

**The Performance of Vehicle Suspensions  
Fitted With Controllable Dampers**

by

Gregory R. Firth, B.Sc.

Submitted in fulfilment of the  
requirements for the degree of  
Doctor of Philosophy

Department of Mechanical Engineering  
The University of Leeds

June 1991

To Donna and Jet

## Abstract

First, techniques for modelling the vehicle and road surface are discussed, and the standard linear and nonlinear analysis methods are reviewed. Then, using the quarter car model and a single idealised road surface, a brief analysis of the passive and active suspensions, including full and limited state feedback schemes, is presented. The performance in terms of ride comfort, road holding ability and suspension travel for both systems is established, providing a yardstick against which the controllable damper systems can be compared.

Three suspensions fitted with controllable dampers are then analysed. In order of increasing complexity these are; a three-state adaptive system, a two-state switchable system, and a continuously variable system. After a performance comparison of the ideal system, the practical limitations present in real hardware are included in the damper model. Their effect on performance is quantified and realistic response targets are set.

The model is then extended to a two dimensional “bicycle” model, which enables control laws to be generated which take into account the correlation between front and rear wheel inputs. Using these laws to drive the active and continuously variable damper system, the advantages of a correlated law are identified. The accelerations and suspension displacements of a passively suspended production vehicle are measured during actual runs over three roads of varying roughness. These are used to estimate the surface roughness properties of the roads. Using this range of typical conditions, the idea of system adaptation is then considered.

The performance of each controllable damper system lies between that of the active and conventional passive systems. The continuously variable system generally offers the best ride comfort, but worthwhile improvements are also possible with the two-state switchable system. The adaptive system offers only marginal improvements for the conditions considered.

## Acknowledgements

Foremost, I would like to thank my academic supervisor, Dr. D.A Crolla, for his guidance throughout the project. I also wish to thank my sponsoring company, Monroe (UK) Ltd, and in particular Peter Hine and Paul Pearce for their valuable advice on the practical aspect of the problem. In The Department of Mechanical Engineering, The University of Leeds, much help has come from discussions with research staff and other students. Dave Horton merits a special mention, not least for the use of his excellent VDAS and PLOT software packages. Others of assistance include, Dave Shuttlewood, Paul Wilkinson and Magdy Abdel-Hady. A theoretical study of this nature requires considerable use of computing facilities. The Vax computer, together with its various plotters and printers, was supported by Ted Allwood. Photographs and slides for the thesis and associated papers were produced by Steve Burrige.

The period of research has been made more enjoyable by many friends within the department. These include; Andrew Winn, Simon Collins, Chris Radcliffe, Barry Gilbert, Jon Cooper, Barry Malone, Pat Hopper and Aref Soliman. Outside the department I would like to acknowledge my mates in Barnsley and all the lads in the Pontefract Road End.

Finally, thanks to my family for their support and to Donna for putting up with me.

# Contents

<b>Abstract</b>	<b>i</b>
<b>Acknowledgements</b>	<b>ii</b>
<b>Contents</b>	<b>iii</b>
<b>Nomenclature</b>	<b>vii</b>
<b>1 Introduction and Review of Previous Work</b>	<b>1</b>
1.1 Introduction . . . . .	1
1.2 Review of Previous Work . . . . .	4
1.2.1 Mathematical modelling . . . . .	4
1.2.2 Passive systems . . . . .	6
1.2.3 Active systems . . . . .	7
1.2.4 Controllable damper systems . . . . .	10
1.2.5 System Comparisons . . . . .	12
1.3 Summary . . . . .	13
<b>2 Vehicle Ride Modelling</b>	<b>15</b>
2.1 Introduction . . . . .	15
2.2 Road Profile Representation . . . . .	16
2.3 The Quarter Car Model . . . . .	19
2.3.1 Justification . . . . .	20
2.3.2 Equations of Motion . . . . .	23
2.4 Linear Analysis . . . . .	25
2.4.1 Frequency Response . . . . .	25
2.4.2 Response to Spectral Density Ground Inputs . . . . .	26
2.5 Non Linear Analysis . . . . .	27
2.6 Performance Criteria . . . . .	28

2.7	VDAS . . . . .	30
2.8	Concluding Remarks . . . . .	31
<b>3</b>	<b>Passive System</b>	<b>32</b>
3.1	Introduction . . . . .	32
3.2	Analysis . . . . .	33
3.3	Results . . . . .	35
3.4	Discussion of Results . . . . .	41
3.5	Concluding Remarks . . . . .	44
<b>4</b>	<b>Active System</b>	<b>46</b>
4.1	Introduction . . . . .	46
4.2	Equations of Motion . . . . .	47
4.3	System Optimization . . . . .	48
4.3.1	Full State Feedback Case . . . . .	51
4.3.2	Limited State Feedback Case . . . . .	54
4.4	Results . . . . .	57
4.5	Discussion of Results . . . . .	61
4.6	Concluding Remarks . . . . .	65
<b>5</b>	<b>Controllable Damper Systems</b>	<b>67</b>
5.1	Introduction . . . . .	67
5.2	Equations of Motion . . . . .	69
5.3	System Definitions . . . . .	70
5.3.1	Continuously Variable Damper System . . . . .	70
5.3.2	Switchable Damper System . . . . .	74
5.3.3	Adaptive Damper System . . . . .	74
5.4	Results . . . . .	76
5.5	Discussion of Results . . . . .	85
5.6	Concluding Remarks . . . . .	88

<b>6</b>	<b>Effect of Practical Limitations</b>	<b>91</b>
6.1	Introduction . . . . .	91
6.2	Modelling of Limitations . . . . .	92
6.2.1	Time Delay Characteristics . . . . .	92
6.2.2	Damping Constraints . . . . .	99
6.3	Results . . . . .	101
6.3.1	Effect of Time Delays . . . . .	101
6.3.2	Effect of Damping Constraints . . . . .	106
6.4	Discussion of Results . . . . .	109
6.5	Concluding Remarks . . . . .	111
<b>7</b>	<b>Half-Vehicle Model Studies</b>	<b>115</b>
7.1	Introduction . . . . .	115
7.2	Equations of motion . . . . .	117
7.2.1	Passive case . . . . .	118
7.2.2	Active case . . . . .	119
7.2.3	Semi-active case . . . . .	120
7.3	Control Laws . . . . .	121
7.3.1	First order equations . . . . .	121
7.3.2	Uncorrelated Case . . . . .	122
7.3.3	Correlated Case . . . . .	125
7.4	Results . . . . .	129
7.5	Discussion . . . . .	132
7.6	Concluding Remarks . . . . .	140
<b>8</b>	<b>Measurements</b>	<b>143</b>
8.1	Introduction . . . . .	143
8.2	Instrumentation . . . . .	144
8.3	Results . . . . .	147

8.4	Discussion . . . . .	149
8.5	Concluding Remarks . . . . .	159
<b>9</b>	<b>Comparison of Systems</b>	<b>160</b>
9.1	Introduction . . . . .	160
9.2	Selected designs . . . . .	161
9.2.1	Continuously variable damper . . . . .	161
9.2.2	Switchable damper . . . . .	162
9.2.3	Adaptive damper . . . . .	163
9.3	Results . . . . .	165
9.4	Discussion . . . . .	172
9.4.1	Scaling effect . . . . .	172
9.4.2	Comparison of results . . . . .	173
9.4.3	Control law adaptation . . . . .	176
9.5	Concluding Remarks . . . . .	177
<b>10</b>	<b>Conclusions</b>	<b>180</b>
	<b>References</b>	<b>186</b>

## Nomenclature

Symbol	Description
$a, b$	distance from C of G to front and rear wheel stations
$A, B, B_1$	coefficient matrices in first order equation of motion
$A_a, B_a, B_{aw}$	coefficient matrices in first order equation of motion (including input) - active quarter car
$A_b, B_b, B_{b1}$	coefficient matrices in first order equation of motion - continuously variable damper quarter car
$A_c, B_c, B_{cw}$	coefficient matrices in first order equation of motion (including input) - continuously variable damper quarter car
$A_d, B_d, B_{dw}$	coefficient matrices in first order equation of motion (including input and delay states) - active half car
$A_e, B_e, B_{ew}$	coefficient matrices in first order equation of motion (including input and delay states) - semi-active half car
$A_\eta, B_\eta$	coefficient matrices in state space representation of wheelbase time delay
$\bar{A}$	state matrix in Liapunov equations
ACC	rms ISO weighted vertical body acceleration ( $\text{m/s}^2$ )
$b_1, b_2$	input matrices - half car with delay states

$c_a, c_{af}, c_{ar}$	actual damping coefficients - controllable damper systems (kNs/m)
$C, C_f, C_r$	demand damping coefficients - controllable damper systems (kNs/m)
$C_{hard}, C_{int},$ $C_{soft}$	discrete damper settings used in switchable and adaptive systems (kNs/m)
$C_{min}, C_{max}$	maximum and minimum damping coefficient - continuously variable damper (kNs/m)
$C_s, C_{sf}, C_{sr}$	passive damping coefficients (kNs/m)
$d$	damping parameter
$D$	connection matrix
DTL	rms tyre load variation (kN)
$D_{\eta}$	output matrix of wheelbase delay equation
$f$	vector of functions
$f_w$	input filter
$F_f, F_r$	front and rear suspension force (kN)
$F_w$	matrix of input filters
$G, G_A, G_B$	road roughness coefficient (or intensity of white noise)
$H$	vector of frequency response functions
$I$	identity matrix
$I_b$	pitch inertia (tonnes.m <sup>2</sup> )
$J$	performance index

$K, K_L$	matrices of full and limited state feedback gains
$K_s, K_{sf}, K_{sr}$	spring stiffnesses (kN/m)
$K_t, K_{tf}, K_{tr}$	tyre vertical stiffnesses (kN/m)
$l$	wheelbase (m)
$M$	measurement matrix
$M_b$	quarter car body mass (tonnes)
$M_{bh}$	half car body mass (tonnes)
$M_c$	mass at centre of vehicle
$M_f$	mass at front of vehicle
$M_r$	mass at rear of vehicle
$M_w, M_{wf}, M_{wr}$	wheel masses (tonnes)
$MXDD, MXD, MX$	coefficient matrices of general equation
$MU, MUD, MF$	of motion
$MXDD_a, MX_a$	coefficient matrices of equation of motion
$MU_a, MF_a$	- active quarter car
$MXDD_c, MX_c$	coefficient matrices of equation of motion
$MU_c, MF_c$	- controllable damper quarter car
$MXDD_p, MXD_p$	coefficient matrices of equation of motion
$MX_p, MU_p$	- passive quarter car
$MXDD_s, MXD_s$	coefficient matrices of equation of motion
$MX_s, MU_s, MF_s$	- controllable damper quarter car (including first order delay)

$MXDD_{ha}, MX_{ha}$	coefficient matrices of equation of motion
$MU_{ha}, MF_{ha}$	- active half car
$MXDD_{hc}, MX_{hc}$	coefficient matrices of equation of motion
$MU_{hc}, MF_{hc}$	- controllable damper half car
$MXDD_{hp}, MXD_{hp}$	coefficient matrices of equation of motion
$MX_{hp}, MU_{hp}$	- passive car
$MXDD_{hs}, MXD_{hs}$	coefficient matrices of equation of motion
$MX_{hs}, MU_{hs}, MF_{hs}$	- controllable damper half car (including first order delay)
$n$	wavenumber (c/m)
$n_0$	wavenumber at discontinuity of spectra (c/m)
$n_{co}$	cut-off wavenumber (c/m)
$n_{max}, n_{min}$	maximum and minimum wavenumbers of interest
$nf$	dimension of vector of functions
$nm$	dimension of measurement matrix
$nq$	dimension of weighting matrix
$nu$	dimension of force vector
$nx_0$	dimension of input vector
$ny$	dimension of output vector
$nz$	dimension of state vector
$N$	order of Pade approximation
$p, p_1, p_2$	exponents in description of surface spectra

$P$	unique solution to Ricatti equation
$q_1 \dots q_6, \rho$	performance index weighting constants
$Q, R$	weighting matrices
$s_1, s_2, s_3$	intermediate variables
$S$	transformation matrix
$S_{x_0}$	input spectral density
$S_z$	output spectral density
SWS	rms suspension displacement (m)
$t$	time (secs)
$T, T_f, T_r$	first order time constants (msecs)
$T_u, T_{uf}, T_{ur}$	
$T_{th}$	threshold delay (msecs)
$TXDD, TXD, TX$	coefficient matrices of output equation
$TU, TUD$	
$u, u_1, u_2$	control forces
$u_a, u_{af}, u_{ar}$	actual damping forces
$V, V_A, V_B$	vehicle forward speeds
$V_{max}, V_{min}$	maximum and minimum speeds of interest
$w, v_f, v_r$	white noise processes
$W_c, W_o$	solutions to Liapunov equations
$x$	general first order state vector

$\bar{x}$	transformed state vector
$x_a$	first order state vector including input - active quarter car
$x_b$	first order state vector - continuously variable damper quarter car
$x_c$	first order state vector including input - continuously variable damper quarter car
$x_d$	first order state vector including delay states - active half car
$x_e$	first order state vector including delay states - semi-active half car
$x_u, x_{uf}, x_{ur}$	damper forces as system states
$x_0, x_{0f}, x_{0r}$	ground input displacements
$Y$	vector of output variables
$z$	state vector
$z_1, z_3$	vertical wheel displacements
$z_2, z_4$	vertical body displacements
$z_b$	body bounce at C of G
$z_s$	state vector including damping coefficient - continuously variable damper quarter car
$z_{hs}$	state vector including damping coefficient - continuously variable damper half car

$Z$	magnitude of output response
$\alpha$	filter coefficient
$\alpha_0 \dots \alpha_4$	constants in the Pade approximation
$\eta$	wheelbase time delay state vector
$\theta_b$	body pitch at C of G
$\tau$	wheelbase time delay
$\phi$	phase shift
$\omega$	angular frequency (rad/s)
$\omega_1, \omega_2$	minimum and maximum frequencies of interest (rad/s)
$\Omega$	frequency (cycles/s)
$\Omega_{min}, \Omega_{max}$	minimum and maximum frequencies of interest (cycles/s)

# Chapter 1

## Introduction and Review of Previous Work

### 1.1 Introduction

An effective automotive suspension system must perform a number of different tasks. It must support the vehicle over a range of loading conditions, maintain directional and attitude control during handling manoeuvres, and also provide isolation from undulations in the road surface. These tasks inevitably lead to conflicting design requirements. For example, suspensions with low stiffnesses and hence low natural frequencies provide good isolation, but at the same time exhibit poor attitude control and also a requirement for large suspension working spaces.

The passive suspension is still to be found on the majority of current production vehicles. Generally, the system consists of conventional springs and dampers, which are constant rate and cannot be changed by external signals. In view of the conflicting requirements and the fact that the vehicle has to operate over a wide range of running conditions, the choice of fixed stiffness and damping parameters must be a compromise. Although some vehicle manufacturers have attempted to overcome the problem by employing self-levelling systems and/or adjustable dampers, the potential of an "intelligent" suspension system with the ability to avoid this compromise is clear.

In recent years the use of microprocessors on vehicles has become commonplace, and this, combined with important technological developments in actuators,

adjustable dampers, and variable springs has led to an upsurge of interest in more advanced suspensions. At the extreme end of the spectrum, the fully active suspension is one in which the conventional elements of the passive suspension are replaced with a hydraulic or pneumatic actuator. The actuator responds to a demand signal, which is typically generated in a microprocessor on receipt of measured information about the vehicle response and possibly the road input. The system is governed by a control law which can readily be changed, either on initiation of a handling manoeuvre, or in response to a change in running conditions. The theoretical and experimental performance improvements are dramatic; however, the added cost and complexity of the system, coupled with the higher energy consumption, has so far restricted its use to a number of racing and prototype vehicles.

The majority of vehicle manufacturers have lowered their sights somewhat in an attempt to find a more realistic alternative. The "slow" active system is one in which a limited bandwidth actuator is mounted in parallel with a conventional passive spring and/or damper. Examples of this type of system are beginning to appear on the market, but although the costs associated with the actuator are lower, much of the complexity of the fully active system is retained. In contrast, the controllable damper system represents the simple end of the intelligent suspension spectrum. The system is essentially one in which a damper, its coefficient controlled according to some law, is mounted in parallel with a conventional passive spring. For obvious reasons this class of suspension has become an attractive proposition to vehicle manufacturers. The actuators, hydraulic pumps and accumulators of the active system, are no longer required, enabling the system to be incorporated in a standard vehicle with few design changes. Also, since only the rate of energy dissipation can be varied, any additional energy costs are minimal. How the performance of these more practical suspensions compares against that of the passive and ideal active suspensions

is the subject of the work presented here.

Computer aided theoretical analysis is fast becoming an important tool in the development of practical suspension systems. Its advantage lies in the ability to determine the effect of parameter changes early in the design process and hence reduce development costs. In general, such investigations of vehicle dynamics problems require reduction of the vehicle to a mathematical model. This can be obtained either by application of the fundamental laws of physics to an idealised representation of the vehicle, or alternatively, from analysis of measured data obtained from the real vehicle. If the modelling is to represent a practical situation it follows that a further model is required to describe the surface roughness properties of the road.

At Leeds University, Horton [1991] has developed the Vehicle Dynamics Analysis Software package, VDAS, which, once a set of equations describing the system is established, is able to deal with both linear and non-linear ride and handling problems. The package is able to generate a wide range of output including eigensolutions, frequency responses, responses to an idealised ground input and time histories from simulation in the time domain. Other analysis packages exist, for example ADAMS or MEDYNA, but these are perhaps more suited to complex simulations of multibody systems with large numbers of degrees of freedom.

The next section presents a review of some of the previous work on the subject. First, the mathematical modelling of the vehicle and road surface are considered. Then selected work on the passive, active and controllable damper systems is discussed, together with suggested techniques for obtaining suitable control laws. Finally, previous theoretical comparisons of competing suspensions are reviewed.

## 1.2 Review of Previous Work

### 1.2.1 Mathematical modelling

The starting point in obtaining an accurate prediction of vehicle response to excitation by the ground input is a suitable representation of the road surface itself. Measurement and analysis of road surfaces has been carried out by a number of workers. La Barre *et al* [1970] describes the development of a profilometer which is then used to conduct an extensive survey of European roads. The results obtained are analysed by Dodds and Robson [1973] who, recognising that a general expression could be used to describe the single track spectra, classify the roads in terms of their roughness coefficient and frequency content (the actual values for these parameters are later corrected by Robson [1979]). The same expression is also used by Healey *et al* [1977], who performs similar measurements and analyses. Using the assumption of isotropy, Dodds and Robson [1973] and Kamash and Robson [1978] show that the spectral density of a single track can also be used to define a two-dimensional road surface model.

For the frequency domain analysis of linear systems, the road spectra can be used directly as the input. However, non-linear analysis requires the road surface description to be in the form of a time or distance dependent profile. These are obtained by applying the inverse discrete Fourier transform to the spectral density function. Techniques for generating single and two correlated parallel profiles using this method are presented in Cebon and Newland [1983].

Once a suitable mathematical description of the ground input is determined the next step is to reduce the vehicle to a manageable model. A 7 d.o.f model is described by Sharp and Hassan [1984] in which the vehicle body is assumed to be rigid and has freedom in bounce, pitch and roll directions. The vertical motion of the front two wheels contribute a further two degrees of freedom, whilst the

remaining degrees of freedom are either the independent vertical motion of the rear wheels, or, the bounce and roll motion of a rear axle. Any structural body vibrations, the vibration of the engine on its mountings and of the driver on his seat are neglected. Sharp and Hassan go on to justify further reductions to 4 d.o.f "bicycle model" and finally a 2 d.o.f quarter car model. Healey *et al* [1977] compares measured accelerations over a known road surface input, with predicted results from 7 d.o.f, 4 d.o.f and 2 d.o.f models. The comparison shows that the 7 d.o.f model is the most accurate but also that the reduction to simpler models does not contribute as much error as might have been expected. The validity of the quarter car model is further confirmed by Chalasani [1986 a] and [1986 b] who obtains theoretical results for an active system using both full and quarter vehicle models. He concludes that the quarter car model is adequate for arriving at a fundamental understanding of many of the issues that are involved in the design of an active suspension. In all the models mentioned, it is assumed that the suspension elements are linear and that the available working space is large enough to prevent any contact with the bump stops. In each case the tyre is modelled as a linear spring which is in constant contact with the road surface.

Techniques for generating the response of the vehicle model to an idealised road surface using linear and non-linear analysis are reviewed by Horton [1986]. They are discussed further in Chapter 2.

The next stage is to determine the output variables which provide a suitable measure of system performance. Ryba [1974 a] and Sharp and Hassan [1984] select three performance criteria; (a) the root mean square (rms) value of vertical acceleration of the passenger on his seat, (b) the rms dynamic tyre load, and (c) the rms dynamic deflection of the suspension spring, representing passenger discomfort, road holding ability and suspension working space usage respectively. To obtain a single figure measure of passenger discomfort, it is necessary

to multiply the accelerations by a frequency dependent weighting factor which takes into account the human sensitivity to vibration at various frequencies. Ryba applies the weighting curves proposed by ISO (ISO/TC 108/WG7) and Simic (see Ryba [1973]), while Sharp and Hassan use weightings based on the later ISO document 2361 [1974]

### 1.2.2 Passive systems

The passive suspension system has been studied in detail in a series of papers by Ryba [1973], [1974 a] and [1974 b]. In the first he excites a model consisting of sprung mass and passenger on seat with a road surface model which is based on white noise. The passenger discomfort and spring deflection are then determined over a range of suspension parameters. He concludes that the comfort can be improved by reducing the natural frequency of the sprung mass but this always results in an increased dynamic spring deflection. In [1974 a] he uses a more realistic quarter car model which takes into account the unsprung mass. This reveals that a reduction in sprung mass natural frequency below a certain level also results in an increase in dynamic tyre loading, and highlights the problem facing the suspension designer. In [1974 b] the possibility of incorporating an dynamic absorber in the suspension is examined. The conclusion is that, providing the absorber is of mass equal to the unsprung mass, a somewhat unrealistic proposition, a high degree of comfort can be achieved without a reduction in road holding ability. The fundamental conflict between ride and suspension working space is also discovered by Sharp and Hassan [1984], who study the performance of both two and three mass passive systems. The latter system is modelled with a dynamic absorber which amounts to only 10% of the unsprung mass, while in both cases two different values of unsprung mass are considered. They conclude that neither a reduction in the unsprung mass,

which is difficult in practice, nor the addition of a dynamic absorber appear to be cost effective.

The conflict between ride comfort, road holding and suspension working space requirements are further complicated by the fact that the vehicle must operate over a range of running and loading conditions. Sharp and Hassan [1986 a] show how the performance of the fixed passive suspension deteriorates when operating at surfaces and speeds away from its design condition. There have been a number of attempts to alleviate the problem with the use of variable parameter suspension elements. These can generally be classified as adaptive systems and examples are given in Section 1.2.4.

The problem of varying payloads can be overcome by employing a self-levelling suspension. Using a pneumatically or hydropneumatically controlled air spring, these are able to provide a constant ride height and sprung mass natural frequency, regardless of the vehicle loading condition. Such systems, used successfully by Citroen for many years, enable softer springs to be used, giving improved ride comfort when compared with a conventional system having the same available working space.

### **1.2.3 Active systems**

The active vehicle suspension has been the subject of numerous theoretical investigations over the last 20 years, and the potential benefits are well documented. Reviews of early work on the subject, outlining analysis procedures, optimisation techniques and hardware developments, have been presented by Hedrick and Wormley [1975] and more recently by Goodall and Kortum [1983].

An important area of discussion has been the optimisation of active systems and a number of methods have been suggested. Thompson [1976] uses a technique

based on linear optimal control theory to generate a full state feedback control law for a quarter vehicle model. The theory requires that the system input is white noise and that the performance index to be minimised by the optimal control is of quadratic form. A coordinate transformation allows a unique set of feedback gains to be obtained from the solution to the algebraic Riccati equation. This full state control law includes a term which is dependent on the measurement of body-to-road height and is consequently difficult to realise in practice. A sub-optimal law avoiding the requirement of a body-to-road height sensor is described by Thompson [1984]. A more practical solution, again based on linear optimal control theory, is presented by Wilson *et al* [1986]. In this case the system input is assumed to be a low pass filtered white noise and, using the solution to the Liapunov equations and a gradient descent method, a control law can be generated for quite general feedback possibilities.

The optimisation problem relating to a full vehicle model is complicated by the fact that the inputs at each wheel are correlated; a coherency exists between the left and right tracks and, more importantly, the rear input is a delayed version of that at the front. The use of control laws which take account of these correlations has been investigated by several workers. Thompson and Pearce [1979] conclude that the speed-dependent time delay between disturbance inputs has no effect on the optimal control law and hence suspension performance. This is later questioned by Fruhauf *et al* [1985], Louam *et al* [1988] and Abdel-Hady [1989] who, using different techniques to model the time delay, obtain promising results at the rear of the vehicle from control laws which take advantage of the "wheelbase preview" information. Foag [1988] takes the idea further and considers an active suspension which has the benefit of look-ahead preview. Although the results are again encouraging, such a system reintroduces the practical difficulties associated with a body-to-road sensor.

Although many of the optimisation techniques mentioned here are based on

linear optimal control theory, a number of alternative methods have been used. For example, Foag [1988] uses a “multi-criteria” approach to determine the optimum control law parameters, while Hall and Gill [1987] favour an approach based on modal control methods. The latter technique involves a scan of the  $s$  plane in order to find the control law which results in the most appropriate pole locations.

A comprehensive review of work into the generation of active control laws is given by Sharp and Crolla [1987 a] while the relative merits of various uncorrelated and correlated control laws are discussed further in Chapters 4 and 7 here.

Despite the performance claims of the theoretical active suspension studies, the increased cost and complexity, coupled with high energy consumption, have restricted development of the fully active design to a number of prototype vehicles. Notable examples of these are the Lotus Turbo Esprit road car, described by Wright and Williams [1984], and more recently the experimental DaimlerBenz system, described by Acker *et al* [1989]

A more commercially attractive alternative is the “slow” active suspension, in which the active elements have a bandwidth of approximately 3Hz and are combined with either fixed or controlled damper elements. To provide suspension action beyond the control bandwidth the actuator must be mounted in series with a conventional spring, which in turn reduces the energy requirements of the system. Sharp and Hassan [1987] model such a system, and predict a ride comfort performance which is close to that of the fully active system over a wide range of running conditions. Actuator costs are lower than for a fully active design, and it is this feature which has led to a number of first generation slow active systems appearing on the market, for example, on the Nissan Infiniti Q45 (Aoyama *et al* [1990]) and the Toyota Celica (Yokoya *et al* [1990]).

## 1.2.4 Controllable damper systems

The term controllable damper system is used here to describe the class of systems, of varying complexity, which occupy the gap between passive and active suspensions. Adjustable dampers in their simplest form have been available for many years and as early as 1963, the Armstrong Selectaride shock absorber (see Poyser [1987]) enabled the driver to select the preferred damping level for the general conditions at the time. In more recent systems an “adaptive” strategy is used, in which the decision to change suspension setting is made by a microprocessor on receipt of information concerning the vehicle operating conditions. The Toyota TEMS system (Yokoya *et al* [1984]) employs a two-state damper which is set soft for normal running conditions and switches hard when manoeuvring, accelerating or braking. Similar systems are employed by Mitsubishi (Mizuguchi *et al* [1984]), Nissan (Konishi *et al* [1988]) and Citroen [1989] although these go one stage further in providing soft and hard spring rates together with self-levelling.

Other adaptive suspensions currently on the market include; the Monroe (formerly Armstrong) ASC system (Hine and Pearce [1988]), the BMW EDC II system (Hennecke and Zieglmeier [1988]) and the system used on the 1989 Cadillac Allante (Reuter [1989]). The switching strategies of these systems are based on suspension displacement, frequency content of road input, and vehicle speed respectively. Each design employs a three setting damper which defaults to the hardest setting in the event of manoeuvring or braking etc.

Advances in valve technology have reduced the damper switching times in some of the more recent adaptive systems to such a level that more complex control strategies are now being considered. Karnopp *et al* [1974] models a two setting semi-active damper which uses a switching strategy based on the direction of absolute and relative velocity of the body. The work does not address the

vehicle problem in particular and uses a single degree of freedom model. They do, however, conclude that a semi-active suspension of this nature can provide many of the performance gains of active systems with much reduced capital and running costs. The strategy is later applied to the vehicle problem by, for example Crolla and Aboul Nour [1988] and Lizell [1988]. The latter system is slightly different in that the semi-active strategy is combined with a frequency dependent adaptive strategy. The system operates according to the Karnopp semi-active concept only in a band of low frequencies (0.5-3Hz) and outside this range the damper setting depends on the frequency content of the wheel motion. Both studies claim significant improvements in ride performance over the fixed passive system.

A different semi-active strategy is considered in the theoretical studies of Sharp and Hassan [1986 a]. The control law used is essentially a fully active linear optimal control law which is modified to account for the fact that the damper can only dissipate energy. A continuously variable damper is required which is theoretically capable of tracking a force demand signal independently of the velocity across the damper. The development of commercially viable proportional valves for use in such systems is currently of interest and prototypes have been built by Parker and Lau [1988] and Doi *et al* [1988].

The distinction to be made between a semi-active and a purely adaptive system is in the length of time spent in each setting. A semi-active system, operating according to a switchable or continuously variable strategy, is constantly changing its damper setting and consequently will require short switching times. In contrast, the adaptive may remain in one particular setting for long periods and the valve response becomes less important.

### 1.2.5 System Comparisons

In an attempt to determine the relative merits of the various competing suspension systems, a number of theoretical comparisons have been performed. For example, using a quarter car model Sharp and Hassan [1986 b] compare the performance of passive, active and semi-active suspensions. Recognising that the suspension designer will have to limit the amount of suspension travel, they introduce a method of comparison which is based around the equal usage of workspace. For a given workspace value, this enables the performance in terms of ride comfort to be plotted against that in terms of road holding ability. Their work reveals that, for a range of suspension working spaces, the active and continuously variable semi-active systems driven by limited state linear optimal control laws, perform almost as well as the full state feedback active system. A similar study is undertaken by Crolla and Aboul Nour [1988] but here the slow active suspension and semi-active damper switching according to the Karnopp strategy are also considered. The latter system is shown to provide significant improvements in ride comfort over a fixed passive system. Although both the above comparisons assume that the active and semi-active systems operate with a first order time delay of around 10ms, the effect this has on performance is not dealt with in any detail. Chalasani [1986 a], [1986 b] uses the quarter car and full vehicle models to compare the performance of the passive and active systems only. Rather than use an equal workspace curve, Chalasani plots body acceleration against suspension travel and completes the picture by including lines of equal tyre deflection. Results show that the active suspension can improve on the ride performance of the passive suspension by around 15% to 20%, with no increase in rms suspension deflection or tyre deflection. The performance gains are achieved through reductions in body accelerations in the frequency range around body resonance.

### 1.3 Summary

The conflicting demands on a vehicle suspension are well understood. It follows that the design of a passive system with fixed damping and stiffness parameters must inevitably involve a compromise. The development of an “intelligent” suspension which can do better in relation to this compromise has been the subject of widespread theoretical and experimental work. The fully active system is one answer to the problem but its dramatic improvements in ride performance are accompanied by equally dramatic increases in cost, complexity and energy consumption. Consequently, most vehicle manufacturers have switched their efforts to finding a more realistic alternative. The first generation of these are now beginning to appear on the market, usually in the form of an adaptive damper system.

There is a considerable interest in the semi-active system. It is hoped that the system, perhaps used in conjunction with a self-levelling system, will provide much of the benefits of the fully active system but with a much reduced energy consumption and component complexity. There have been some theoretical studies with encouraging results. However, many of the performance comparisons so far have assumed systems fitted with ideal components. The valve response has been modelled by some workers as a simple first order lag but its effect on performance has not been studied in any detail, and other factors such as the range of damping available are ignored.

The use of control laws which take advantage of wheelbase preview information has yielded promising results. So far these have only been applied to the ideal fully active system. Whether similar improvements can be obtained in the case of a semi-active system fitted with real components, has yet to be determined.

Most comparisons have concentrated on the performance over a single idealised road surface. This is acceptable for linear systems since a scaling factor can be used to determine the performance at other conditions. For systems with time-varying parameters, for example controllable damper systems, this may not apply and further comparisons are required.

The aim of this work is to compare the performance of controllable damper systems against that of the passive and fully active suspensions. In the next chapter, various modelling techniques, including reduction of the vehicle to a two degree of freedom model and procedures for the analysis of linear and non-linear equations, are reviewed. The techniques are then used in Chapter 3 to briefly analyse and quantify the performance of the passive quarter car over a single idealised surface. The performance of the active system, using both full and limited state linear optimal control laws, is established in Chapter 4, providing a target for other less complex designs. In Chapter 5, various controllable damper systems are described and modelled, initially using ideal components. The response limitations of a real system are then introduced to the model in Chapter 6 and their effect on performance is studied in detail. Chapter 7 uses a half vehicle model and the Pade approximation technique to investigate the use of wheelbase preview on the semi-active continuously variable damper system. In Chapter 8, measured accelerations of the vehicle body and suspension arm are used to estimate the road surface description of three typical roughness/speed combinations. These are used in Chapter 9 where selected controllable damper systems, modelled with realistic suspension parameters and response limitations, are compared against the passive and ideal active systems over the three idealised conditions.

# Chapter 2

## Vehicle Ride Modelling

### 2.1 Introduction

The first step in analysing the response of the vehicle to road roughness is to obtain an adequate model of the surface itself. It is widely recognised that road surfaces approximate to Gaussian random processes, and can be classified using the equation describing its amplitude squared spectral density. These expressions, in terms of frequency or wavenumber, can then be used directly as inputs for the frequency domain analysis of linear models. Non-linear analysis is carried out in the time domain, and in this case the input is required in the form of a time or distance dependent profile.

The vehicle itself may be reduced to a two degree of freedom quarter vehicle model, from which the equations of motion are easily formulated using Newtonian methods. Linear equations allow the frequency response and, when combined with the input spectral density, the response to an idealised input to be determined. If non-linearities or time varying parameters are present in the model, the equations may be solved numerically to give time histories, and subsequently processed to give results in the frequency domain.

This chapter describes the representation of road profiles based on amplitude squared spectral density, and also outlines the procedure to obtain a time or distance dependent profile from such a description. Justification of the quarter car model is then discussed and a general form for the equations of motion is

adopted. The procedures for analysing the linear or non-linear equations are reviewed, and finally the output variables of interest are decided upon.

## 2.2 Road Profile Representation

The random road profile may be considered as a continuous spectrum of sine waves. A corresponding graph of squared amplitude against wavenumber is called the amplitude spectral density, and the units of spectral density, for an amplitude in metres and wavenumber in cycles/m, is  $\text{m}^2/(\text{cycle}/\text{m})$ . Such spectra have been obtained from measured road profiles by several workers including LaBarre *et al* [1970] and Healey *et al* [1977]. Subsequent analysis by these and others, has revealed that the shape of these spectra, regardless of road quality is generally the same. Fig 2.1, taken from Dodds and Robson [1973], shows the spectral density of a typical principal road using log-log axes.

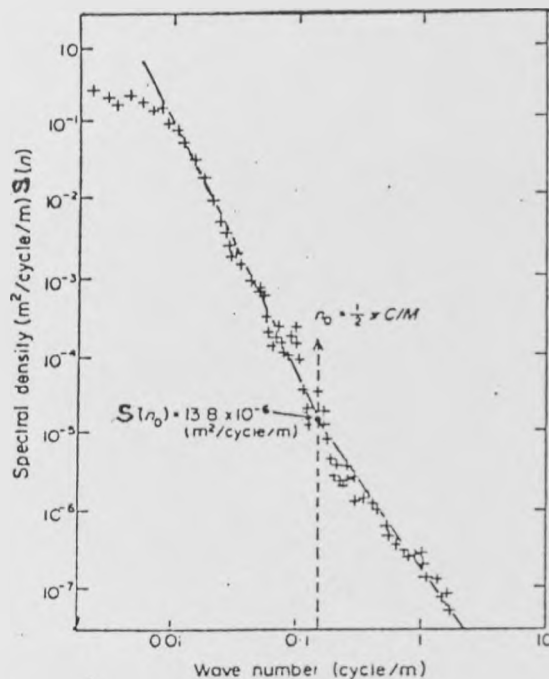


Figure 2.1: The spectral density of a typical principal road

Dodds and Robson recognise that in general a discontinuity appears in the spectrum and consequently approximate it by an equation of the form ;

$$S_{x_0}(n) = \begin{cases} G \left(\frac{n}{n_0}\right)^{-p_1} & ; \quad n \leq n_0 \\ G \left(\frac{n}{n_0}\right)^{-p_2} & ; \quad n \geq n_0 \end{cases} \quad (2.1)$$

where  $n_0$  is the wavenumber at the discontinuity and  $G$  is the roughness coefficient (equal to the value of  $S_{x_0}(n)$  at  $n_0$ ). The exponents  $p_1$  and  $p_2$  are the slopes of each section of the log-log spectrum. The discontinuity in Eqn (2.1) is found by Robson [1979] to correspond generally to a wavelength of approximately 6.3m, giving a value of  $1/2\pi$  cycle/m to  $n_0$ . Although the exponent  $p_1$  varies typically between 2.9 and 3.4, and  $p_2$  between 2 and 2.5, in most cases  $p_1$  and  $p_2$  are very similar and allow Eqn (2.1) to be simplified further to a single slope equation :

$$S_{x_0}(n) = Gn^{-p} \quad (2.2)$$

Typical values for the roughness coefficient ( $G$ ) are quoted by Robson [1979] and shown in Table 2.1. The units of  $G$  are compatible with the other terms in Eqn (2.2)

Surface	Range	Mean
Motorway	$3 \times 10^{-8} - 50 \times 10^{-8}$	$10 \times 10^{-8}$
Principal road	$3 \times 10^{-8} - 800 \times 10^{-8}$	$50 \times 10^{-8}$
Minor road	$50 \times 10^{-8} - 3000 \times 10^{-8}$	$500 \times 10^{-8}$

Table 2.1: Typical surface roughness coefficients,  $G$ .

To be useful, the Eqn (2.2) must describe the road spectra over a range of wavenumbers which are likely to be relevant in response prediction. The highest

wavenumber of interest (corresponding to the shortest wavelength) is obtained from the lowest speed ( $V_{min}$ ) and highest frequency ( $\Omega_{max}$ ) :

$$n_{max} = \frac{\Omega_{max}}{V_{min}} \quad (2.3)$$

Conversely, the lowest wavenumber of interest is obtained from the highest speed ( $V_{max}$ ) and lowest frequency ( $\Omega_{min}$ ) :

$$n_{min} = \frac{\Omega_{min}}{V_{max}} \quad (2.4)$$

For reasons discussed later, the frequency range of interest here is 0.15Hz to 15Hz and a typical vehicle speed range is taken to be 17.9m/s to 31.3m/s (40mph to 70mph), therefore  $n_{max}$  and  $n_{min}$  are 0.84 and 0.005 cycle/m respectively.

An equation of the form (2.2) implies that the input amplitude tends to infinity for very low wavenumbers. As Fig 2.1 shows, this is not the case in reality and the input spectra levels off at low wavenumbers. Although this section of the spectrum is likely to be below the minimum wavenumber of interest it can be described easily by introducing a cutoff wavenumber  $n_{co}$ , below which the amplitude spectral density remains constant.

This form of surface description has been used by, amongst others, Sharp and Hassan [1986 b] and Crolla and Aboul-Nour [1988]. Since this work is initially a continuation of the work by Hassan, the description is also used here, with Chapters 3 to 7 using an exponent ( $p$ ) of 2.5 together with a roughness coefficient ( $G$ ) of  $5 \times 10^{-6}$  and cutoff wavenumber ( $n_{co}$ ) 0.005 c/m.

Later, in Chapter 8, body and wheel accelerations are measured during runs over three typical road surfaces at three different speeds. The spectra of these surfaces are then estimated from comparisons between measured and theoretical results. The roughness coefficients ( $G$ ) and exponents ( $p$ ) are adjusted accordingly to provide three road roughness/speed conditions which represent a range of typical operation of the vehicle.

If the same surface is now traversed at a constant speed,  $V$ , then Eqn (2.2) may be rewritten in terms of frequency rather than wavenumber ;

$$S_{x_0}(\Omega) = \frac{GV^{p-1}}{\Omega^p} \quad (2.5)$$

where  $\Omega$  = frequency in cycles/s.

If the vehicle model is linear, the road spectra described by Eqn (2.5) can be used directly as the input for frequency domain analysis. However, systems which have time variant parameters require non-linear analysis and road surface representation in the form of a time or distance dependent profile. A single track road profile is generated essentially by adding together a discrete number of sine waves. The amplitude of each sinewave is derived from the assumed spectral density of the surface of interest, while the phase angles are determined through a random number generator. The result is a profile which is approximately Gaussian in nature. Throughout the work here, profile generation is carried out using a subsidiary program of the main vehicle dynamics software package (VDAS) developed by Horton [1991].

## 2.3 The Quarter Car Model

A vehicle with a wheel at each corner may be represented by a seven degree of freedom model. The vehicle body is assumed to be rigid and undergoes bounce, pitch and roll motions. The vertical motion of the front wheels contribute a further two degrees of freedom, whilst the remaining degrees of freedom are either the independent vertical motion of the rear wheels, or, the bounce and roll motion of a rear axle. Although a much simplified model of the actual vehicle, in that structural body vibrations, and the vibration of the engine on its mountings and driver on his seat have been neglected, this 7 d.o.f model is still rather complicated for basic ride analysis. Further reduction to a 2 d.o.f.

quarter car model is justified by Sharp and Hassan [1984], the reasoning being outlined below.

### 2.3.1 Justification

First, assuming linearity, the model can be reduced to the two-dimensional model seen in Fig 2.2(a) by ;

1. Observing that for long wavelengths, the coherence between the left and right tracks is likely to be high, and the road surface may be regarded as cylindrical. Consequently the two sides of the vehicle will behave in a similar fashion.
2. Noting that for shorter wavelengths the motions excited in the vehicle will mostly involve wheel hop. Little body motion will occur, and left and right will interact very little.

This “bicycle” model is used later in Chapter 7, where it is required to generate active control laws which take into account the correlation between front and rear wheel ground inputs. The reduction to a quarter car is completed by replacing the bicycle model with a dynamically equivalent system, shown in Fig 2.2(b). This three mass system is equivalent to the rigid beam system if the following conditions are true :

- the total masses are equal.

$$M_f + M_c + M_r = M_{bh} \quad (2.6)$$

- the mass centres are in the same position.

$$M_f a = M_r b \quad (2.7)$$

- the pitch inertias are equal.

$$M_f a^2 + M_r b^2 = I_b \quad (2.8)$$

It can be shown that  $M_c$  will be zero if  $I_b = M_{bh}ab$ . Typical vehicle parameters, including those used here (see Table 3.1), reveal that in general  $I_b \approx M_{bh}ab$  and therefore  $M_c$  is small. This implies that there is little interaction between front and rear and allows separation into two quarter car problems. The validity of this simplification is confirmed by Chalasani [1986 a] and [1986 b] who compares predicted results using both the 7 d.o.f and 2 d.o.f models. The 2 d.o.f. model will be used for the bulk of the work here and the passive version is depicted in Fig 2.2(c). The state variables  $z_1$  and  $z_2$  denote vertical displacement of the wheel and body respectively whilst  $x_0$  represents the ground input displacement. Body and wheel masses are represented by  $M_b$  and  $M_w$  respectively. The tyre is represented by a linear spring throughout, with vertical stiffness  $K_t$ . A tyre model of this form obviously has its limitations in that, (a); a point contact with the road surface is assumed and (b); any separation between the tyre and ground is ignored. More complex tyre models have been suggested by, for example, Bakker *et al* [1987] and Sharp [1989]. However, these models are aimed at the more complicated problem of cornering and braking, rather than straight running at a constant speed, and the use of the simple spring representation is justified here for two reasons. First, the tyre contact length (approx. 0.2m) will be much less than the minimum wavelength of interest (1.3m for a vehicle speed of 20m/s), and second the work is largely of a comparative nature and the tyre model is likely to affect each system model to an equal extent.

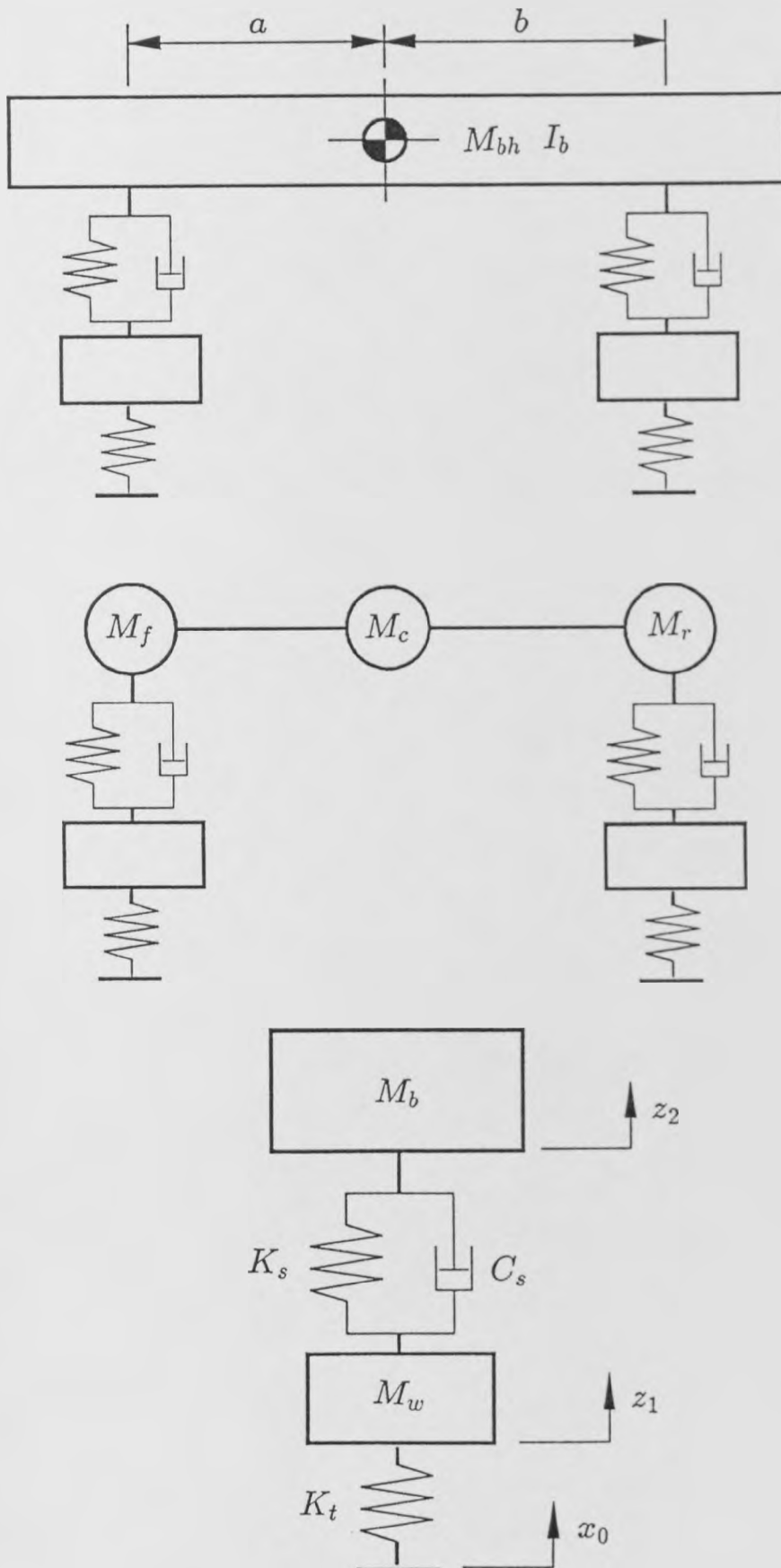


Figure 2.2: Justification of quarter vehicle model

### 2.3.2 Equations of Motion

The equations of motion are formulated using Newtonian methods and, using the passive quarter car case (Fig 2.2(c)) as an example, can be written as follows;

$$M_w \ddot{z}_1 = K_t(x_0 - z_1) - K_s(z_1 - z_2) - C_s(\dot{z}_1 - \dot{z}_2) \quad (2.9)$$

$$M_b \ddot{z}_2 = K_s(z_1 - z_2) + C_s(\dot{z}_1 - \dot{z}_2) \quad (2.10)$$

where  $K_s$  is the passive spring stiffness and  $C_s$  is the damping coefficient.

A more general analysis has been carried out by Horton [1986] for a model which has  $nz$  degrees of freedom. The masses are connected to each other and the ground by various connecting elements (eg. springs, dampers, tyres). This results in the second and/or first order equations of motion being written in matrix form ;

$$MXDD\ddot{z} + MXD\dot{z} + MXz = MUx_0 + MUD\dot{x}_0 + MFf \quad (2.11)$$

where  $z = z(t)$  is a state vector of  $nz$  generalised coordinates,  $x_0 = x_0(t)$  is the input vector of dimension  $nx_0$ , and  $f = f(z, \dot{z}, t)$  is a vector of functions of dimension  $nf$ . The coefficient matrices  $MXDD$ ,  $MXD$ , and  $MX$  are of dimension  $(nz, nz)$ ,  $MU$  and  $MUD$  are  $(nz, nx_0)$  and  $MF$  is  $(nz, nf)$ .<sup>1</sup>

Systems which consist solely of linear connecting elements (ie. the forces are a linear function of relative displacements and velocities across the elements) are conveniently described using the  $z$ ,  $\dot{z}$ ,  $x_0$  and  $\dot{x}_0$  terms in Eqn (2.11). The passive system shown in Fig 2.2(c) is assumed to be such a system, the spring and damper forces being linearly related to  $(z_1 - z_2)$  and  $(\dot{z}_1 - \dot{z}_2)$  respectively.

Eqns (2.9) and (2.10) describing the passive system can now be rearranged and written in the form of Eqn (2.11). Using the suffix  $p$  to denote the passive case,

<sup>1</sup>The matrix notation is taken from FORTRAN code used in the analysis package VDAS.

the coefficient matrices become ;

$$\begin{aligned} MXDD_p &= \begin{bmatrix} M_w & 0 \\ 0 & M_b \end{bmatrix}, MXD_p = \begin{bmatrix} C_s & -C_s \\ -C_s & C_s \end{bmatrix} \\ MX_p &= \begin{bmatrix} K_s + K_t & -K_s \\ -K_s & K_s \end{bmatrix}, MU_p = \begin{bmatrix} K_T \\ 0 \end{bmatrix} \end{aligned} \quad (2.12)$$

Tyre damping is assumed to be negligible, and therefore in this case  $MUD$  is a null matrix.  $MF$  is also a null matrix since the vector of functions,  $f$ , is not required.

The  $nz$  second order equations may be transformed into  $2nz$  first order equations by defining a new state vector  $x = [z \quad \dot{z}]^T$ . The equations describing the passive quarter car can now be written :

$$\dot{x}_1 = x_3 \quad (2.13)$$

$$\dot{x}_2 = x_4 \quad (2.14)$$

$$\dot{x}_3 = \frac{K_t(x_0 - x_1) - K_s(x_1 - x_2) - C_s(x_3 - x_4)}{M_w} \quad (2.15)$$

$$\dot{x}_4 = \frac{K_s(x_1 - x_2) + C_s(x_3 - x_4)}{M_b} \quad (2.16)$$

These equations lead to a different general form ;

$$\dot{x} = Ax + B_1x_0 \quad (2.17)$$

where  $A$  is  $(2nz, 2nz)$  and  $B_1$  is  $(2nz, nx_0)$ , and are related to  $MXDD$ ,  $MXD$ ,  $MX$  and  $MU$  by ;

$$\begin{aligned} A &= \begin{bmatrix} 0 & I \\ -MXDD^{-1}MX & -MXDD^{-1}MXD \end{bmatrix} \\ B_1 &= \begin{bmatrix} 0 \\ MXDD^{-1}MU \end{bmatrix} \end{aligned} \quad (2.18)$$

where  $I$  is the identity matrix.

If the vehicle model contains active or semi-active elements, Eqn (2.17) may be extended to ;

$$\dot{x} = Ax + Bu + B_1x_0 \quad (2.19)$$

where  $u$  represents a vector of control forces and can be included in Eqn (2.11) using the vector of functions  $f$ , such that :

$$B = \begin{bmatrix} 0 \\ MXDD^{-1}MF \end{bmatrix} \quad (2.20)$$

This standard form of equation is used to generate control laws, and ultimately the elements in matrix  $B$ , for both active and semi-active systems. The techniques used are based on linear optimal control theory and are outlined in Chapter 4.

## 2.4 Linear Analysis

The passive and active models considered in Chapters 3 and 4 respectively, contain only time invariant elements and therefore lend themselves to linear analysis. Basically, the problem is to excite the vehicle model and its equations of motion (2.11) with a road input which has a spectra described by an equation of the form (2.5), and obtain any desired output. First, it is necessary to derive the frequency response of the model to an input comprising a sine wave of unit amplitude.

### 2.4.1 Frequency Response

The derivation of the frequency response function is covered in detail by, for example, Van de Vegte [1990] or Horton [1986] and the procedure outlined here.

Suppose a system has a single input and takes the form :

$$x_0 = e^{i\omega t} \quad (2.21)$$

where  $\omega$  is the frequency in rads/sec.

It follows that, after the decay of transients, the vector of system states  $z$  will respond in a similar form ;

$$\begin{aligned} z &= Z(\omega)e^{i(\omega t + \phi)} \\ &= Z(\omega)e^{i\phi} \cdot x_0 \end{aligned} \quad (2.22)$$

ie. at the same frequency  $\omega$ , but with different magnitude  $Z$  and phase  $\phi$ . Eqn (2.22) may be written as ;

$$z = H(\omega)x_0 \quad (2.23)$$

where  $H(\omega)$  is a complex vector of frequency response functions.

Since  $\dot{x}_0 = i\omega x_0$ ,  $\dot{z} = i\omega z$ , and  $\ddot{z} = -\omega^2 z$ , Eqn (2.11) can be rewritten ;

$$\left(-\omega^2 MXDD + i\omega MXD + MX\right) z = (i\omega MUD + MU) x_0 \quad (2.24)$$

Comparison of Eqns (2.23) and (2.24) shows the frequency response equation to be :

$$H(\omega) = \frac{(i\omega MUD + MU)}{(-\omega^2 MXDD + i\omega MXD + MX)} \quad (2.25)$$

Since the random road profile is regarded as a continuous spectrum of sinewaves, the response at a single wavenumber is of little use. The response to a road profile having a spectral density described by Eqn (2.5) must now be considered.

## 2.4.2 Response to Spectral Density Ground Inputs

Once the frequency response function has been obtained it is possible, with knowledge of the amplitude spectral density of the input, to obtain spectral densities for the output variables of interest. From Eqn (2.23) it follows that

the output amplitude squared spectral density matrix ( $S_z$ ) is related to the single input spectral density ( $S_{x_0}$ ) by :

$$S_z = H^2 S_{x_0} \quad (2.26)$$

Individual responses can be expressed in terms of root mean square values ( $\sigma_z$ ) by integrating the output spectral density function ( $S_z$ ) over the frequency range of interest :

$$\sigma_z = \sqrt{\int_{\omega_1}^{\omega_2} S_z(\omega) d\omega} \quad (2.27)$$

Throughout the work here, the upper frequency limit ( $\omega_2$ ) is set at 94.25 rad/s (15Hz), recognising that above this frequency the problem will be of a structural nature rather than ride comfort. The lower limit ( $\omega_1$ ) is set at 0.94 rad/s (0.15Hz), since there is no requirement of the suspension system to filter out very long wavelengths and dynamic effects at such wavelengths will, in any case, be negligible.

Since the output spectral density is equal to the input spectral density multiplied by the frequency response, from Eqn (2.5) it follows that the rms values are proportional to  $\sqrt{G}$  and  $\sqrt{V^{p-1}}$ , allowing scaling of the values between different operating conditions. However, this is not the case if the half vehicle, bounce/pitch model is used, since the presence of a wheelbase time delay means that the rms values are no longer directly proportional to  $\sqrt{V^{p-1}}$ .

## 2.5 Non Linear Analysis

The bulk of the work here will concentrate on systems which use time varying coefficient controllable dampers. The forces generated across such a damper depend on the control strategy, but in general are a function of displacements, velocities, and time. Eqn (2.11) remains valid but must now be solved numerically, using non-linear analysis to obtain time histories for the desired outputs.

The time varying forces are included in the equation using the vector of functions  $f$ , and the connection matrix  $MF$ . Time domain analysis also requires that the input to the system takes the form of a distance or time dependent ground profile. The input vector,  $x_0$ , will then depend on the profile, together with the vehicle speed and configuration (eg. number of axles). Profiles here are generated from amplitude squared spectral densities described by Eqn (2.2) and the procedure is outlined in Section 2.2. The time histories of the state variables, and any other desired output, are obtained from simulation over the profile. Processing into the frequency domain then yields power spectral densities (psd's) and root mean square (rms) values as required. The length of simulation and number of sample points required are determined after an examination of psd's obtained with various sampling frequencies. At 20 m/s, an adequate resolution is achieved with 2048 sample points and a profile length of 340m. In Chapter 9, to maintain the same sampling frequency, the length of run is adjusted to suit the three different vehicle speeds.

## 2.6 Performance Criteria

The performance of each suspension system can be assessed quantitatively in terms of three parameters. These are chosen to represent each of the conflicting requirements of the suspension, and have been widely used and accepted as a measure of system performance (Sharp and Hassan [1986]) :

- Discomfort (ACC)

This provides a single number index of system performance in terms of ride quality. It can be defined as the rms value of frequency weighted vertical body acceleration. The weighting function is applied to the multifrequency acceleration spectrum prior to integration, and reflects the

fact that the human body is most sensitive to vertical vibrations in the frequency range 4 to 8Hz. Weightings used here are based on the ISO document 2631 Part 1 [1985] and are described in Table 2.2.

Frequency (Hz)	Weighting Factor
less than 1	1/4
1 to 4	1/4 × freq.
4 to 8	1
above 8	64/freq <sup>2</sup>

Table 2.2: ISO weighting function for vertical acceleration

- Suspension Working Space (SWS)

This parameter is defined as the rms value of wheel to body displacement ( $z_1 - z_2$ ) and measures the variation of the displacement about its static position. Since the excitation of the system by the road surface is considered random and Gaussian in nature, it follows that the responses, at least for a linear system, will also be Gaussian and can be described using a normal distribution. Applying this argument to suspension working space, it can be said that wheel to body displacement will remain within  $\pm$ SWS,  $\pm$ 2SWS, and  $\pm$ 3SWS of the static position for 68.3%, 95.4%, and 99.7% of the time respectively. From the rms value therefore, it is possible to determine the necessary dynamic suspension travel for the vehicle when traversing any particular road. For example, suppose a vehicle has an allowable suspension travel of 0.12m. If the SWS value for this vehicle when travelling over a minor road is 0.02m, then the dynamic suspension

displacement from static position would be within  $\pm 0.06\text{m}$  for 99.7% of the time. In the remaining 0.3% the end stops will come into contact.

- Tyre Loading Parameter (DTL)

Defined as the rms value of tyre load variations from the static value. DTL can be considered as a measure of road holding ability, since a variation in the tyre load results in a varying contact length and consequently a net reduction in side or braking force.

These outputs are functions of the state variables ( $z$ ), their derivatives and the input ( $x_0$ ) and as such do not lend themselves to frequency response analysis using Eqn (2.26). In general they may be combined to give  $ny$  output variables using the following transformation :

$$Y = TXz + TXD\dot{z} + TXDD\ddot{z} + TUx_0 + TUD\dot{x}_0 \quad (2.28)$$

where the dimension of  $Y$  is  $ny$  and the matrices  $TX$ ,  $TXD$ ,  $TXDD$  are  $(ny, nz)$  and  $TU$ ,  $TUD$  are  $(ny, nx_0)$ . For the three outputs here ( $ny = 3$ ) and using the quarter car model ( $nz = 2$ ) we have ;

$$TXDD = \begin{bmatrix} 1 & 0 \\ 0 & 0 \\ 0 & 0 \end{bmatrix}, TXD = \begin{bmatrix} 0 & 0 \\ 1 & -1 \\ -1 & 0 \end{bmatrix}, TU = \begin{bmatrix} 0 \\ 0 \\ 1 \end{bmatrix} \quad (2.29)$$

and  $TXD$ ,  $TUD$  are null matrices.

## 2.7 VDAS

Throughout the project, all linear and non-linear analyses has been performed on a VAX 8600 mainframe computer, using the Vehicle Dynamics Analysis Software package (VDAS) developed at the University of Leeds by Horton [1991].

The models are supplied to the software using equations of the form (2.11) and input can be user supplied, or generated within the package. Outputs, in a vector described by Eqn (2.28), take the form of frequency responses, output spectral densities, or time histories. The matrix elements of Eqn (2.11) and Eqn (2.28) are supplied to VDAS using a model (MDL) file and the vehicle data, which can be altered interactively, is supplied in a parameter (PAR) file. If necessary the time dependent behaviour of suspension elements can be supplied in a simulation (SIM) file. VDAS is also used for the generation of control laws using linear optimal control theory (see Chapter 4). In addition to the main analysis package, several subsidiary programs exist, of which the following have been used here ;

- PROFILE - generates input profiles which are a function of time or distance (see Section 2.2).
- ACCDTL - gives the relationship between ACC and DTL for a given value of SWS (see Section 3.3).

## 2.8 Concluding Remarks

This chapter describes the basic vehicle ride modelling techniques which are to be used extensively throughout the rest of the thesis. First, the idea of representing the road surface using a single equation describing its amplitude spectral density is introduced, together with the subsequent technique for generating a road profile. Then the reduction of a 7 d.o.f “full” vehicle model to a 2 d.o.f quarter vehicle model is justified and, using Newtonian methods, the equations of motion for the latter are formulated. The linear and non-linear analysis procedures are reviewed and finally the criteria used in performance comparisons are defined.

# Chapter 3

## Passive System

### 3.1 Introduction

Despite the fact that the first generation of “intelligent” systems are beginning to appear on the market, the passive suspension is still to be found on the majority of current production vehicles. The system is one comprising only of springs and dampers which are fixed rate and cannot be changed by external signals. There is no external energy source and therefore the system can only store, restore, and dissipate energy. The fundamental behaviour and performance of passive systems has been analysed by several investigators including Ryba [1973], [1974 a], [1974 b] and Sharp and Hassan [1984]. In general, their conclusions emphasise the fact that, due to the conflicting requirements of the suspension system, any choice of fixed spring or damper rate by the vehicle designer is a compromise. Performance improvements over a well designed passive system must therefore be achieved using some form of controllable suspension element.

The aim of this chapter is to quantify the ride behaviour of the passive suspension. The behaviour of more advanced systems can then be compared against this “baseline” performance in an effort to quantify potential improvements.

## 3.2 Analysis

In line with previous work, for example by Sharp and Hassan [1984], the analysis is carried out using the quarter car model, which is justified in Section 2.3.1. The passive version of the model is shown in Fig 2.2(c) and its equations of motion are formulated as an example in Section 2.3.2. The vehicle data used throughout the quarter car analysis is shown in Table 3.1, and refers to the rear suspension of a current production saloon car.

$M_b$	0.3175	Body mass (tonne)
$M_w$	0.0454	Wheel mass (tonne)
$K_s$	22	Spring stiffness (kN/m)
$C_s$	1.5	Damping coefficient (kNs/m)
$K_t$	192	Tyre vertical stiffness (kN/m)

Table 3.1: Quarter vehicle data

It is assumed that the designer can only exercise control over the spring stiffness  $K_s$  and the damping coefficient  $C_s$ , both of which are considered as linear time-invariant parameters. This may not be the case in practice and it is more likely that the passive damper has an asymmetric force/velocity relationship, with the ratio of compression to rebound damping being approximately 1:2. For the vehicle described by Table 3.1, the actual damping characteristic and its linear equivalent are shown in Fig 3.1. The linearised characteristic has a damping coefficient of 1.5 kNs/m and is obtained by considering the energy dissipation of the damper. Both cases must dissipate the same energy and therefore the areas under the linear and non-linear force/velocity curves must be equal.

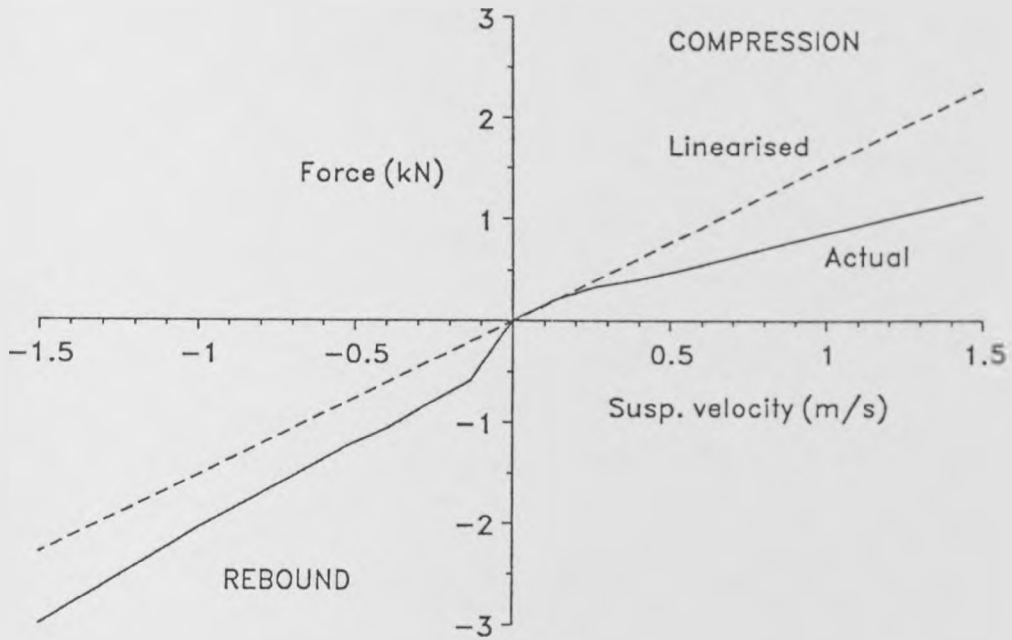


Figure 3.1: Linearisation of damping characteristics

Although the linearised characteristic appears to be a considerable simplification, its use is justified by the results in Table 3.2, where the effect on predicted root mean square (rms) values is shown to be small.

	ACC ( $\text{m/s}^2$ )	SWS (m)	DTL (kN)
Actual	2.18	0.0290	1.30
Linearised	2.20	0.0289	1.29

Table 3.2: Effect of damper linearisation on rms values

The procedures for linear analysis are outlined in Section 2.4 and are used to obtain rms values and power spectral densities (psd's) for the outputs of interest. The three main outputs of interest are represented by the performance criteria ACC, SWS, and DTL, defined in Section 2.6, which provide a measure of system performance in terms of ride comfort, suspension travel, and road holding ability

respectively. Analysis is performed using the VDAS software package which requires the equations of motion to be supplied in matrix form. Section 2.3.2 introduces a general form of matrix equation (2.11), and the coefficient matrices  $MXDD_p$ ,  $MXD_p$ ,  $MX_p$  and  $MU_p$  for the passive case are determined as an example. VDAS also requires the output variables to be written in matrix form, using the transformation outlined in Section 2.6. Eqn (2.28) describes the general form, whilst Eqn (2.29) defines the output matrices required to obtain ACC, SWS and DTL. The frequency range of interest when calculating rms values is taken as 0.15Hz to 15Hz. The reasoning behind this choice has been previously explained in Section 2.4.

The road surface input used throughout this chapter is assumed to have a psd which can be described by Eqn (2.5). The roughness coefficient ( $G$ ) and exponent ( $p$ ) are taken to be  $5 \times 10^{-6}$  and  $-2.5$  respectively, and the forward vehicle speed is assumed to be a constant 20m/s. Eqn (2.5) then becomes :

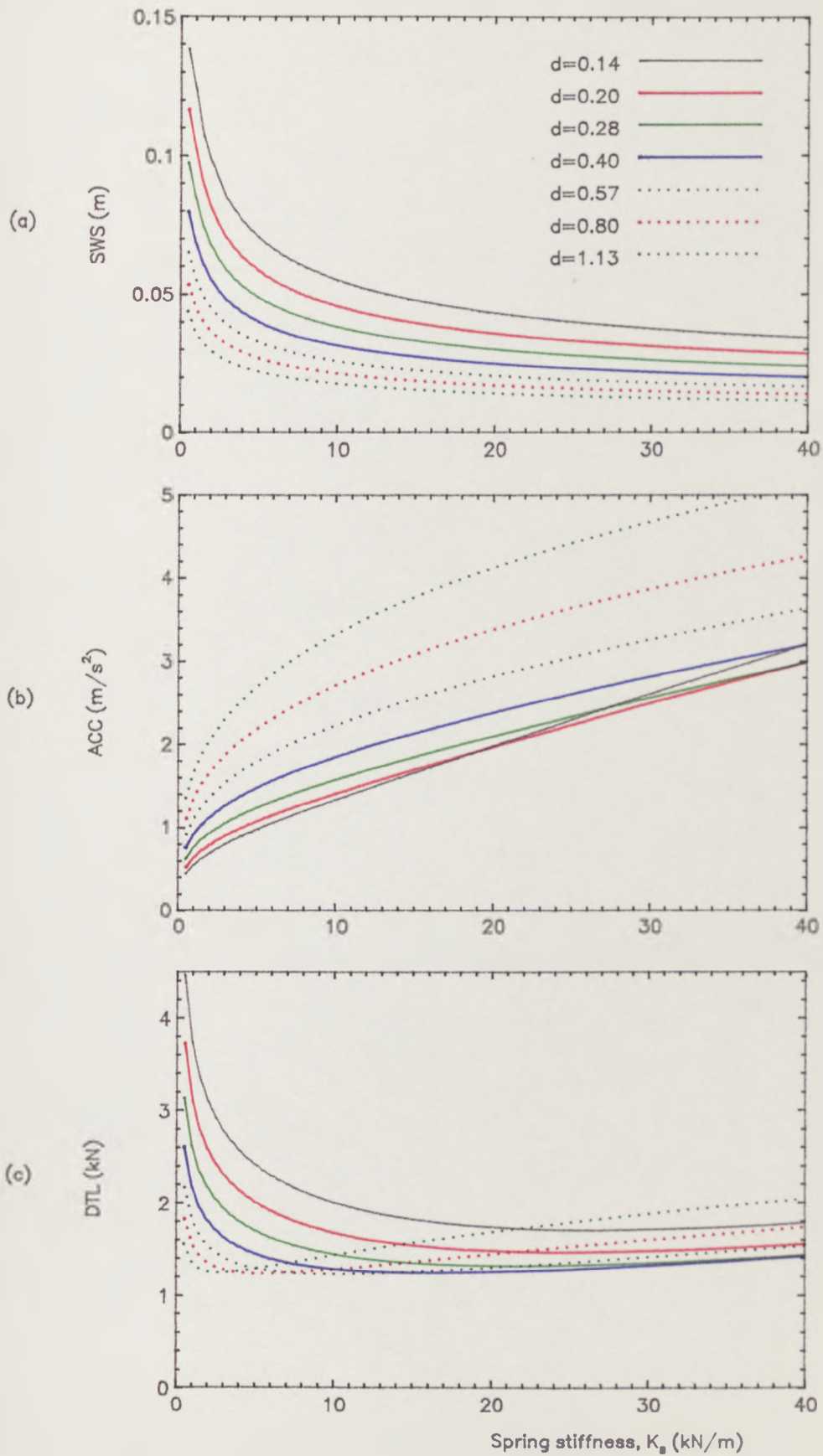
$$S_{x_0}(\Omega) = \frac{(5 \times 10^{-6}).20^{1.5}}{\Omega^{2.5}} \quad (3.1)$$

### 3.3 Results

The rms values of weighted body acceleration, suspension working space and dynamic tyre load are calculated over a range of spring and damping rates. Damping is expressed here in terms of parameter ( $d$ ), which is defined by ;

$$d = \frac{C_s}{2\sqrt{K_s M_b}} \quad (3.2)$$

and varied between 0.14 and 1.13 using a geometric progression in the style of Sharp and Hassan [1986 b]. The resulting sets of curves for the three performance criteria (SWS, ACC and DTL) are shown in Figs 3.2(a),(b) and (c) respectively.

Figure 3.2: Effect of varying spring stiffness ( $K_s$ ) and damping parameter ( $d$ )

Although all the required information is present in these graphs, an insight into the relative performance of competing systems, ie./ combinations of  $K_s$  and  $d$ , is not readily obtained. A good starting point for such comparisons is the equal workspace contour. This method has been used extensively by, for example, Sharp and Hassan [1986 b], Sharp and Crolla [1987], and Crolla and Aboul Nour [1988]. It is based on the fact that the suspension designer will only have a limited amount of available suspension travel. The vehicle studied here (see Table 3.1) has design values for  $K_s$  and  $d$  of 22kN/m and 0.28 respectively, together with a total available dynamic working space of 0.22m ( $\pm 0.11$ m from static position). From Fig 3.2(a), the rms value of SWS for such a system operating in conditions described by Eqn (3.1) is approximately 0.029m. Using the argument that the suspension working space response can be described by a normal distribution (Section 2.6), it follows that the suspension displacement for this system, at these conditions, will be within  $\pm 0.087$ m ( $\pm 3$ SWS) for 99.7% of the time. For these conditions therefore the workspace usage is within the available limits, only occasional bump and rebound stop contact occurs, and the linear analysis remains valid.

An equal workspace contour is shown in Fig 3.3 . Each point on the curve represents a different combination of stiffness ( $K_s$ ) and damping parameter ( $d$ ), and gives their relative performance in terms of ride comfort and road holding for a suspension working space of 0.029m. The points are generated as follows. Various combinations of stiffness and damping with an rms SWS value of 0.029m can be read off Fig 3.2(a). Once these systems have been established, their performance in terms of ACC and DTL can be readily obtained from Figs 3.2(b) and (c) respectively. In practice this procedure can be carried out using ACCDTL, a subsidiary program of VDAS, which generates values of ACC and DTL for a given SWS.

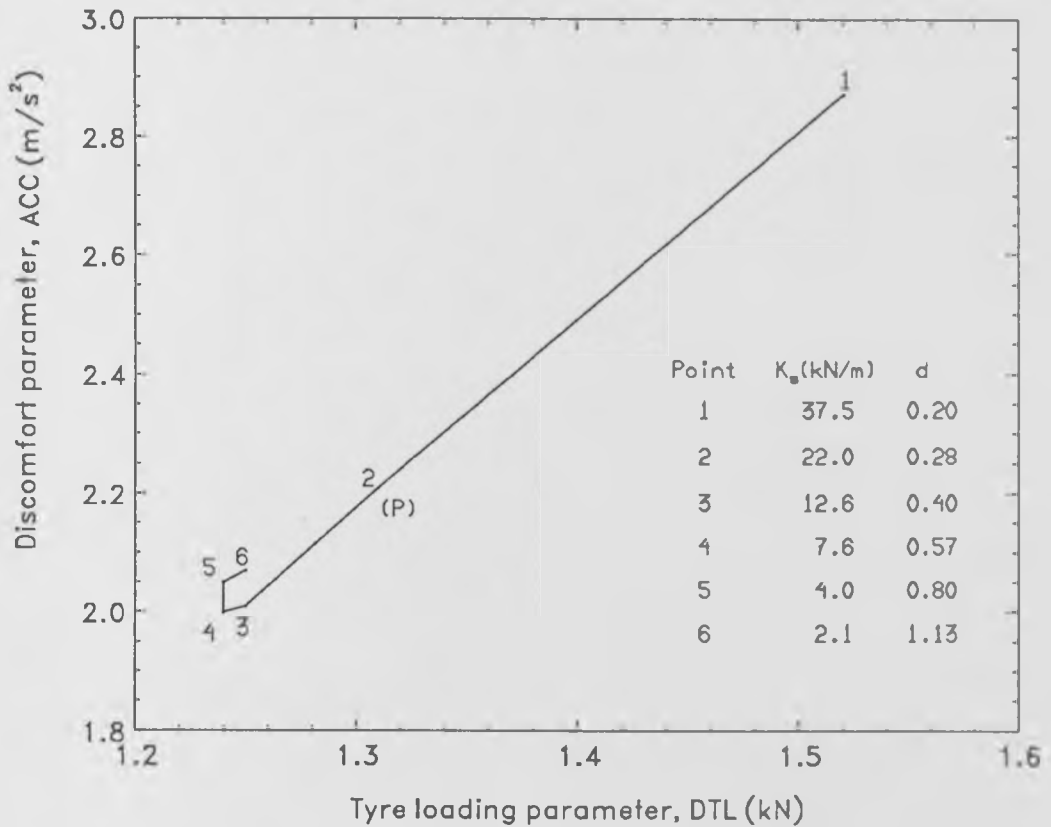


Figure 3.3: Comparison of passive systems using an equal workspace contour

Once the equal SWS contour is obtained, further analysis may be carried out by examining the psd's relating to selected points of interest. The psd's of ISO weighted body acceleration and dynamic tyre load for points 1 to 6 in Fig 3.3 are shown in Fig 3.4(a) and (b) respectively.

In Fig 3.5 the idea of the equal SWS contour is extended to include a family of such curves. Also shown are lines of constant stiffness and damping, creating a matrix of possible systems. The ranges of damping ratio (0.15 to 0.40) and stiffness (10kN/m to 30kN/m) are this time narrowed to concentrate on parameter values which could feasibly be found on production vehicles. Therefore, given the vehicle masses and tyre stiffness, Fig 3.5 reveals the performance of any stiffness/damping combination over a rough minor road at 20m/s. Point P (Fig 3.3 and Fig 3.5) represents the performance of the baseline production vehicle described in Table 3.1 ( $K_s=22\text{kN/m}$ ,  $d=0.28$ ).

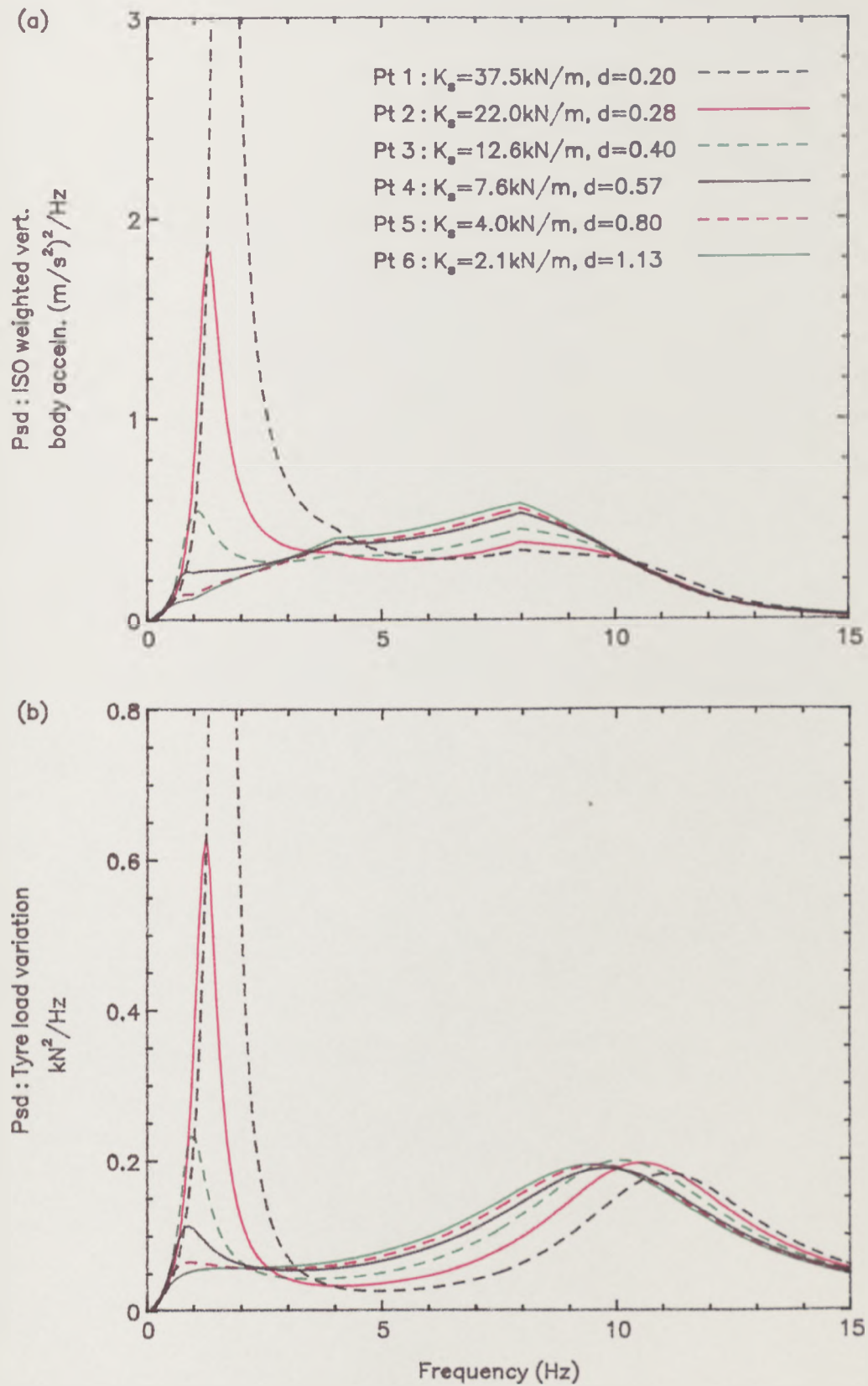


Figure 3.4: PsD's of ISO weighted vertical body acceleration and dynamic tyre load for selected passive systems

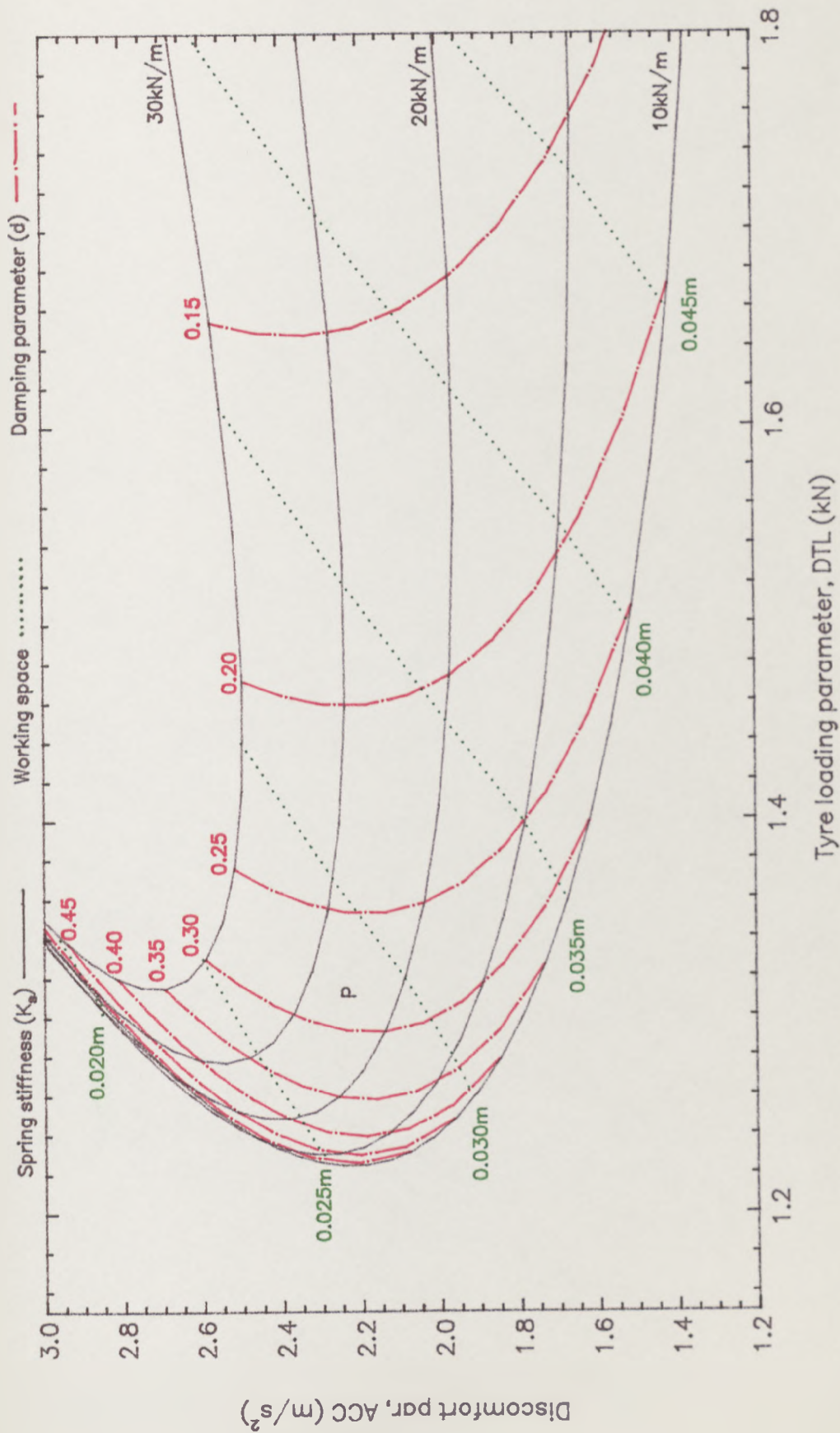


Figure 3.5: Performance envelope of the passive system, showing lines of equal suspension stiffness, damping and working space.

### 3.4 Discussion of Results

The effect of varying the stiffness and damping of the passive system has been well established by amongst others Hassan [1986] and Chalasani [1986 a] [1986 b], and can be clearly seen in Fig 3.2(a),(b) and (c). The best ride comfort is achieved with the softest spring and very light damping. However, any improvements gained by employing such a system are always at the expense of suspension working space. The best performance in terms of dynamic tyre load is achieved by systems having spring stiffnesses between 15kN/m and 20kN/m and a damping parameter of around 0.5.

The three performance criteria can be effectively reduced to two by recognising that in practice the usage of workspace must be limited. The resulting equal workspace contour (Fig 3.3) reveals the performance, in terms of ACC and DTL, once this restriction has been imposed. The optimum passive systems are clearly seen (points 3, 4 and 5) and have spring rates between 4kN/m and 12kN/m and damping parameters between 0.4 and 0.8 . The performance improvements as the system approaches optimum can also be seen in Fig 3.4(a) and (b), where they appear as a reduction in the psd resonance peaks for both body acceleration and tyre load variation.

The final choice of system is subject to further practical considerations. First of all, the spring stiffness must be high enough to support changes in static loads without excessive deflection. Secondly, attitude changes during cornering may be too great with the softer systems, and result in deterioration of vehicle handling and/or subjective objections to manoeuvring behaviour. Consequently, the best performing systems in Fig 3.3 may be impractical due to their low stiffness, and the vehicle designer has to select a system which is a compromise in terms of its ride and handling performance. The problem of the design conflict can be eased by employing a self-levelling system, as used by Citroen for

example. The advantage of this system is that none of the available working space is used up by changes in the static loading condition. This allows softer springs to be used, giving improved ride comfort over the conventional passive system with the same available workspace. However, unless the levelling system can also be used to keep the vehicle level during manoeuvring, the attitude changes will remain a problem.

The passive system (P) is shown within the matrix of possible passive systems in Fig 3.5, where its performance is compared against that of systems utilising different workspaces, and lies approximately in the centre of the performance envelope. In general, stiffer more heavily damped sports cars will lie in the upper left-hand region of this performance space, while softer lightly damped “luxury” vehicles lie towards the lower right-hand region.

At this stage, it must be remembered that any suspension must operate over a range of road surface roughnesses and vehicle speeds. System P is an effective design for the input used so far ( $G = 5 \times 10^{-6}$ ,  $V=20\text{m/s}$ ) but may not be ideal under different conditions. The performance of the fixed parameter system is now compared with that of a system which is able to adapt its stiffness and damping to suit different running conditions. Since increasing road surface roughness and vehicle speed have a similar scaling effect on rms values (Section 2.4.2), it is only necessary to vary one or the other to obtain a range of conditions. Here, vehicle speed is varied ( $V=10, 20$  and  $30\text{m/s}$ ) and the road roughness remains constant. Table 3.3 compares the performance of passive system P with systems which are purpose designed for each condition. These best stiffness/damping combinations are selected using equal workspace contours, similar to Fig 3.3, for each condition. A commercial implementation of the adaptive strategy would require a controller to switch the springs and dampers to hard during manoeuvring.

Speed	Passive			Adaptive		
	ACC (m/s <sup>2</sup> )	SWS (m)	DTL (kN)	ACC (m/s <sup>2</sup> )	SWS (m)	DTL (kN)
10m/s	1.38	0.017	0.78	0.83	0.029	1.06
20m/s	2.20	0.029	1.31	1.99	0.029	1.24
30m/s	2.97	0.039	1.78	3.61	0.029	1.72

Table 3.3: Comparison of Passive and Adaptive Systems

At 10m/s, the passive system only uses a fraction of the available working space and consequently its ride performance is much worse than the adaptive. The softer, lightly damped adaptive system shows some increase in rms dynamic tyre load, although for straight running at low speeds this is probably not a practical problem. At 20m/s, system P is at design conditions and any adaptive performance gains are achieved by virtue of the fact that a softer spring setting is available. This allows a selection of spring and damper rates which is nearer to the optimum combination seen in the equal workspace contour (Fig 3.3). If the speed is increased to 30m/s the passive system has a demand for working space which is greater than is available, resulting in frequent bump and rebound stop contact. In this case the linear calculations are strictly no longer accurate. The effect of hitting the stops is equivalent to increasing the spring stiffness ( $K_s$ ) and, since  $d = C/2\sqrt{K_s M_b}$ , reducing the damping parameter ( $d$ ). The equivalent linear system is therefore stiff and lightly damped and its performance will in any case be poor in comparison with the adaptive system.

The main point to emerge from this analysis is that if a suspension with fixed working space is to perform well over a range of conditions, it must have adap-

tive elements of some kind. The changes in spring and/or damping rate can generally be relatively slow as the system adapts to the new surface, although from a handling aspect, there should be an immediate return to stiff settings during cornering, braking, and accelerating manoeuvres. Adaptive systems have been commercially available for some time and, although variable springs and dampers have been employed in some systems eg. Mitsubishi (Mizuguchi *et al* [1984]) and Citroen [1989], they usually take the form of adjustable rate dampers with conventional springs eg. Toyota (Yokoya *et al* [1984]) or Armstrong (Hine and Pearce [1988]). The Armstrong system, employing a three position damper and switching according to a strategy based on suspension displacement and vehicle speed, is described further in Chapter 5 and compared against other systems over a range of conditions in Chapter 9.

### 3.5 Concluding Remarks

This chapter presents a brief performance analysis of the passive suspension using the quarter vehicle model. The main aim is to quantify the ride behaviour of the system and provide a yardstick against which other, more advanced, systems can be compared. In establishing this a number of results are generated, the conclusions drawn being similar to those given by several other workers including Ryba [1974 a] and Sharp and Hassan [1984] :

1. Suspensions with low spring stiffness and light damping provide the best performance in terms of ride comfort. Unfortunately, such systems also require large suspension working spaces.
2. For a given running condition and suspension working space, the optimum passive suspensions in terms of body acceleration and road holding can be identified using an equal SWS contour. However, from a handling point

of view, the suspension must also be able to prevent excessive attitude changes during manoeuvring. The result is a further design conflict, with the best performing systems on the equal workspace contours becoming impractical due to their low stiffness. The final selection of stiffness and damping must therefore be a compromise between ride and handling performance.

3. If the performance of the passive suspension with fixed working space is to be improved over a range of running conditions ie. surfaces and speeds, it must have the ability to adapt between a number of discrete spring and damper settings.

The potential of a more advanced suspension which will overcome these design compromises and also adapt to the prevailing conditions is clear.

# Chapter 4

## Active System

### 4.1 Introduction

The fully active suspension system has been studied in detail by several workers in recent years eg. Thompson [1976], [1984], Chalasani [1986 a], [1986 b] and Sharp and Hassan [1986], and the potential performance improvements have been well established. The system is one in which the conventional spring and damper of the passive system are replaced with a hydraulic or pneumatic actuator which responds to a force demand signal. The demand signal, typically generated in a microprocessor on receipt of measured state variable information, is governed by a control law which is based, for example, on linear optimal control theory. A number of prototype vehicles fitted with fully active suspensions have been built and tested, most notably by Lotus (Wright and Williams [1984]). However, the added cost and complexity coupled with high energy costs has meant the system has yet to appear commercially.

Recently a number of vehicles which employ limited bandwidth actuators in conjunction with controllable dampers and conventional springs have become available, eg. the Toyota Celica (Yokoya *et al* [1990]) and the Nissan Infiniti Q45 (Aoyama *et al* [1990]). Although these systems are marketed as “full active” suspensions they are probably more correctly defined as slow active systems (Sharp and Crolla [1987]).

The purpose of this work on the active system is twofold. First, to describe

briefly the various techniques, based on linear optimal control theory, which are used to derive control laws for both the full and limited state feedback active systems. These techniques will also later be used in Chapter 5 to obtain control laws for the continuously variable (semi-active) damper system. Secondly, results will enable the predicted behaviour of the active system over a given road surface to be quantified. This chapter concentrates on an ideal active system ie. one in which actuator response times and force limitations are ignored. The results therefore, represent a “best possible” suspension performance for the given conditions. This performance, together with the passive performance described in Chapter 3, provide notional limits against which the results of the more practical controllable damper systems can be assessed.

## 4.2 Equations of Motion

A quarter car model of the active system is shown in Fig 4.1 and the equations of motion can be written as follows ;

$$M_w \ddot{z}_1 = K_t(x_0 - z_1) - u \quad (4.1)$$

$$M_b \ddot{z}_2 = u \quad (4.2)$$

where  $u$  is the control force generated by the actuator. Eqns (4.1) and (4.2) can then be rearranged and written in the general matrix form of Eqn (2.11);

$$MXDD\ddot{z} + MXD\dot{z} + MXz = MUx_0 + MUDx_0' + MFf$$

Using the suffix  $a$  to denote the active system and letting the control force  $u$  become an element in the vector of functions  $f$ , the coefficient matrices can be written :

$$MXDD_a = \begin{bmatrix} M_w & 0 \\ 0 & M_b \end{bmatrix}, MX_a = \begin{bmatrix} K_t & 0 \\ 0 & 0 \end{bmatrix}$$

$$MU_a = \begin{bmatrix} K_t \\ 0 \end{bmatrix}, MF_a = \begin{bmatrix} -1 \\ 1 \end{bmatrix} \quad (4.3)$$

The matrices  $MXD_a$  and  $MUD_a$  are both zero.

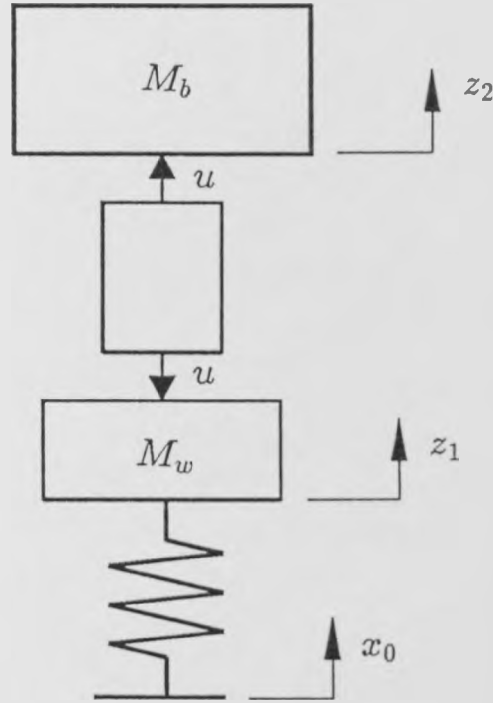


Figure 4.1: Quarter vehicle model of the active system.

### 4.3 System Optimization

The derivation of a control law which optimises system performance is an essential part of the design of any advanced suspension. The active control laws discussed here, and also the laws governing the continuously variable damper (semi-active) system in Chapter 5, are derived using techniques which are based on linear optimal control theory (see for example Van de Vegte [1990]). These techniques have been used extensively by several workers including Thompson [1976], [1984], Hac [1985] and Crolla and Aboul-Nour [1989]. They are discussed in detail by Wilson *et al* [1986], and the principles are outlined here.

Using the transformation outlined in Section 2.3.2, the equations of motion can be written in first order matrix form of Eqn (2.19) ;

$$\dot{x} = Ax + Bu + B_1x_0$$

where  $A$ ,  $B$  and  $B_1$  are related to  $MXDD_a$ ,  $MX_a$ ,  $MF_a$  and  $MU_a$  by :

$$\begin{aligned} A &= \begin{bmatrix} 0 & I \\ -MXDD_a^{-1}MX_a & 0 \end{bmatrix}, B = \begin{bmatrix} 0 \\ MXDD_a^{-1}MF_a \end{bmatrix} \\ B_1 &= \begin{bmatrix} 0 \\ MXDD_a^{-1}MU_a \end{bmatrix} \end{aligned} \quad (4.4)$$

If a practical solution is to be obtained, optimal control theory requires that, rather than use an equation of the form (3.1), the disturbance input is modelled as the output of a linear system driven by white noise. This has generally taken one of two forms :

1. Integrated white noise.

The disturbance input ( $x_0$ ) can be described by the equation ;

$$\dot{x}_0 = w \quad (4.5)$$

where  $w$  is a zero mean white noise process. This implies that the road surface must have an amplitude spectral density of the form ;

$$S_{x_0}(n) = \frac{G}{n^2} \quad (4.6)$$

with  $G$  in this case representing the intensity of the white noise.

2. Filtered white noise.

This alternative and more realistic description has been used by several workers, eg. Hac [1985] and Wilson *et al* [1986]. Here a filtered white noise

signal is used and the input is a solution to the first order differential equation ;

$$\dot{x}_0 + 2\pi V\alpha x_0 = w \quad (4.7)$$

where  $\alpha$  is the filter coefficient and  $V$  is the vehicle speed. The amplitude spectral density is now bounded and given by an equation of the form :

$$S_{x_0}(n) = \frac{G}{n^2 + \alpha^2} \quad (4.8)$$

Eqn (4.8) is a more accurate representation of measured spectral densities, since the constant  $\alpha$ , given a value of 0.005 in line with the cut-off wavenumber  $n_{co}$ , ensures that the displacements remain finite at vanishingly small wavenumbers.

Combining Eqn (2.19) with Eqn (4.5) or (4.7) gives a new state equation in terms of an augmented vector  $x_a = [x \ x_0]^T$  ;

$$\dot{x}_a = A_a x_a + B_a u + B_{aw} w \quad (4.9)$$

where

$$A_a = \begin{bmatrix} A & B_1 \\ 0 & f_w \end{bmatrix}, B_a = \begin{bmatrix} B \\ 0 \end{bmatrix}, B_{aw} = \begin{bmatrix} 0 \\ I \end{bmatrix} \quad (4.10)$$

and  $f_w = 0$  for the integrated white noise case or  $-2\pi V\alpha$  if the input is taken to be filtered white noise.

The optimization goal is to minimize the vertical body acceleration and dynamic tyre load, whilst at the same time maintain a suspension deflection which is within the allowable limits. A performance index, defined by the weighted sum of the integral square values for these outputs of interest, can be written as follows;

$$J = \frac{1}{2} \int_0^\infty [q_1(x_0 - x_1)^2 + q_2(x_1 - x_2)^2 + \rho u^2] dt \quad (4.11)$$

where  $q_1$ ,  $q_2$ , and  $\rho$  are weighting constants and represent the importance attached to each element in the performance index. Here it is assumed that the actuator is the only suspension element. Therefore, the actuator force ( $u$ ) is directly proportional to the vertical body acceleration and can be considered a measure of ride comfort. The quantities in the performance index, known as the output variables, are related to the state variables by :

$$y = Dx \quad (4.12)$$

The connection matrix  $D$  in this case is defined by :

$$D = \begin{bmatrix} 1 & -1 & 0 & 0 & 0 \\ 0 & 1 & -1 & 0 & 0 \end{bmatrix} \quad (4.13)$$

Eqn (4.11) can then be rearranged to a general form ;

$$J = \int_0^{\infty} \left[ y^T(t) Q y(t) + u^T(t) R u(t) \right] dt \quad (4.14)$$

where  $Q(nq, nq)$  and  $R(nu, nu)$  are matrices containing the weighting constants.

The determination of the control force  $u(t)$  for the system described by Eqn (4.9) which minimizes the performance index (Eqn (4.14)) is called the stochastic optimal linear regulator problem. When applied to the vehicle problem, two separate solutions exist; full state feedback available, and the more practical limited state feedback available.

### 4.3.1 Full State Feedback Case

A solution to the optimal linear regulator problem for a system having full state feedback and an integrated white noise input (Eqn (4.6)) is described in detail by Thompson [1976]. Briefly, the optimal force  $u(t)$  is given by ;

$$u = -Kx \quad (4.15)$$

where the matrix of feedback gains  $K$  is defined by ;

$$K = B_a^T P R^{-1} \quad (4.16)$$

and  $P$  is the unique solution to the algebraic Ricatti equation ;

$$A_a^T P + P A_a + D^T Q D - P B_a B_a^T P R^{-1} = 0 \quad (4.17)$$

under the condition that the system is completely :

1. stabilizable ie. any uncontrollable modes are stable.
2. detectable ie. any unstable modes are observable.

These properties, defined by the pairs of matrices  $(A_a, B_a)$  and  $(A_a, D)$  respectively, are discussed in greater detail by Wilson *et al* [1986]. If the input is assumed to be integrated white noise, since Eqn (4.6) is unbounded, it is clear that condition (1) is not true. However, the requirement is satisfied by Thompson through a well known coordinate transformation :

The variables  $x_a$  in Eqn (4.9) are transformed into new variables  $\hat{x}$  by ;

$$\hat{x} = S x_a \quad (4.18)$$

where

$$S = \begin{bmatrix} 1 & 0 & 0 & 0 & 0 \\ -1 & 1 & 0 & 0 & 0 \\ -1 & 0 & 1 & 0 & 0 \\ 0 & 0 & 0 & 1 & 0 \\ 0 & 0 & 0 & 0 & 1 \end{bmatrix} \quad (4.19)$$

or

$$\hat{x}_0 = x_0, \quad \hat{x}_1 = x_1 - x_0, \quad \hat{x}_2 = x_2 - x_0, \quad \hat{x}_3 = x_3, \quad \hat{x}_4 = x_4 \quad (4.20)$$

The state equations then become ;

$$\dot{\hat{x}} = SA_aS^{-1}\hat{x} + SB_a u + SB_{aw}w \quad (4.21)$$

$$y = DS^{-1}\hat{x} \quad (4.22)$$

where

$$SA_aS^{-1} = \begin{bmatrix} 0 & 0 & 0 & 0 & 0 \\ 0 & 0 & 0 & 1 & 0 \\ 0 & 0 & 0 & 0 & 1 \\ 0 & -\frac{K_t}{M_w} & 0 & 0 & 0 \\ 0 & 0 & 0 & 0 & 0 \end{bmatrix}, SB_a = \begin{bmatrix} 0 \\ 0 \\ 0 \\ -\frac{1}{M_w} \\ \frac{1}{M_b} \end{bmatrix}$$

$$DS^{-1} = \begin{bmatrix} 0 & 1 & 0 & 0 & 0 \\ 0 & -1 & 1 & 0 & 0 \end{bmatrix} \quad (4.23)$$

The coordinate transformation results in the uncontrollable disturbance input becoming also unobservable ie. it no longer appears in the performance index. A controllable, and therefore stabilizable, subspace now exists in the lower partitions of matrices  $SA_aS^{-1}$ ,  $SB_a$  and  $DS^{-1}$  and can therefore be solved using the Ricatti equation (4.17). The optimal control law now depends only on  $\hat{x}_1$ ,  $\hat{x}_2$ ,  $\hat{x}_3$  and  $\hat{x}_4$  and is written :

$$u = -K\hat{x} = -[K_1\hat{x}_1 + K_2\hat{x}_2 + K_3\hat{x}_3 + K_4\hat{x}_4] \quad (4.24)$$

In terms of the original coordinates the control law can be rearranged and becomes :

$$u = -[K_1(x_1 - x_2) + K_3(x_3 - x_4) + (K_1 + K_2)(x_2 - x_0) + (K_3 + K_4)x_4] \quad (4.25)$$

The optimal control force  $u(t)$  is calculated using Eqn (4.25) providing all state variables are available for feedback. The value of gains  $K_1$  to  $K_4$  depends on the solution to the Ricatti equation, which in turn depends on the selected values of  $q_1$ ,  $q_2$  and  $\rho$  in the performance index. A different gain matrix  $K$  exists for each combination of weighting constants.

### 4.3.2 Limited State Feedback Case

The control law described in the last section requires the measurement of full state information in some form. This includes the body height above the road surface ( $x_2 - x_0$ ), requiring the use of a body mounted height sensor. The cost implications and practical difficulties associated with such a sensor are great, and the importance of a control law which does not require availability of all the state variables becomes clear.

Thompson [1984] defines a sub-optimal control law in which, rather than measuring the body height relative to the road ( $x_2 - x_0$ ), the displacement relative to the wheel ( $x_2 - x_1$ ) is measured instead. Substituting this in Eqn (4.25) we have :

$$u = - [K_1(x_1 - x_2) + K_3(x_3 - x_4) + (K_1 + K_2)(x_2 - x_1) + (K_3 + K_4)x_4] \quad (4.26)$$

The gain matrix  $K$  in this equation, however, is calculated assuming the measurement ( $x_2 - x_0$ ) is still available.

Further analysis, considering the case of general feedback possibilities, is carried out by Wilson *et al* [1986], and the control law is chosen to be of the form ;

$$u = -K_L M x \quad (4.27)$$

where the  $nm$  available measurements are defined by the matrix  $M$ .

The gain matrix  $K_L$  is this time of dimension  $(nm, nu)$ . For example, if the relative displacement ( $x_1 - x_2$ ), plus the absolute body and wheel velocities,  $x_3$  and  $x_4$ , are available for feedback, then ;

$$M = \begin{bmatrix} 0 & 1 & -1 & 0 & 0 \\ 0 & 0 & 0 & 1 & 0 \\ 0 & 0 & 0 & 0 & 1 \end{bmatrix} \quad (4.28)$$

and the control law becomes :

$$u = -[K_2(x_1 - x_2) + K_3x_3 + K_4x_4] \quad (4.29)$$

Once again the elements of the matrix  $K_L$  are required to minimise the performance index (4.14). However, the detectability condition ensuring the existence of a unique solution to the Ricatti equation is no longer applicable and further techniques are required to find  $K_L$ . The approach of Wilson and the one which shall be used throughout the rest of the work, is to use a gradient search routine. The basic steps are as follows :

1. Estimate initial values for feedback gains  $K_L$ . The gains obtained for the corresponding full state feedback case are often a reasonable first approximation.
2. Solve the following "Liapunov" equations for  $W_c$  and  $W_o$ .

$$\tilde{A}W_c + W_c\tilde{A}^T + V = 0 \quad (4.30)$$

$$\tilde{A}^TW_o + W_o\tilde{A} + D^TQD + M^TK^TRKM = 0 \quad (4.31)$$

where

$$\tilde{A} = A_a - B_aKM \quad (4.32)$$

3. Calculate the performance index ( $J$ ) and its gradient  $dJ/dK$  from :

$$J = \text{tr} [W_c(D^TQD + M^TK^TRKM)] \quad (4.33)$$

$$dJ/dK = 2 [RKMW_cM^T - B_a^TW_oW_cM^T] \quad (4.34)$$

4. Update  $K_L$  using a gradient search routine and repeat from step (2) until a satisfactory convergence is achieved.

Since the feedback can only affect the controllable modes of the system, it follows that, for the design to be stable any uncontrollable and/or unobservable modes must also be stable. The stability of the closed loop system is checked at each stage of the iteration by calculating the eigenvalues of the matrix  $\bar{A}$ . Eqns (4.30) to (4.34) assume a road surface description based on filtered white noise. Since the input  $x_0$  is bounded and neutrally stable (Eqn (4.8)) it is no longer necessary to prevent it from contributing to the performance index ( $J$ ). If the disturbance is taken to be integrated white noise the input becomes unbounded (Eqn (4.6)) and Thompsons transformation is once again required, the matrices  $A_a$ ,  $B_a$ ,  $D$  etc. becoming  $SA_aS^{-1}$ ,  $SB_a$ ,  $DS^{-1}$  etc. respectively.

It is worth noting that this procedure may also be used to generate gains for the full state feedback case. If the measurement matrix is defined as ;

$$M = \begin{bmatrix} -1 & 1 & 0 & 0 & 0 \\ -1 & 0 & 1 & 0 & 0 \\ 0 & 0 & 0 & 1 & 0 \\ 0 & 0 & 0 & 0 & 1 \end{bmatrix} \quad (4.35)$$

and substituted into Eqn (4.27), the control law becomes equivalent to Thompsons law requiring feedback of body-to-road displacement. This time, the gradient search routine generates four gains which are equal to the ones obtained from the solution of the Ricatti equation. Furthermore, if  $M$  is taken to be the identity matrix, the control law is again full state and described by ;

$$u = -[K_0x_0 + K_1x_1 + K_2x_2 + K_3x_3 + K_4x_4] \quad (4.36)$$

the extra gain  $K_0$  allowing the independent feedback of the absolute road surface height  $x_0$ .

Both techniques described here have been included in the VDAS software by Horton using an appropriate NAG library routine, EO4KCF, to perform the gradient search process.

## 4.4 Results

In contrast to the relatively straightforward passive system, with only spring stiffness and damping parameter as design parameters, the active quarter car has a control law in which a number of gains can be varied in response to changes in the three performance index weighting constants. Consequently a wide range of performance is possible and the analysis becomes more complex.

Using the techniques described in Section 4.2 the optimal gain vector  $K$  or  $K_L$  is calculated for a range of weighting constants  $\rho$ ,  $q_1$  and  $q_2$ . Root mean square values of the three performance criteria, (ACC, SWS and DTL), can then be found by substituting  $-Kx$  for  $u$  in the equations of motion (4.1 and 4.2) and performing the linear analysis described in Section 2.3.2.

In the same style as Chapter 3 the comparisons here are performed on an equal workspace basis. The problem can be simplified by realizing that it is the ratio between  $\rho$ ,  $q_1$  and  $q_2$  rather than their actual values which is of importance. The constant  $\rho$  can therefore be set to unity without any subsequent loss in generality, allowing a two dimensional sweep to be performed. The process is now similar to the search for passive systems using equal workspace, except that the variables are now the weighting constants,  $q_1$  and  $q_2$ , rather than stiffness  $K_s$  and damping parameter  $d$ . Using the remaining vehicle parameters as described in Table 3.1 and an input psd described by Equ (3.1), the effect of varying  $q_1$  for three fixed values of  $q_2$  is shown in Figs 4.2(a), (b) and (c). Systems using the same working space (SWS) can be identified using Fig 4.2(a). The corresponding performance in terms of ACC and DTL can then be read off Figs 4.2(b) and (c) respectively.

Various active systems, using full state feedback, limited state feedback, and sub-optimal control laws, are compared in Fig 4.3 using an rms suspension

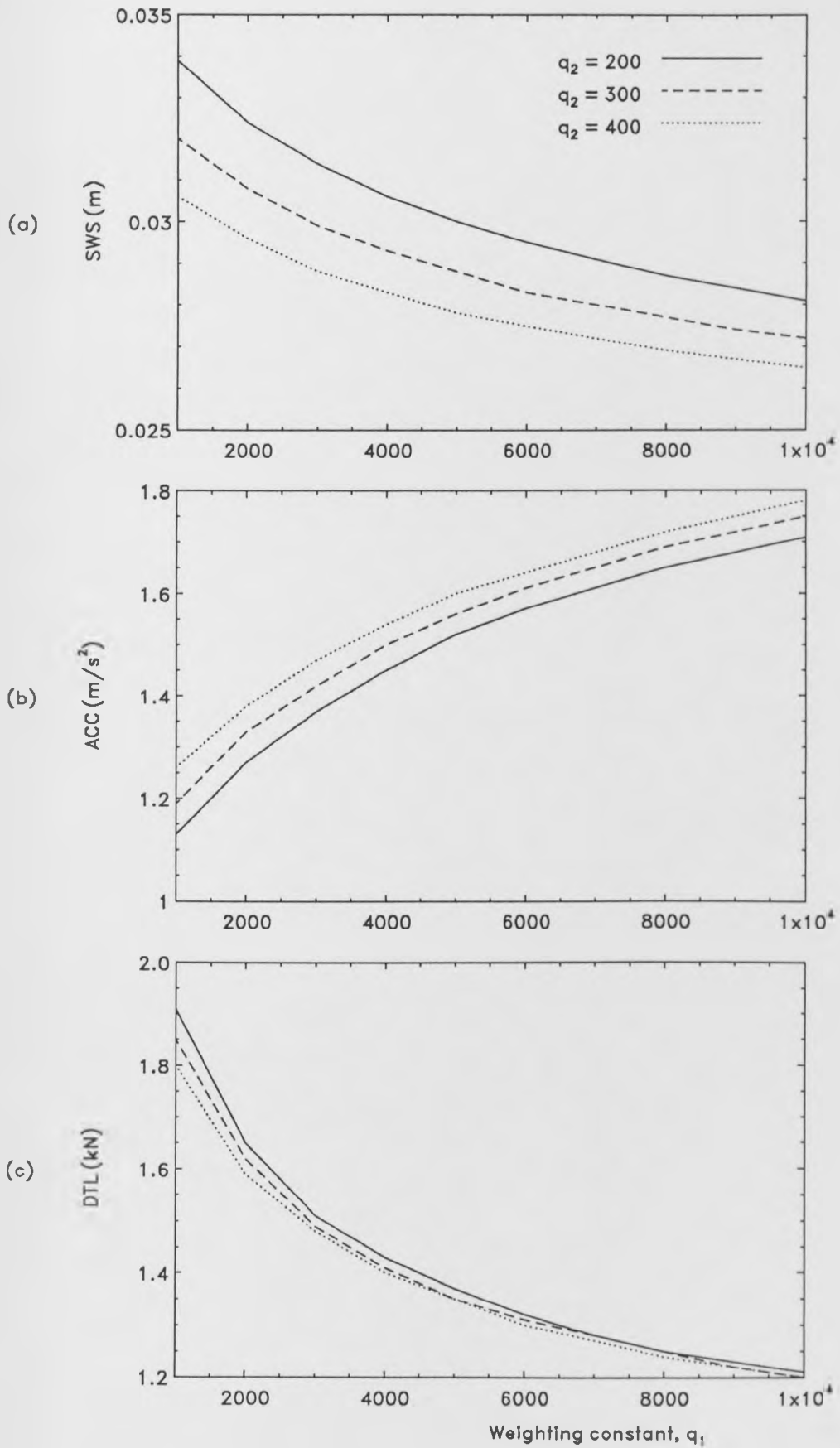


Figure 4.2: Effect of varying the performance index weighting constants,  $q_1$ ,  $q_2$ .

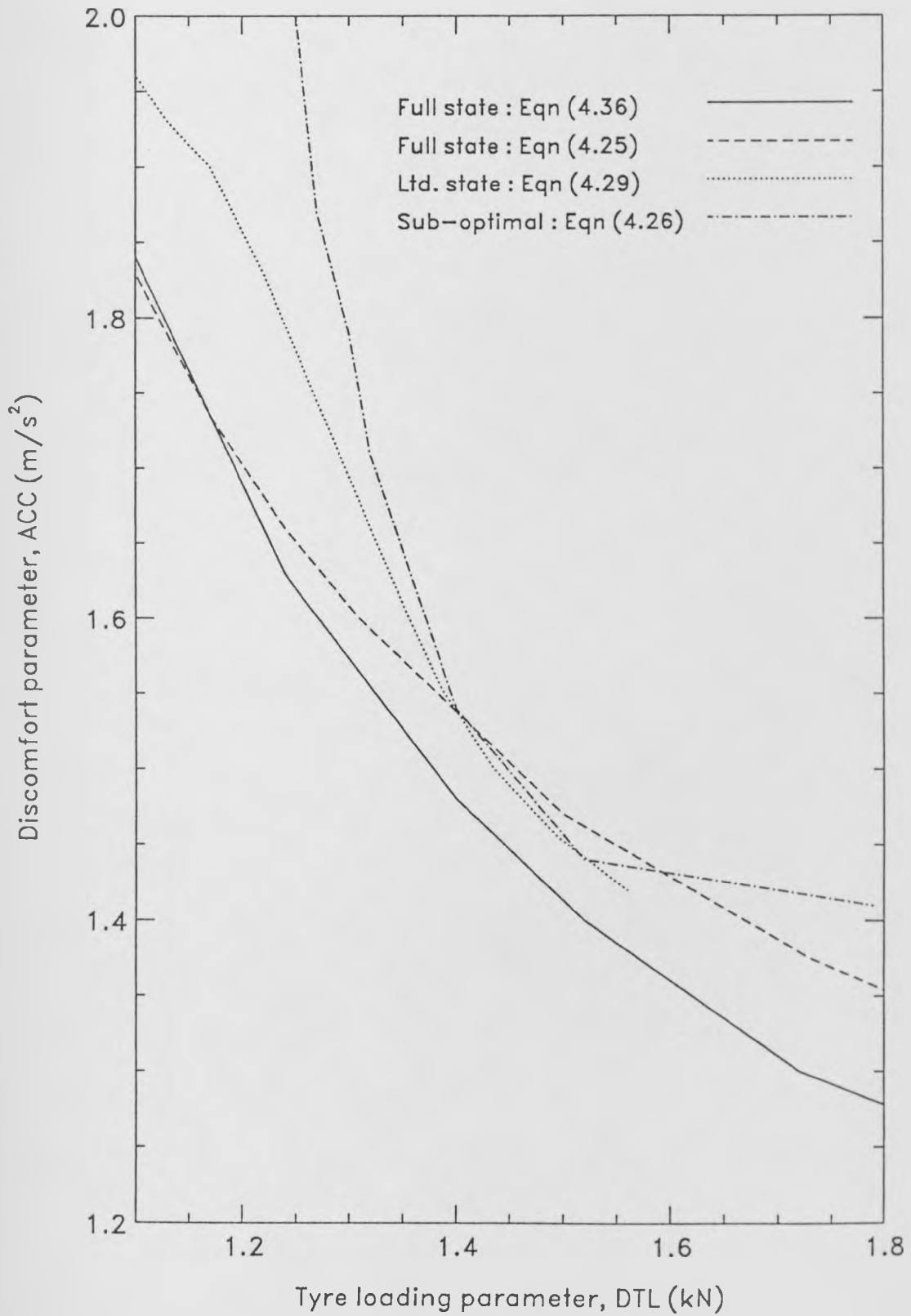


Figure 4.3: Performance comparison of various active control laws.

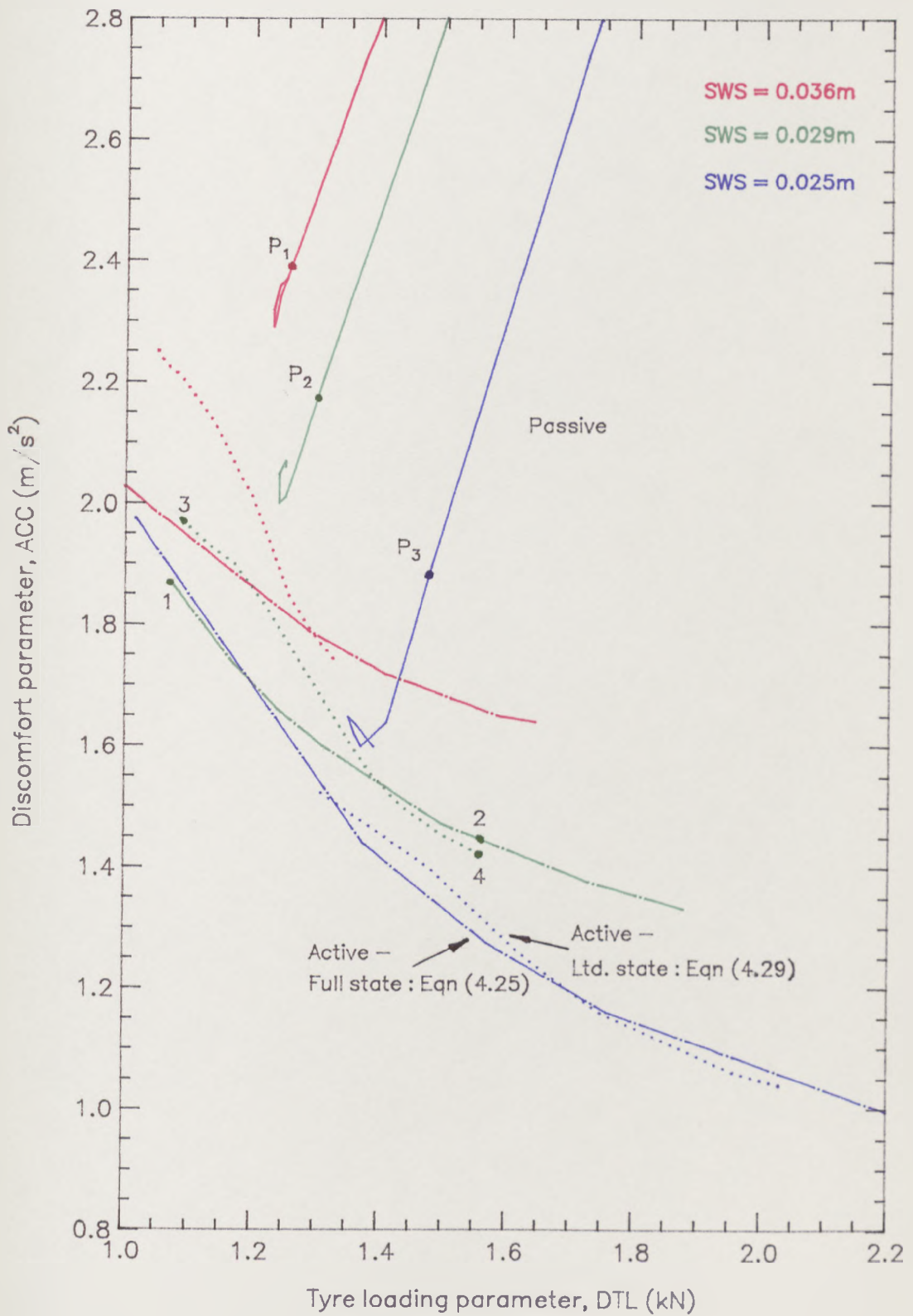


Figure 4.4: Performance of active and passive systems at three suspension workspaces.

workspace of 0.029m. Fig 4.4 compares the more important of these systems against their passive equivalent over a range of suspension workspace values. Each point on the active curves is a different system and has a control law with a different combination of feedback gains. The psd's of ISO weighted vertical body acceleration and dynamic tyre load for selected full state and limited state active designs are compared against the passive system in Figs 4.5 and 4.6.

## 4.5 Discussion of Results

Fig 4.3 shows the best performing active system to be one which uses full state control, with feedback gains being obtained using the gradient search method and a measurement matrix  $M$  equal to the identity matrix. A control law having five separate terms is used, allowing the independent feedback control of each state variable, including  $x_0$  the absolute road surface height. Rms values of ISO weighted vertical body acceleration for this system are typically 5% lower, for any given tyre load performance, than those obtained from a system based on Thompson's full state control law. The trade-off between ride comfort and dynamic tyre load is evident along each curve, and reflects the change in emphasis in the performance index as the weighting constants  $q_1$  and  $q_2$  are varied.

Although the benefit of using either full state feedback system is clear, obvious practical difficulties exist with both systems, namely the measurement of body-to-road displacement. In addition to this, the five gain control law (Eqn (4.35)) requires absolute measurement of each state, implying double integration of accelerometer output to obtain  $x_1$  and  $x_2$ . Thompson's sub-optimal system, which uses the Ricatti equation to generate the feedback gains, but substitutes body-to-wheel for body-to-road displacement in the control law, is one solution

to the problem. Thompson [1984] shows that this system will actually be optimal when  $K_2 = -K_1$  in Eqn (4.26). This can be seen in Fig 4.3 when the two curves for full state and sub-optimal control coincide briefly. Away from this condition however, the performance of the sub-optimal design is seen to drift markedly. The second solution, which caters for general feedback possibilities, is the limited state feedback system suggested by Wilson *et al* [1986]. If a measurement matrix defined by Eqn (4.28) is used the performance again drifts away from that of the full state if the system is weighted toward road holding, although this time the loss in comfort is not so severe.

Fig 4.4 selects the limited state (Eqn (4.29)) and Thompson's full state system (Eqn (4.25)) for comparison with equivalent passive systems at three different rms suspension working space values, SWS=0.025, 0.029 and 0.036m. Since the vehicle considered here has an available suspension travel of 0.22m this latter value represents the maximum allowable rms suspension displacement (see Section 2.6). Points  $P_1$ ,  $P_2$  and  $P_3$  represent the performance of a typical passive suspension in each case, and are chosen on the basis that a sensible spring stiffness (approx. 22kN/m) will be required to prevent excessive attitude changes during manoeuvring.

Assuming that the optimum control laws are subject to additional algorithms which are able to control vehicle attitude, it is clear that, for any active system, a much wider range of possible systems exist at each workspace. In the full state case, significant gains in ride comfort and/or road holding are possible depending on how the control law is weighted. Systems which are heavily weighted toward comfort show improvements in ride of up to 45%, however, this is always at the expense of road holding. At the other extreme, systems which are weighted in favour of road holding show up to 50% reduction in dynamic tyre loading with little or no improvement in ride over the passive equivalent.

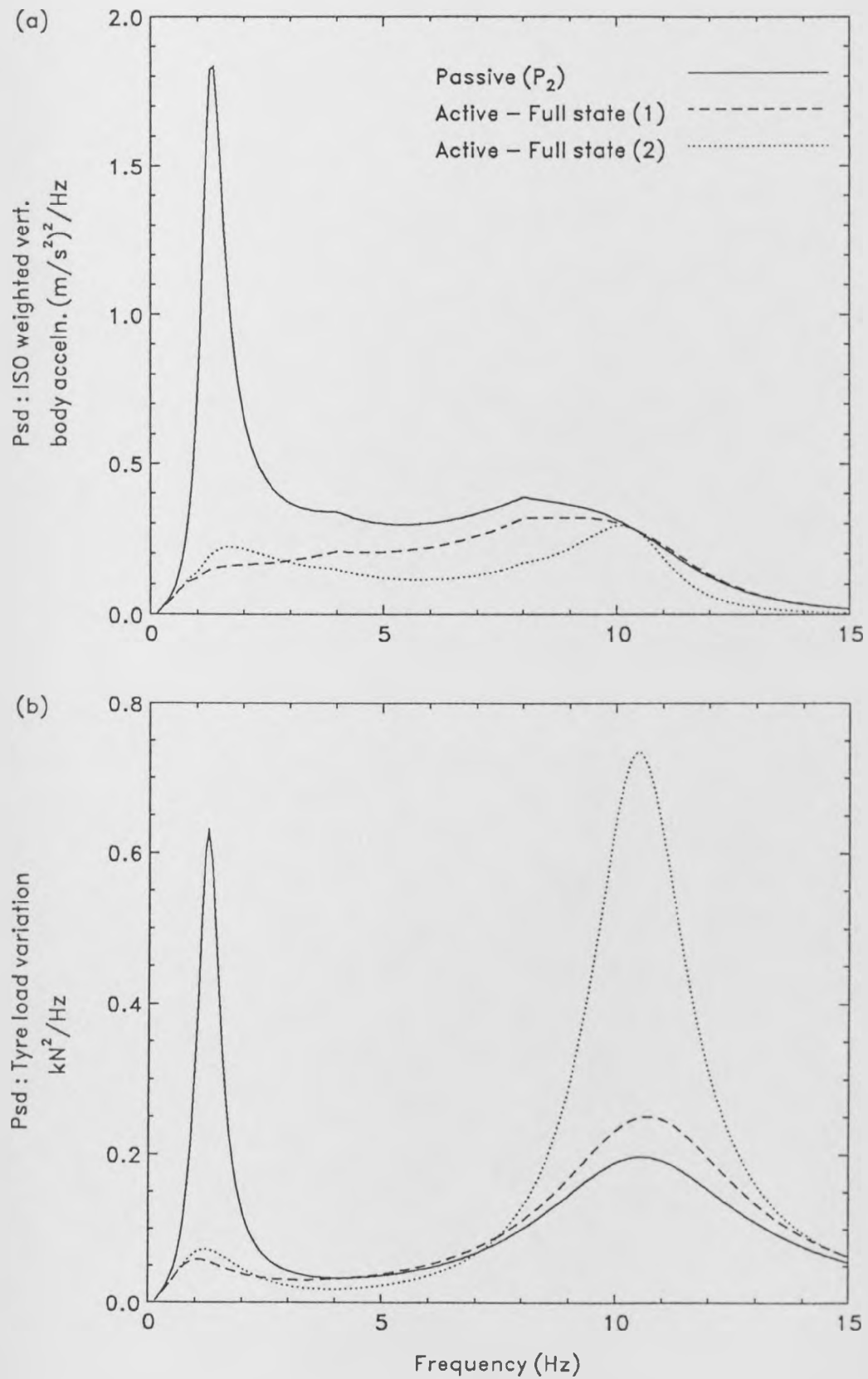


Figure 4.5: Psd's of ISO weighted vertical body acceleration and dynamic tyre load - full state feedback active systems.

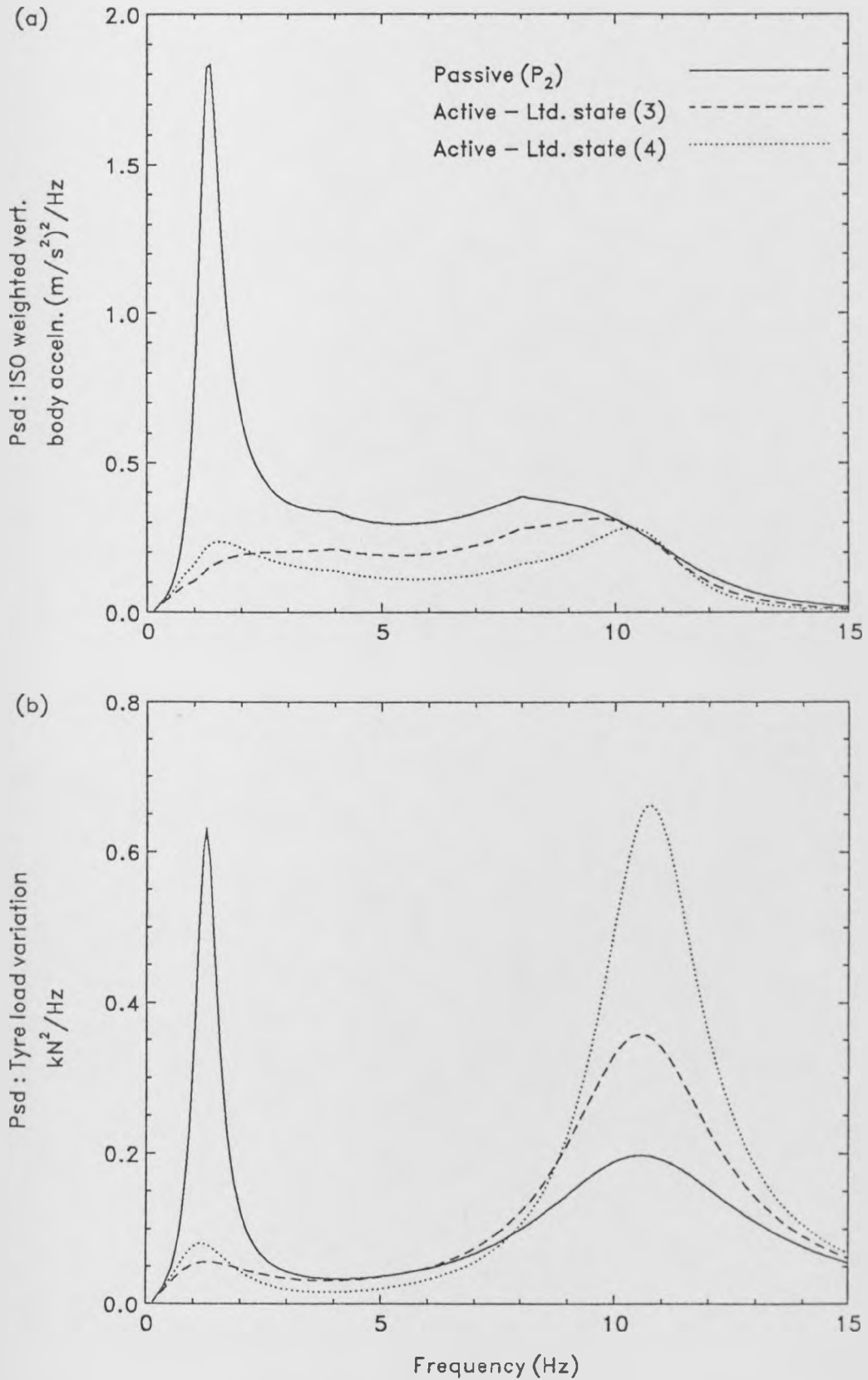


Figure 4.6: Psd's of ISO weighted vertical body acceleration and dynamic tyre load - limited state feedback active systems.

Although the range of limited state designs is restricted to some extent, the performance is also favourable. At  $SWS=0.036m$  the behaviour is very similar to that of the full state system, and it appears that at this workspace there is no advantage to be gained in measuring body-to-road displacement. However, as the workspace is reduced, the trade-off between ride comfort and road holding becomes steeper and the performance curves separate.

Points 1 and 2 on the full state curve, and 3 and 4 on the limited state curve, each at  $SWS=0.029m$ , are examined further using the spectral densities in Figs 4.5(a), (b) and 4.6(a), (b) respectively. Points 1 and 3 are selected to represent systems which employ control laws weighted in favour of road holding, while points 2 and 4 represent systems weighted toward ride comfort. In both the full and limited state cases, the improvement in ride comfort over the passive system appears as a dramatic reduction in the body resonance peak of ISO weighted vertical body acceleration. It is clear from the psd's of dynamic tyre load that any improvements in rms value, seen in Fig 4.3, are also achieved through a reduction in activity at body resonance. At "wheelhop" even systems 1 and 3 cannot better the performance of the well designed passive system, and in the extreme case of the comfort biased active systems (points 2 and 4) there is a large increase in the wheel resonance peak.

## 4.6 Concluding Remarks

This chapter describes the techniques used to generate various control laws. Two solutions to the stochastic optimal linear regulator problem are discussed, one providing a control law for the special case when all system states can be measured, and the other considering more general feedback possibilities. The performance of active systems operating according to these optimal full

and limited state feedback control laws is then analysed. The systems are compared with equivalent passive suspensions on an equal workspace basis, and the following conclusions can be drawn :

1. Substantial improvements in ride comfort and/or road holding are possible if an active suspension is employed. A system operating according to a full state feedback control law is generally the most effective, however, the more practical limited state feedback case still offers significant performance gains, particularly at higher rms suspension working space values.
2. The improvements seen are achieved mainly through effective control of events at frequencies around body resonance. At the “wheelhop” frequency, active systems cannot improve upon the performance of the well designed passive system.

The analysis here assumes an ideal actuator. Although it is anticipated that practical limitations of the real system will have an adverse effect on performance, the results serve as a target for the more practical controllable damper systems. A further advantage of the active system over the fixed passive suspension does not emerge from these results, namely its ability to adapt to the prevailing running conditions. With the hardware already present in the active car, it will be a relatively straightforward task to include a discrete number of control laws, each suitable for a different running condition. This aspect is dealt with in Chapter 9.

# Chapter 5

## Controllable Damper Systems

### 5.1 Introduction

The results of Chapter 4 show clearly the advantages of the active system operating under various control laws. However, the increased cost and complexity of these systems has left their commercial viability in some doubt, and it is necessary to investigate the behaviour of other, less complex, systems.

This chapter will consider suspensions employing controllable dampers which, in comparison to the active systems, represent the simple end of the intelligent suspension spectrum. The system can take various forms but is essentially one in which a damper, its coefficient controlled according to some law, is mounted in parallel with a conventional passive spring. A minimal amount of energy is required since the damper does not supply energy - only dissipates it, but in a more intelligent way than the passive system. The attraction of such a suspension is obvious. Although microprocessors, transducers and additional wiring are still required, the actuators, hydraulic pumps, and accumulators of the active system are replaced by adjustable dampers and consequently, few design changes are necessary on the vehicle itself.

Three systems of differing complexity, namely the continuously variable, the two-state switchable, and the three-state adaptive systems, are selected for comparison here. The most advanced is the continuously variable damper system. The proportional valve technology required for this system has been around

for many years, however, its use has so far been restricted to specialist areas, for example the aerospace industry, and has therefore been very expensive. It is only recently that commercially attractive versions of the valve have been considered for use within vehicle suspensions, eg. Parker and Lau [1988] or Doi *et al* [1988]

The switchable damper system is selected from a class of systems which employ fast acting dampers to switch between a number of discrete settings. A number of control strategies have been suggested, for example by Alanoly and Sankar [1987], but the one modelled here is based on a strategy first proposed by Karnopp *et al* [1974] and later used by, amongst others, Crolla and Aboul-Nour [1988] and Lizzell [1988].

Slow acting adaptive dampers have been around for some time and a number of systems are currently available, for example, the Citroen Hydractive[1989], the Monroe (formerly Armstrong Patents) Adaptive Suspension Control (Hine and Pearce [1988]), and the BMW/Boge Electronic Damping Control (Hennecke and Zieglmeier [1988]). The Monroe system is selected for the work here.

This chapter, first establishes the general equation of motion and then, following descriptions of each selected system, goes on to compare the performance of controllable damper systems with that of the passive and active systems discussed in Chapters 3 and 4 respectively. At this stage, the systems are modelled using ideal components only. The effect of the practical limitations present in real components is discussed later in Chapter 6.

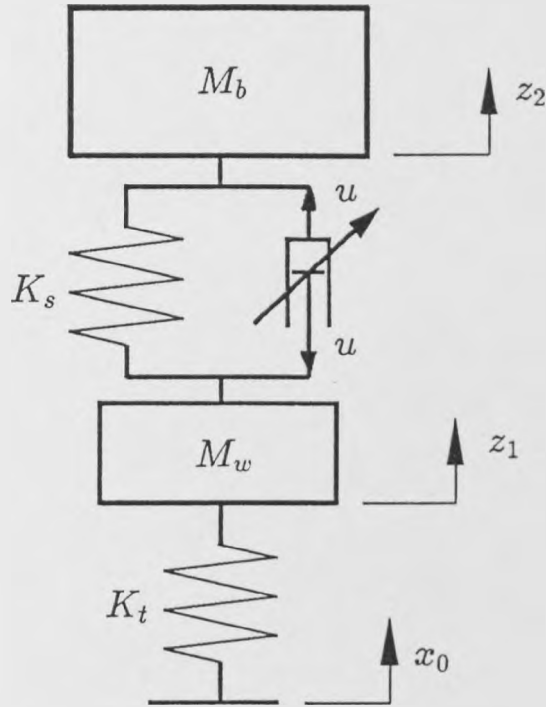


Figure 5.1: Quarter vehicle model of the controllable damper system.

## 5.2 Equations of Motion

The quarter car controllable damper model is shown in Fig 5.1 and the equations of motion are written as follows ;

$$M_w \ddot{z}_1 = K_t(x_0 - z_1) - K_s(z_1 - z_2) - u \quad (5.1)$$

$$M_b \ddot{z}_2 = K_s(z_1 - z_2) + u \quad (5.2)$$

where this time,  $u$  is the force across the controllable damper. In a similar way to the active system, the equations can be rearranged and written in the form of Eqn (2.11). Using the suffix  $c$  to denote the controllable damper system the coefficient matrices in Eqn (2.11) become :

$$MXDD_c = \begin{bmatrix} M_w & 0 \\ 0 & M_b \end{bmatrix}, \quad MX_c = \begin{bmatrix} K_t + K_s & -K_s \\ -K_s & K_s \end{bmatrix}$$

$$MU_c = \begin{bmatrix} K_t \\ 0 \end{bmatrix}, MF_c = \begin{bmatrix} -1 \\ 1 \end{bmatrix} \quad (5.3)$$

$MXD_c$  and  $MUD_c$  are both null matrices.

## 5.3 System Definitions

### 5.3.1 Continuously Variable Damper System

This is essentially the semi-active system described by Sharp and Crolla [1987], and studied by Crolla and Aboul-Nour [1988], in which the actuator is a continuously variable damper. The damper is theoretically capable of tracking a force demand signal independently of the velocity across the damper. The demand signal, as for the active system, is generated in a microprocessor and is governed by a control law which is based on the linear optimal control theory outlined in Chapter 4. The system considered here uses the more practical limited state feedback law and the available state information is taken to be suspension displacement ( $z_1 - z_2$ ), wheel velocity  $\dot{z}_1$  and body velocity  $\dot{z}_2$ . In terms of the transformed variable  $x$ , the control law can be described by Eqn (4.29) :

$$u = -[K_2(x_1 - x_2) + K_3x_3 + K_4x_4]$$

The elements of gain vector  $K$  are calculated by the gradient search routine described by Wilson *et al* [1986] using a measurement matrix  $M$  defined by Equ (4.28). However, the problem is slightly different to the active case presented in Chapter 4, in that the controllable element is mounted in parallel with a conventional spring. There are now two ways of approaching the calculations. The first method is to include the spring in the vehicle model and equations used to obtain feedback gains. In this case, the vertical body acceleration is no longer proportional to the force across the controllable element alone, and the

performance index must be modified slightly to enable direct weighting of the ride comfort term. The damper force is allowed to become one of the system states,  $x_u$ , using the first order equation :

$$T_u \dot{x}_u + x_u = u \quad (5.4)$$

Eqn (5.4) does not represent a physical delay within the system and is used solely as an artefact to generate the control law. The time constant  $T_u$  is given the small value of 0.001s.

Combining Eqn (5.4) with Eqn (2.19) the first order equation of motion becomes ;

$$\dot{x}_b = A_b x_b + B_b u + B_{b1} x_0 \quad (5.5)$$

where the vector  $x_b = [x \ x_u]^T$  and the matrices  $A_b$ ,  $B_b$  and  $B_{b1}$  are defined by :

$$A_b = \begin{bmatrix} 0 & I & 0 \\ -MXDD_c^{-1}MX_c & 0 & MXDD_c^{-1}MF_c \\ 0 & 0 & -T^{-1} \end{bmatrix}, B_b = \begin{bmatrix} 0 \\ 0 \\ T^{-1} \end{bmatrix}$$

$$B_{b1} = \begin{bmatrix} 0 \\ MXDD_c^{-1}MU_c \\ 0 \end{bmatrix} \quad (5.6)$$

The body acceleration,  $\dot{x}_4$ , is now given by ;

$$\dot{x}_4 = \frac{1}{M_b} [K_s(x_1 - x_2) + x_u] \quad (5.7)$$

and to include this in the performance index, the control matrix,  $D$ , is written :

$$D = \begin{bmatrix} -1 & 1 & 0 & 0 & 0 \\ 0 & -1 & 1 & 0 & 0 \\ 0 & \frac{K_s}{M_b} & -\frac{K_s}{M_b} & 0 & \frac{1}{M_b} \end{bmatrix} \quad (5.8)$$

An additional constant,  $q_3$ , is then used to weight the acceleration term,  $(\dot{x}_4)^2$ , in the performance index. To generate feedback gains using the gradient search routine, Eqn (5.5) is then combined with the equation for a filtered white noise input (4.7) using the vector  $x_c = [x_b \ x_0]^T$ , and the first order matrix equation becomes ;

$$\dot{x}_c = A_c x_c + B_c u + B_{cw} w \quad (5.9)$$

where

$$A_c = \begin{bmatrix} A_b & B_{b1} \\ 0 & f_w \end{bmatrix}, B_c = \begin{bmatrix} B_b \\ 0 \end{bmatrix}, B_{cw} = \begin{bmatrix} 0 \\ I \end{bmatrix} \quad (5.10)$$

The second approach is to ignore the spring when calculating the gains, ie. use fully active gains, and then subtract the spring force to obtain the force required of the controllable damper. The control law becomes :

$$u = -[K_2(x_1 - x_2) + K_3 x_3 + K_4 x_4] - K_s(x_1 - x_2) \quad (5.11)$$

Both techniques are considered and results compared, the best one being chosen to generate results throughout the rest of the project.

The major difference between this system and the active system described in Chapter 4 is that the controllable damper can only dissipate energy. Consequently an additional law is required :

$$\text{If } (\dot{z}_1 - \dot{z}_2)u > 0 \quad \text{then} \quad \text{demand signal} = u \quad (5.12)$$

$$\text{Otherwise} \quad \text{demand signal} = 0$$

Eqn (5.12) is shown graphically in Fig 5.2. Each point on the graph represents one step in a simulated run over a typical rough minor road (the input profile has a psd described by Equ (3.1)) at 20 m/s, and shows values of damper force and suspension velocity at each time step.

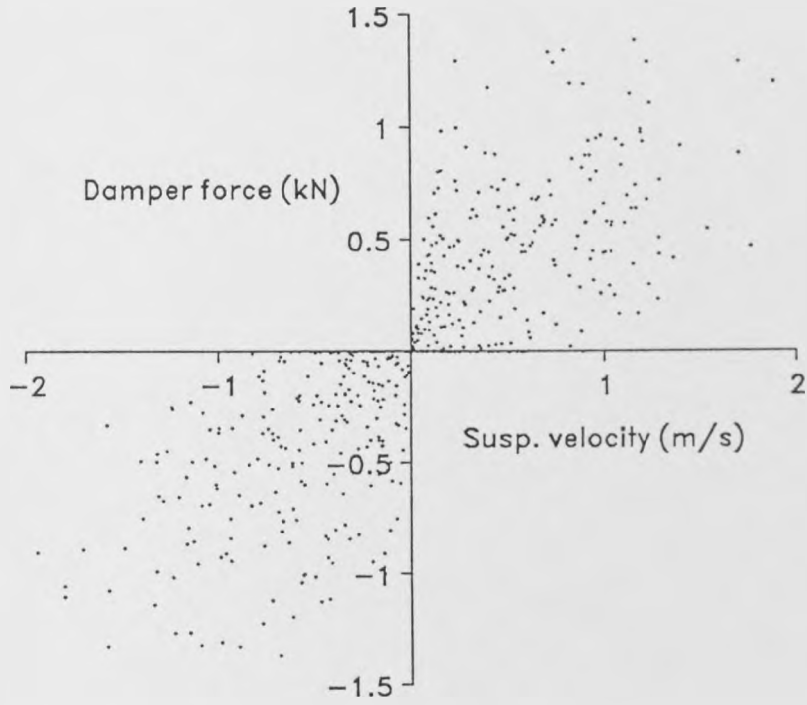


Figure 5.2: Force/velocity plot of the continuously variable damper.

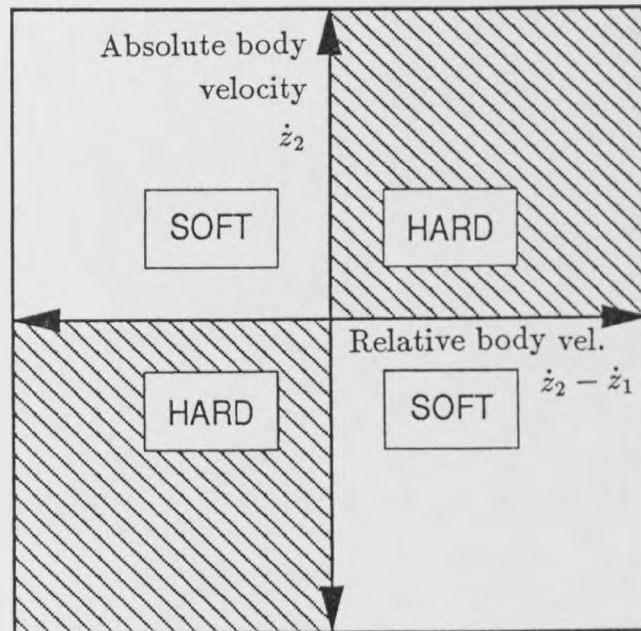


Figure 5.3: Control strategy for the two-state switchable damper.

### 5.3.2 Switchable Damper System

This system uses a two-state switchable damper in parallel with a passive spring. The damper used here is switched according to a strategy first proposed by Karnopp *et al* [1974] and later described by Crolla and Aboul-Nour [1988]. The control law relies on the measurement of the absolute and relative body velocities and is defined by ;

$$\text{If } \dot{z}_2(\dot{z}_2 - \dot{z}_1) > 0 \quad \text{then} \quad C = C_{hard} \quad (5.13)$$

$$\text{Otherwise} \quad C = C_{soft}$$

where  $C$  is the damping coefficient. The choice of hard and soft settings has so far been arrived at empirically by ride engineers. At each time step, the force  $u$  in Eqn 2.11 is then given by ;

$$u = C(\dot{z}_1 - \dot{z}_2) \quad (5.14)$$

The strategy, shown pictorially in Fig 5.3, is simple in comparison with the continuously variable system. However, a fast acting valve is still required to effect the constant switching between hard and soft settings. Such hardware is currently available, for example, the piezo-electric operated valve used in the Toyota TEMS system (Tsutsumi *et al* [1990]).

### 5.3.3 Adaptive Damper System

The adaptive damper system analysed here is an example of a class of system which has been commercially available for some years. It is based on the Monroe ASC system (Hine and Pearce [1988]), and consists of a three-state damper

mounted in parallel with a passive spring. As a simpler alternative to the systems described so far, the control strategy uses an “adaptive” approach in which the damper setting is selected on the basis of suspension displacement and vehicle speed. The softest damper setting, ( $C_{soft}$ ), is used under normal driving conditions, the higher levels, ( $C_{int}$ ) and ( $C_{hard}$ ) being invoked when necessary for ride (or handling) control. In the Monroe system, the highest level of damping is controlled by conventional valves within the shock absorber and, in event of power failure, the unit defaults to this condition for maximum safety. The intermediate and soft damper settings are controlled through electro-magnetic valves on the body of the damper, which can be energised individually. Constant suspension movement information is provided by non-contacting displacement sensors housed within the dirt-shield. For a particular vehicle speed, suspension displacement limits are set, outside of which the damper switches first to the intermediate setting, and ultimately to the hard setting. The damper then remains in the new setting for a minimum time, typically 0.5 seconds.

The important distinction to make between this system and the two-state switchable system is in the length of time the damper spends in each setting. In contrast to the switchable damper, which is constantly changing setting, the adaptive damper may remain in one particular setting for long periods.

The damper settings and switching levels are again arrived at empirically from the results of practical vehicle testing. The Monroe ASC settings for the vehicle considered here are 1.0, 1.5 and 2.0 kNs/m while the displacement switching limits over a range of vehicle speeds can be seen in Fig 5.4.

The aim of this strategy is to allow more of the available suspension working space to be used, particularly on the smoother surfaces, giving increased ride comfort.

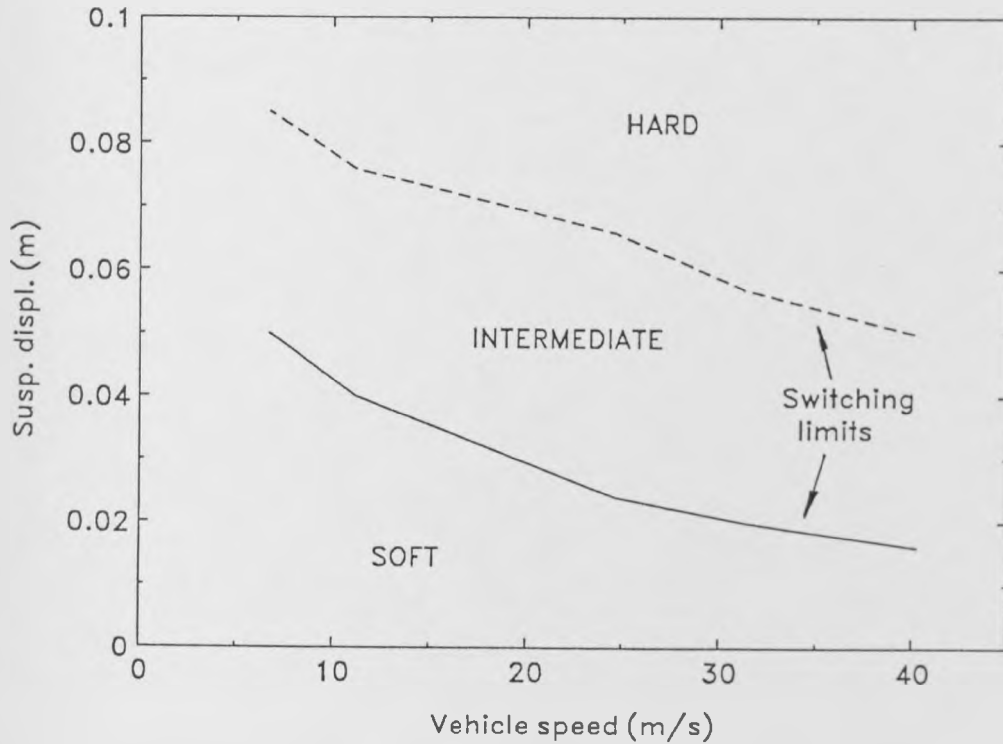


Figure 5.4: Displacement switching limits of the Monroe ASC adaptive suspension.

## 5.4 Results

Since the force across the controllable damper is a function of the system states and time, the equations of motion now require an numerical solution, using the non-linear analysis techniques outlined in Section 2.5. To ensure that all predicted results are directly comparable however, it is necessary to perform all calculations, including those for the linear passive and active systems, in the time domain. The road profile used for the simulation is generated from an input psd described by Eqn (3.1).

In the same style as results in Chapter 4, an initial insight into the relative performance of competing systems is achieved by using the equal workspace contour. Fig 5.5 compares the performance of various controllable damper

systems with that of the passive and active suspensions. Once again, point P on the passive curve denotes the performance of the system described in Table 3.1 ( $K_s=22\text{kN/m}$ ,  $C_s=1.5\text{kNs/m}$ ). Assuming that for attitude control purposes the controllable damper systems will require a similar spring to that of point P, the parallel passive spring for these designs is also taken to be of stiffness  $22\text{kN/m}$ . Two performance curves are shown for the continuously variable damper system, representing the different methods of calculating the control law feedback gains (see Section 5.2.2). Curve (a) is generated using a control law described by Eqn (4.29) which has taken into account the passive spring, while the control law for curve (b) is based on a fully active control law (Eqn (5.11)). Like the active systems discussed in Chapter 4, each point on these curves has a different gain vector  $K_L$ , which changes in response to variations in the performance index weighting constants.

The switchable system curve has been generated in the following manner. First, point P on the passive curve is selected as the starting point. The damping coefficient of this system ( $C_s=1.5\text{kNs/m}$ ) is then taken to be the hard damper setting ( $C_{hard}$ ) of the switchable system. Fig 5.5 shows the effect of introducing the soft damper setting ( $C_{soft}$ ). One end of the curve coincides with point P, since at this stage the ratio,  $C_{soft}/C_{hard}$ , is equal to 1. Moving along the curve, the ratio is reduced until at the other end  $C_{soft}/C_{hard}$  is equal to 0.2. It is a feature of these results that the introduction of a soft switching option does not necessarily result in an increased working space requirement. In this case, for a system having a spring stiffness  $22\text{kN/m}$  and a hard damper setting  $1.5\text{kNs/m}$ , the SWS does not increase significantly until the soft to hard ratio is less than 0.2. This allows the comparison with other systems to be made on an equal workspace basis. It follows that similar curves must also exist starting at each point on the passive curve, although the value of  $C_{soft}/C_{hard}$  beyond which the workspace increases may be different in each case.

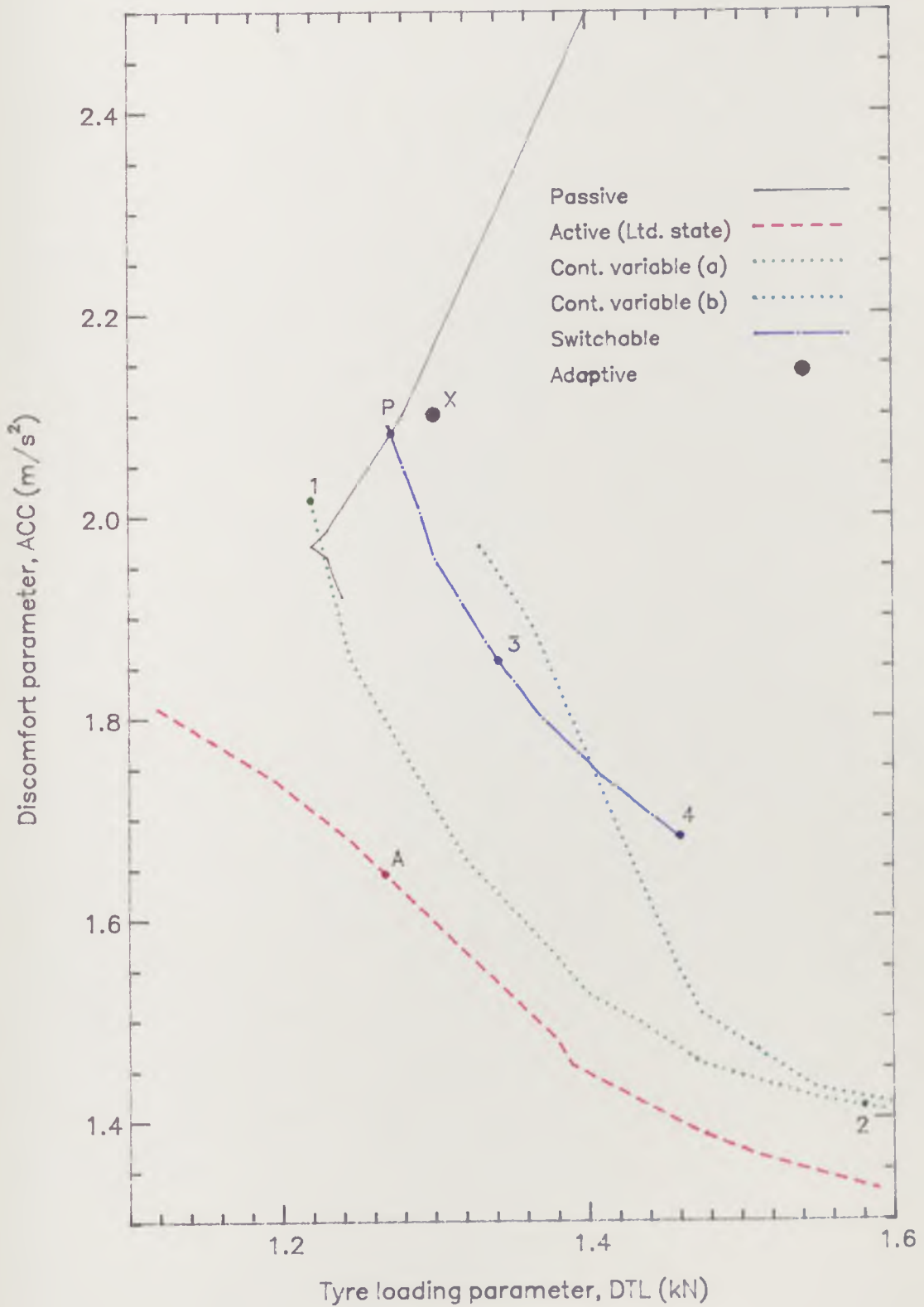


Figure 5.5: Equal workspace comparison of passive, active and controllable damper systems (SWS=0.029m).

Psd's of ISO weighted vertical body acceleration and tyre load variation, for selected continuously variable and switchable damper systems in Fig 5.5, are compared against those of the passive and active systems in Figs 5.6 and 5.7.

The increased number of possible parameter variations render it difficult to plot the adaptive three-state damper on an equal workspace basis. However, one possible combination of damper settings ( $C_{soft}=1.2\text{kNs/m}$ ,  $C_{int}=1.7\text{kNs/m}$ ,  $C_{hard}=2.0\text{kNs/m}$ ) and displacement limits (soft to intermediate = 0.031m, intermediate to hard = 0.068m), used as a Monroe prototype, results in the performance shown (point X), with no increase in suspension working space.

Fig 5.8 concentrates on the continuously variable damper system, and in particular the effect on performance of varying the passive spring stiffness. In this case the spring has been included in the model used to generate feedback gains, and the three values of  $K_s$  considered are 10kN/m, 20kN/m, and 30kN/m.

The switchable damper system is studied further in Figs 5.9 and 5.10. In Fig 5.9 the spring stiffness remains constant at 22kN/m whilst the three hard damper settings considered are 1.32, 1.85 and 2.38kNs/m (corresponding to damping ratios of 0.25, 0.35 and 0.45 respectively). The three curves shown, each having a different suspension working space, are obtained by progressively reducing the soft damper setting until the suspension working space increases beyond +1% of its original value. The systems indicated by the first point on each curve ( $C_{soft}/C_{hard} = 1$ ) are actually conventional passive systems with a damping coefficient specified by the  $C_{hard}$  parameter.

Fig 5.10 examines the effect of stiffness variation for the switchable damper system. Three groups of curves are shown representing  $K_s$  values of 10kN/m, 20kN/m, and 30kN/m. Each group contains three curves, having  $C_{hard}$  values of 1.32, 1.85 and 2.38kNs/m, which follow the style of those in Fig 5.9.

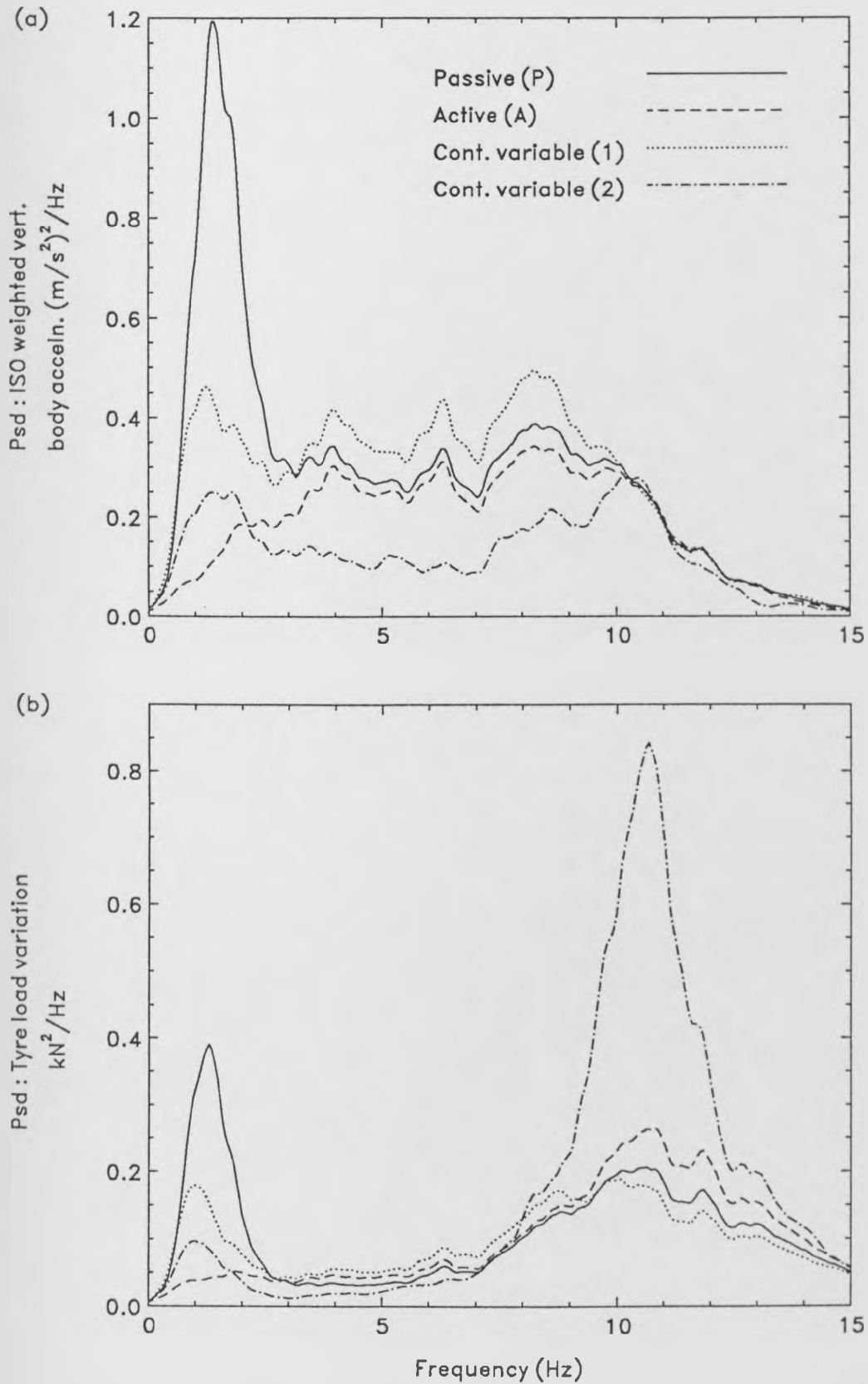


Figure 5.6: Psd's of ISO weighted vertical body acceleration and dynamic tyre load - continuously variable damper systems.

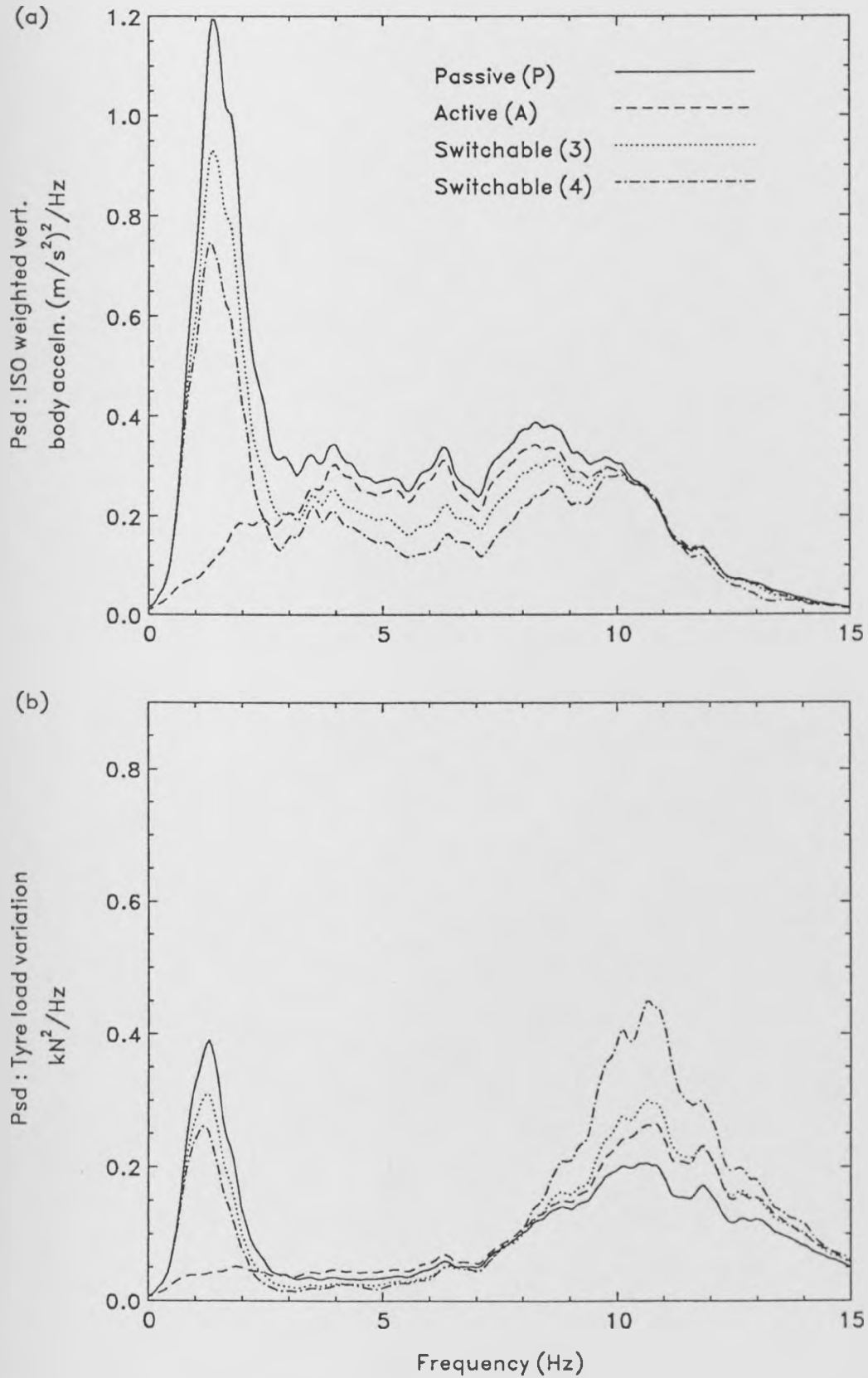


Figure 5.7: Psd's of ISO weighted vertical body acceleration and dynamic tyre load - two-state switchable damper systems.

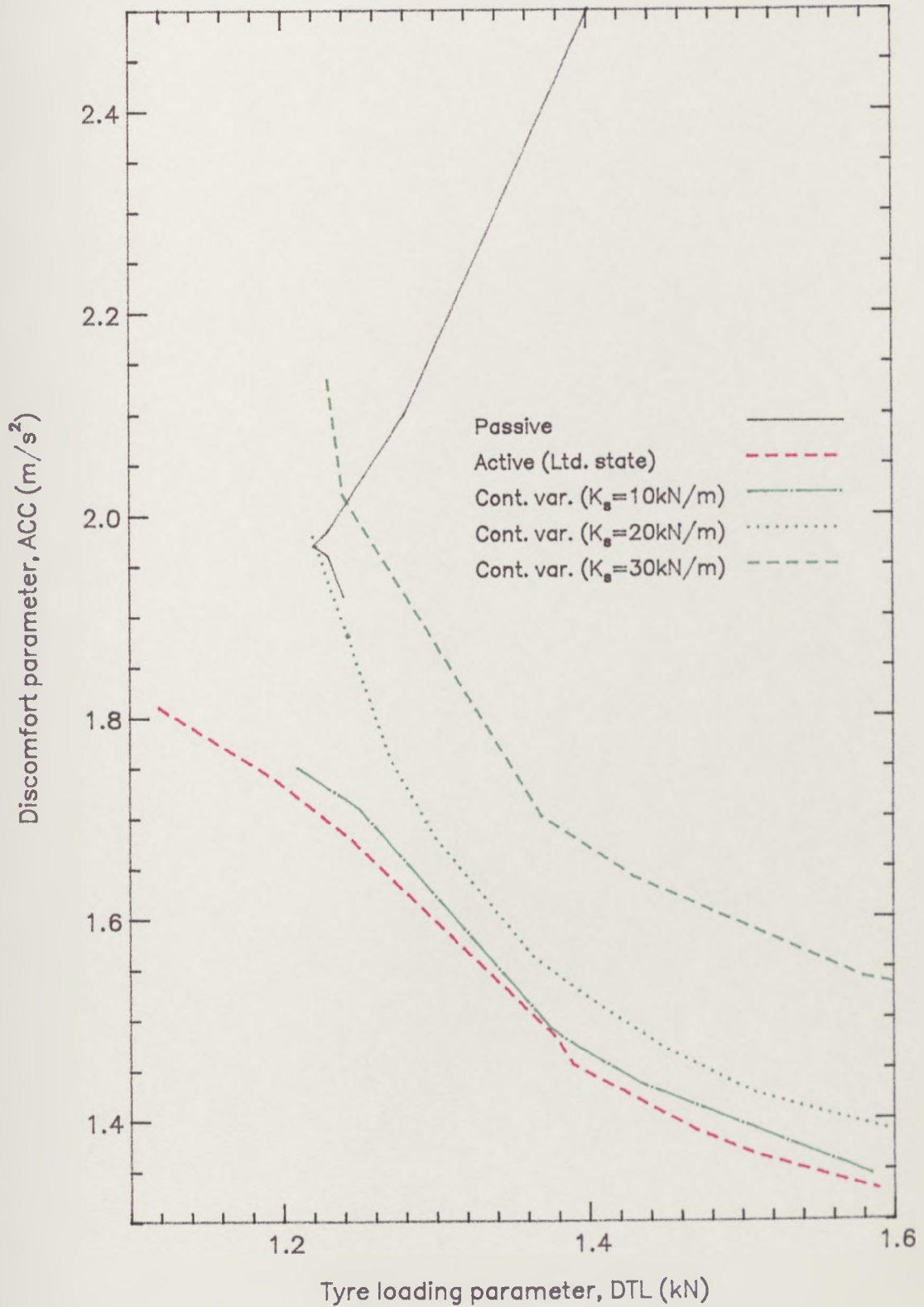


Figure 5.8: Continuously variable damper system - effect of variation in spring stiffness,  $K_s$  (SWS = 0.029m).

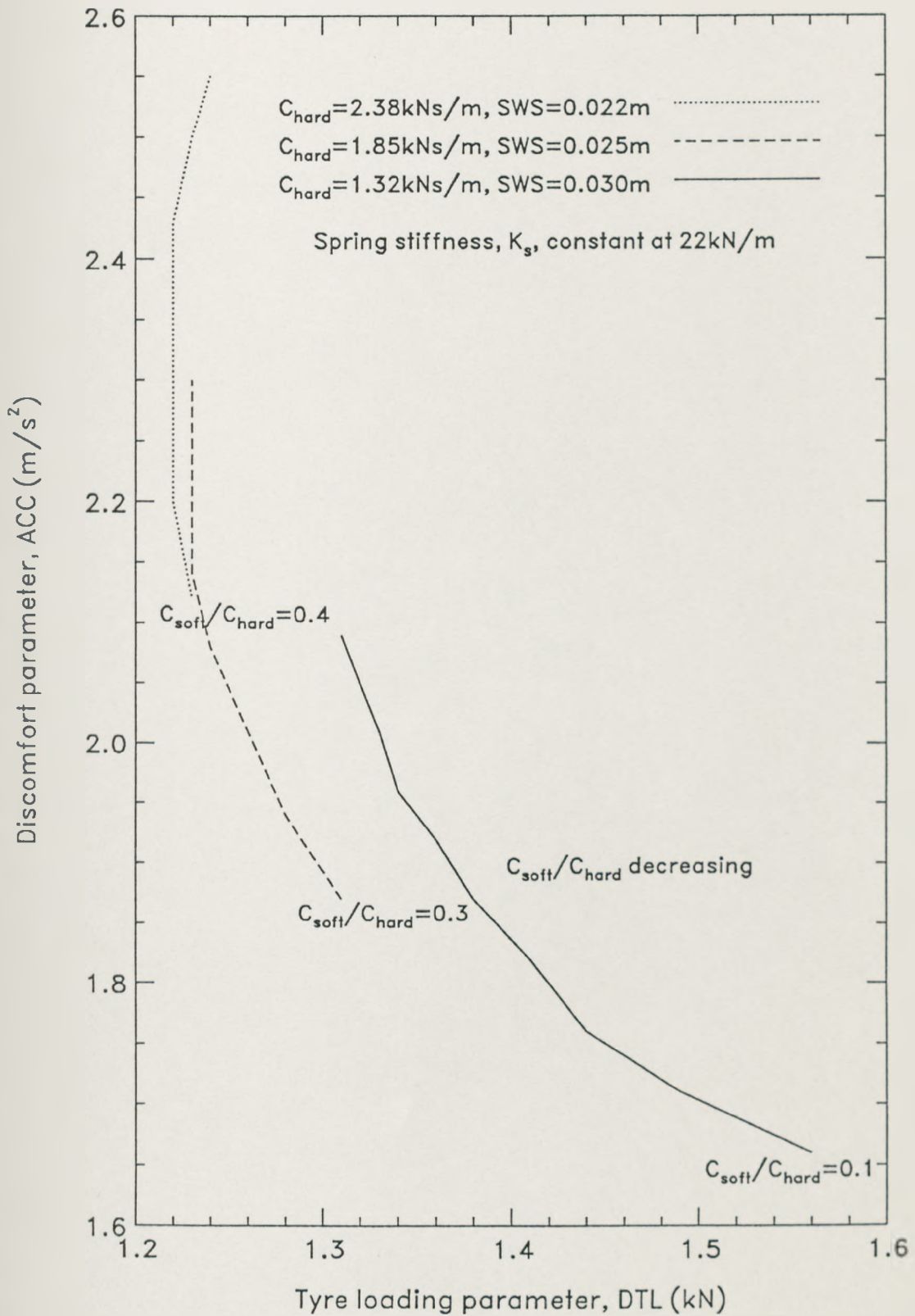


Figure 5.9: Switchable damper system - effect of variation in  $C_{soft}/C_{hard}$  for three values of  $C_{hard}$ .

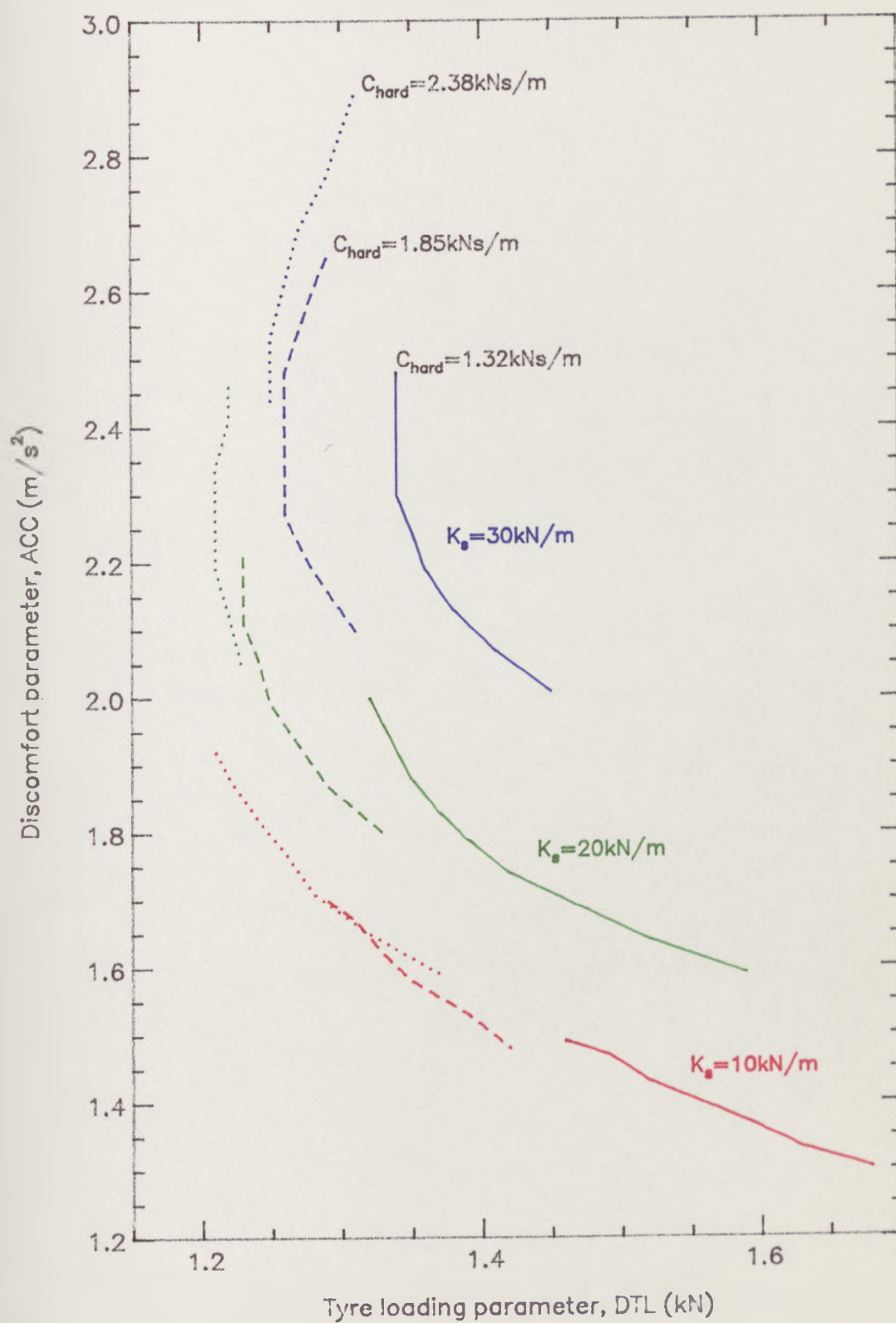


Figure 5.10: Switchable damper system - effect of variation in spring stiffness,  $K_s$ .

## 5.5 Discussion of Results

The first point to be drawn from Fig 5.5 is the marked difference in performance of the two continuously variable damper systems, operating according to the control laws described by Eqns (4.29) and (5.11). If the passive spring is included in the model used to generate the gains, resulting in Eqn (4.29), the behaviour of the continuously variable system is encouraging. Its performance curve lies close to that of the limited state active system, and improvements in ride comfort of around 15% over the passive design (P) are possible, with no increase in DTL. Conversely, if a fully active control law is used, and the spring force then subtracted to obtain the force required at the damper (Eqn (5.11)), the performance deteriorates significantly, especially when the system performance index is weighted in favour of tyre loading. The former method is obviously the most suitable, as it attempts to minimize body acceleration rather than the controllable damper force. It is therefore used throughout this and the remaining chapters to generate feedback gains for the continuously variable damper system.

Since the switchable system shown in Fig 5.5 has a spring stiffness of 22kN/m and a hard damper setting of 1.5kNs/m, it follows that the end of its performance curve coincides with the performance of passive system (P). A reduction in the ratio  $C_{soft}/C_{hard}$  results in an improvement in ride comfort at the expense of dynamic tyre loading. At the extreme, when  $C_{soft}/C_{hard}=0.2$ , the ACC value is approximately 20% lower than the passive system P, whilst the DTL value is increased by around 16%. If the switchable system is compared with the continuously variable damper, it can be seen that both curves follow the same trend but, for a given value of DTL, the switchable curve has a 14% higher discomfort parameter.

The adaptive system shown in Fig 5.5 (point X) shows no improvement over the

passive suspension. However, it is unfair to judge this type of suspension using an equal workspace comparison, since the idea of the system is to maximise the usage of suspension workspace, within the available limits. Only when the equal workspace restriction is relaxed and the performance considered over a range of road surfaces (Chapter 9) will the benefits of the adaptive system be revealed.

Systems 1 and 2 on the continuously variable curve (a) are examined more closely using the psd's for ISO weighted vertical body acceleration and tyre load variation in Fig 5.6(a) and (b) respectively. These points, representing the extreme performance index weighting conditions, are compared against the passive system (P) and the limited state active system (A).

Although not as effective as the active system, ride comfort improvements over the passive appear in Fig 5.6(a) as large reductions in the body resonance peak. Psd's for both continuously variable systems, 1 and 2, have the same general shape, and it seems that a change in performance index weighting affects responses over the frequency range 0-10Hz to an equal extent, rather than controlling events specifically at either body or wheel hop resonance peaks.

The psd's for dynamic tyre load in Fig 5.6(b), show that any improvements over the passive system are always achieved through a reduction in the body resonance peak and, like the active system, comfort-biased systems show a large increase in activity around the "wheelhop" frequency.

The psd's of points 3 and 4 on the switchable curve, representing systems having  $C_{soft}/C_{hard}$  ratios of 0.5 and 0.2 respectively, are shown in Fig 5.7(a) and (b). In this case the shape of the body acceleration psd's closely resembles that of the passive system and any rms ride comfort improvements are due to equal reductions in acceleration over the frequency range 0-10Hz. The increase in rms dynamic tyre loading with the switchable system is seen in Fig 5.7(b), again as

an increased peak in the psd at the “wheelhop” frequency.

The difference between the passive system peak values in Figs 5.6 or 5.7, and those obtained from linear analysis in, for example, Fig 4.5, is due to the smoothing of the psd’s in this chapter to allow easier interpretation of results. The process has little effect on the rms values.

Fig 5.8 shows clearly the effect of varying the parallel conventional spring stiffness in the continuously variable system. At low stiffnesses (10kN/m), the system behaves almost like the limited state active option. However, as  $K_s$  is increased the spring inevitably begins to dominate the suspension behaviour and there is less scope for the controllable damper to improve performance. Nevertheless, even at  $K_s=30\text{kN/m}$  (higher than passive system P), comfort improvements of around 10% are still possible with no increase in DTL.

Two points emerge from Fig 5.9. Firstly, it is clear that suspensions with harder damper settings benefit most from the introduction of a soft switching option. The trade-off between increased comfort and loss in road holding becomes less, and at  $C_{hard}=2.38\text{kNs/m}$ , with  $C_{soft}/C_{hard}=0.4$ , a 17% improvement in comfort is possible with no increase in DTL. Secondly, for each system, the discomfort parameter is always reduced as the softer damper setting is increased.

Fig 5.10 examines the effect of stiffness change on the switchable system. It is evident that softer suspensions ( $K_s=10\text{kN/m}$ ) benefit little from the introduction of soft switching systems, regardless of the hard damper setting. The same effect can be gained simply by employing a lightly damped conventional suspension. However, systems having stiffer springs ( $K_s=20\text{kN/m}$ ,  $30\text{kN/m}$ ) show encouraging performance gains when employing a soft switching damper. The improvements in ride comfort relative to an equivalent passive system can be quantified by comparing any point on a particular curve with the first point ( $C_{soft}/C_{hard} = 1$ ). So, taking the case of  $K_s=30\text{kN/m}$  and  $C_{hard}=1.85\text{kNs/m}$

for example, a 20% reduction in discomfort parameter is available - without a significant increase in the tyre loading parameter - by introducing the switching option. There is another practical implication of these results. The advantages of the switchable system could be exploited by choosing a higher than conventional value of spring stiffness, and at the same time, using less workspace and retaining the tyre loading parameter and ride comfort of the equivalent passive system. The higher spring stiffness would result in improved body attitude control for both static and dynamic conditions. Although the details are not shown here, the results indicate that it is possible to increase the spring stiffness with a hard/soft switching damper and maintain the same overall ride performance (ie. ACC, DTL and SWS figures) as the equivalent softer passive suspension.

## 5.6 Concluding Remarks

This chapter examines the performance of selected controllable damper systems. Three suspensions are described, namely the continuously variable, two-state switchable, and three-state adaptive damper designs, each design being mounted in parallel with a conventional passive spring. A single road surface description, representing a rough minor road, together with a single vehicle speed of 20 m/s, has been used throughout. Since the advantages of the adaptive system will only appear over a range of surfaces (Chapter 9), work in this chapter concentrates on the continuously variable and two-state switchable damper systems. These theoretical results lead to the following conclusions :

1. Performance of the continuously variable damper system is considerably improved if the conventional spring is taken into account when calculating feedback gains.

2. Although not as effective as the limited state active suspension, the continuously variable design shows worthwhile improvements in ride comfort over the passive system. This performance deteriorates as the spring stiffness is increased; however some improvements over the passive system are still possible when  $K_s=30\text{kN/m}$  (ie. higher than the passive system stiffness of  $22\text{kN/m}$ ).
3. Switchable system performance depends more heavily on the spring stiffness. Stiff suspensions employing a soft switching damper show significant comfort improvements. These improvements, particularly at high damping levels, can be obtained whilst retaining the road holding ability of the passive system. Soft suspensions, on the other hand, benefit little from the introduction of soft switching.
4. The psd comparison shows that the performance of the continuously variable system is achieved in a similar manner to that of the active system. Both systems are effective at controlling events around the body resonance frequency, but can do little to improve performance at the “wheelhop” frequency. Consequently any improvements in dynamic tyre loading are achieved through a reduction in the body resonance peak. Conversely, the switchable system psd more closely resembles that of the passive suspension, and ride comfort improvements are achieved through reductions in the frequency range up to  $10\text{Hz}$ . However, these improvements are at the expense of an increase in dynamic tyre loading at the wheel resonance frequency.

The results in this chapter assume ideal components and therefore represent the best possible performance of each system under the given conditions. The effect of practical limitations in the real system will be established in Chapter 6.

6. Any practical implementation of the controllable strategy will include ad-

ditional algorithms, allowing the damper to return to a hard or conventional passive setting during manoeuvring or braking. This will involve a separate control loop, and does not affect the comparisons of ride performance for straight running at constant vehicle speed.

# Chapter 6

## Effect of Practical Limitations

### 6.1 Introduction

In recent years the majority of research into intelligent suspension systems, for example by Thompson [1984] and Chalasani [1986 a] [1986 b], has concentrated on systems having idealised components. Published details of hardware limitations and their effect on performance are still scarce. Miller [1988] has studied the effect of such limitations on a two-state switchable damper system - but only with reference to a single degree of freedom model, which appears to misrepresent the important aspect of dynamic tyre/ground load. Others, including Sharp and Hassan [1986 b] and Crolla and Aboul-Nour [1988] include a time response in their calculations but do not consider in detail the effect this has on performance.

The aim of this chapter is to compare the selected controllable damper systems in a similar style to Chapter 5, but this time incorporating realistic practical constraints in the vehicle model. Firstly, the response of damper valves used for each system will be subject to some form of time delay. Secondly, in the case of the continuously variable damper, constraints will exist on the maximum and minimum levels of damper valve setting.

## 6.2 Modelling of Limitations

### 6.2.1 Time Delay Characteristics

#### Continuously variable damper

In practice the continuously variable damper is likely to respond to the demand signal by opening or closing some orifice. A number of designs have been proposed, including those by Parker and Lau [1988], who describe the development of an electrically controlled floating disc valve fitted to a modified conventional shock absorber, and Doi *et al* [1988] who considers a prototype valve which is positioned in the oil flow between a hydraulic actuator and gas spring accumulator.

It would be impractical to assume that the response of any valve is instantaneous and therefore, in a similar style to Doi, first order lag dynamics are used here to represent the switching action. The modelling procedure is as follows ;

1. At each step in the simulation a demand damping coefficient ( $C$ ) is calculated using the linear relationship ;

$$C = \frac{u}{\dot{z}_1 - \dot{z}_2} \quad (6.1)$$

where  $u$  is the force demanded by the control law (Eqn (4.29)).

If the demand force is dissipative (determined by Eqn (5.12)) the valve will respond by changing the orifice size to achieve the damping coefficient  $C$ . Alternatively, if the value of  $u$  represents a demand for power input, the orifice will open fully and the damping coefficient becomes zero (or more correctly, some minimum value - see Sect 6.2.2). In both cases the response will be subject to a delay.

2. Using the standard equation describing a first order lag, the delay is incorporated in the model by letting the actual damping coefficient become one of the system states,  $c_a$ , such that ;

$$T\dot{c}_a + c_a = C \quad (6.2)$$

where  $T$  is the time constant, and represents the time taken taken for the actual damping coefficient to reach 63% of its required value (see for example, Schwarzenbach and Gill [1984]).

3. The actual damping force at each time step is then given by :

$$u_a = c_a(\dot{z}_1 - \dot{z}_2) \quad (6.3)$$

The demand damping coefficient,  $C$ , and the actual damping force,  $u_a$ , are both represented in Eqn (2.11) by elements of the vector  $f$ , such that  $f = [C \ u_a]^T$ . Eqn (6.2) is then combined with Eqn (2.11) using the extended vector  $z_s = [z \ c_a]^T$ , and the resulting coefficient matrices are related to those of the basic controllable damper by :

$$\begin{aligned} MXDD_s &= \begin{bmatrix} MXDD_c & 0 \\ 0 & 0 \end{bmatrix}, MXD_s = \begin{bmatrix} 0 & 0 \\ 0 & T \end{bmatrix} \\ MX_s &= \begin{bmatrix} MX_c & 0 \\ 0 & I \end{bmatrix}, MF_s = \begin{bmatrix} 0 & MF_c \\ I & 0 \end{bmatrix} \\ MU_s &= \begin{bmatrix} MU_c \\ 0 \end{bmatrix} \end{aligned} \quad (6.4)$$

### Switchable damper

In contrast to the continuously variable damper, the two-state switchable damper involves hardware which has been available for some time. The switchable valve modelled here is based on an existing electro-magnetic valve used by Monroe

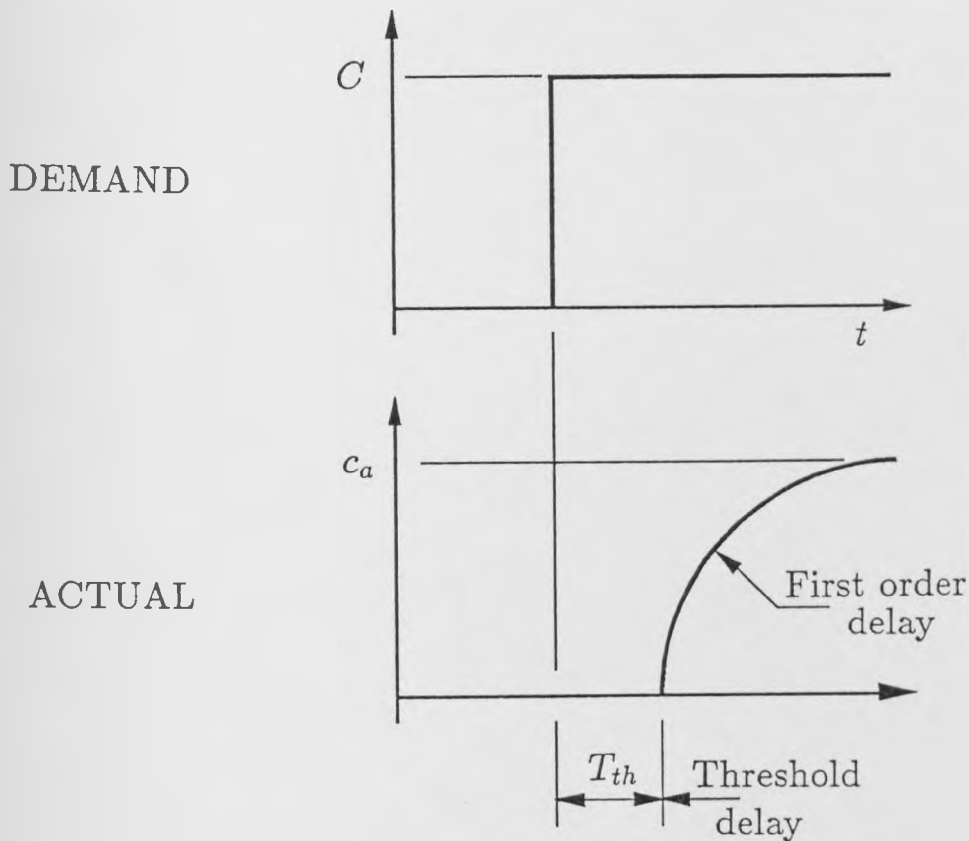


Figure 6.1: Valve response details of the switchable damper.

(UK) Ltd. Practical work on the valve, by Monroe, has shown the response to consist typically of a threshold delay followed by a first order lag (Fig 6.1). On a change in demand signal, the valve will remain in its original position until the threshold delay,  $T_{th}$ , has elapsed (typically 10 msec) and then will respond according to first order lag dynamics. The valve will not respond to any change in demand signal which is of duration less than the threshold delay. This delay time is different to a conventional transport delay in that no output occurs unless a certain time threshold is exceeded and hence the use of the term “threshold” delay to describe it.

The threshold delay is included in the vehicle model using a counter within the simulation (SIM) file used in VDAS, which resets to zero every time there is a change in demand signal. The counter advances at each step through the simulation, and will not allow an actual change in damping until the threshold

delay has elapsed. It follows that the length of the modelled delay is a multiple of the length of each time step, which in turn depends on the number of points in the simulation, the length of profile, and the vehicle speed. In this chapter 2048 points are used over a 340m profile, and therefore, with a vehicle speed of 20m/s, the threshold delay is a multiple of 8ms. The subsequent first order lag is modelled in the same way as the continuously variable damper and the equations of motion are as described by Eqn (6.4). A computer flow chart describing the simulation of the switchable damper is shown in Fig 6.2.

Using dampers with  $T_{th}$  values of zero and 16ms, Figs 6.3 and 6.4 show the time histories of a simulated run over a road profile with psd described by Eqn (3.1). In each case the damper is assumed to have a first order delay which has a time constant of 10ms. For clarity, only one second of a 17 second simulation is shown, with each figure displaying plots of absolute and relative body velocity together with their associated demand and actual damping coefficients. The effect of the first order lag on actual damping coefficient can clearly be seen in both figures, whilst in Fig 6.4, the graph of actual damping coefficient highlights the models lack of response to any signal of shorter duration than its threshold delay, for example, the demand changes; soft to hard after 15.3 seconds, or hard to soft after 15.65 seconds.

### **Adaptive damper**

Valve switching dynamics included in the three-state adaptive system model, based on the Monroe ASC system, also consist of a threshold delay followed by a first order lag. However, in this case, the switching times will be short compared to the minimum time spent in each setting and consequently, it is expected that variation in time constants and delays will have little effect on system performance.

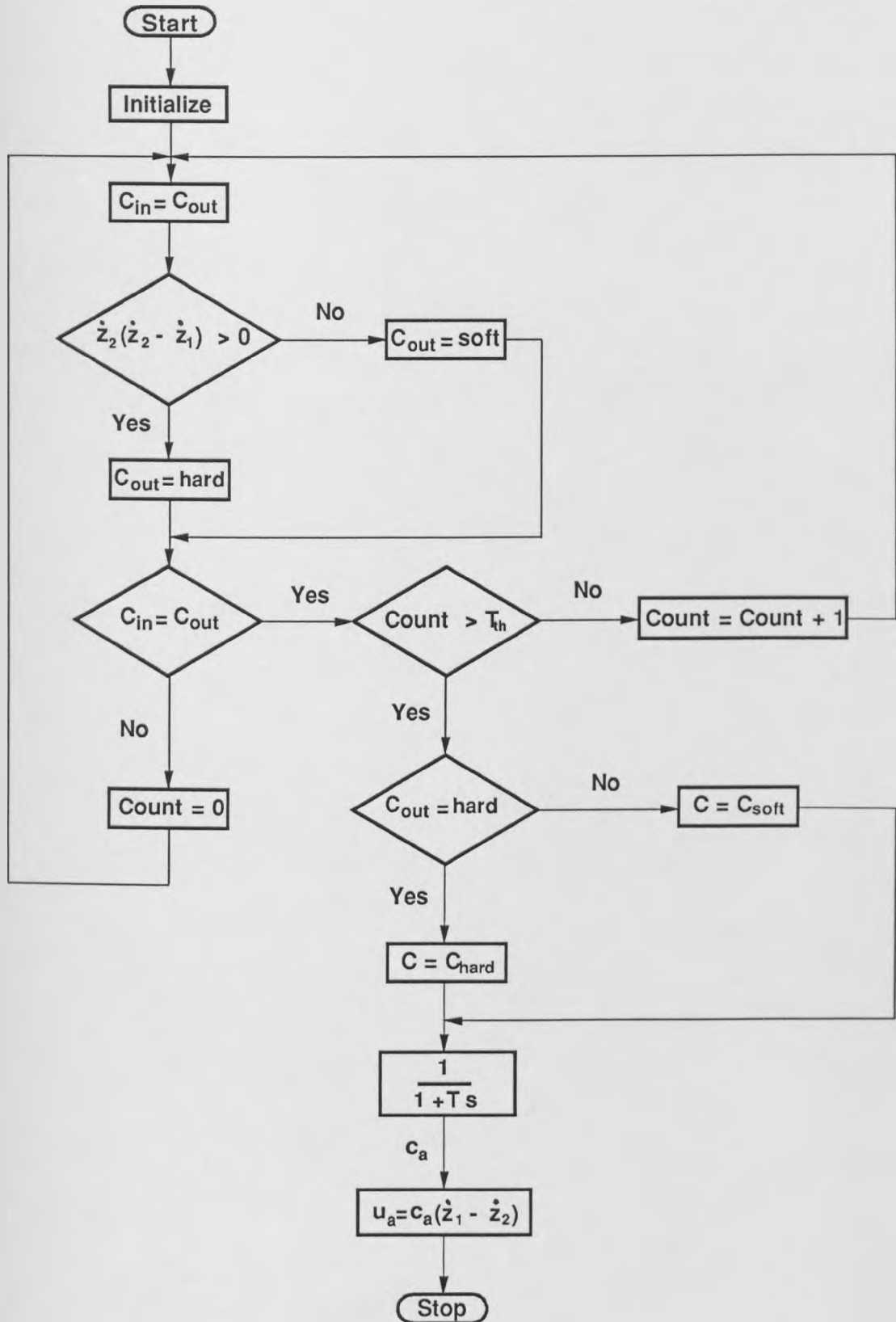


Figure 6.2: Computer simulation of the switchable damper system.

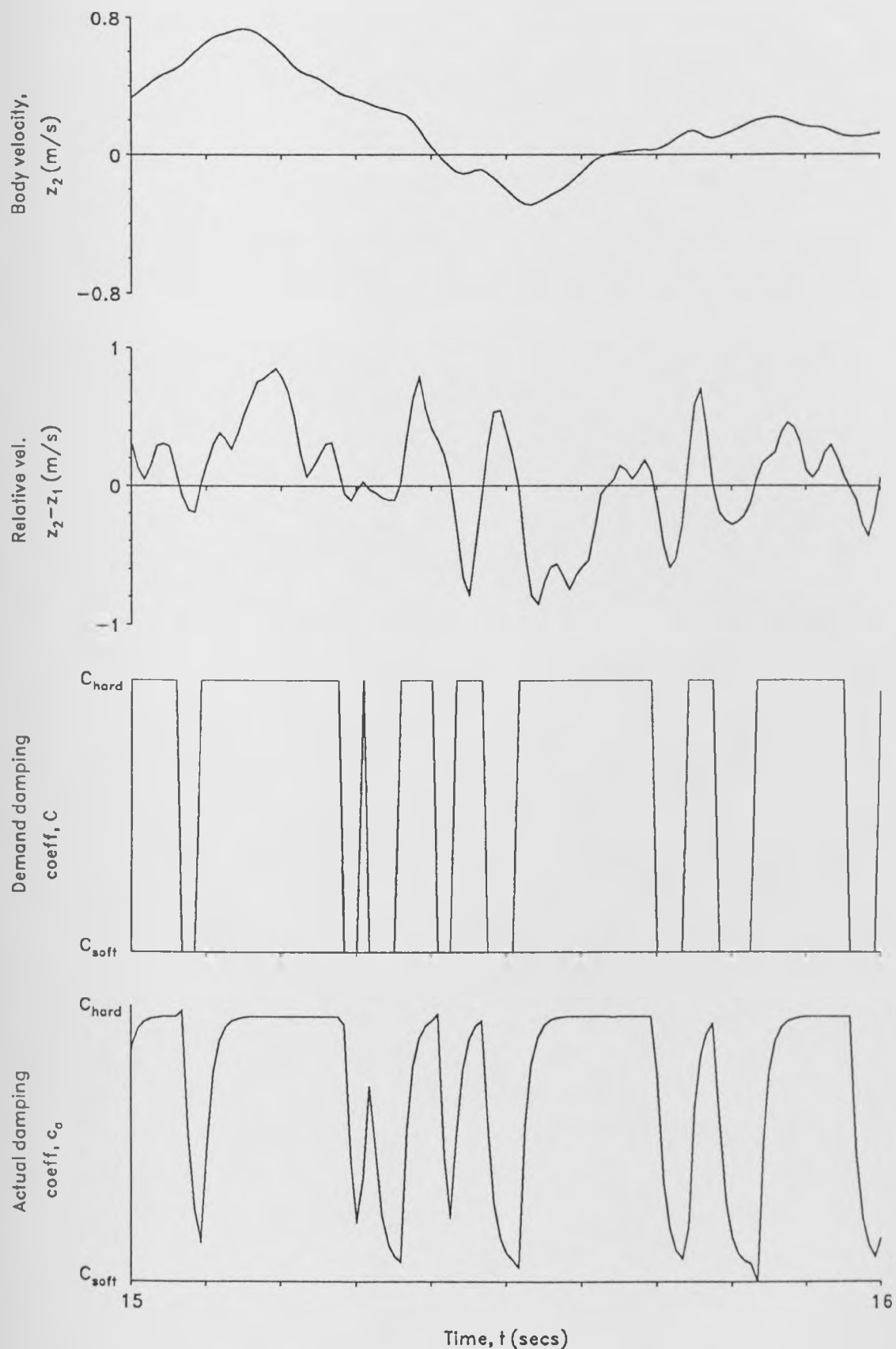


Figure 6.3: Switchable damper system - time histories of absolute and relative body velocity with associated demand and actual damping coefficients ( $T=10\text{ms}$ ,  $T_{th}=0$ ).

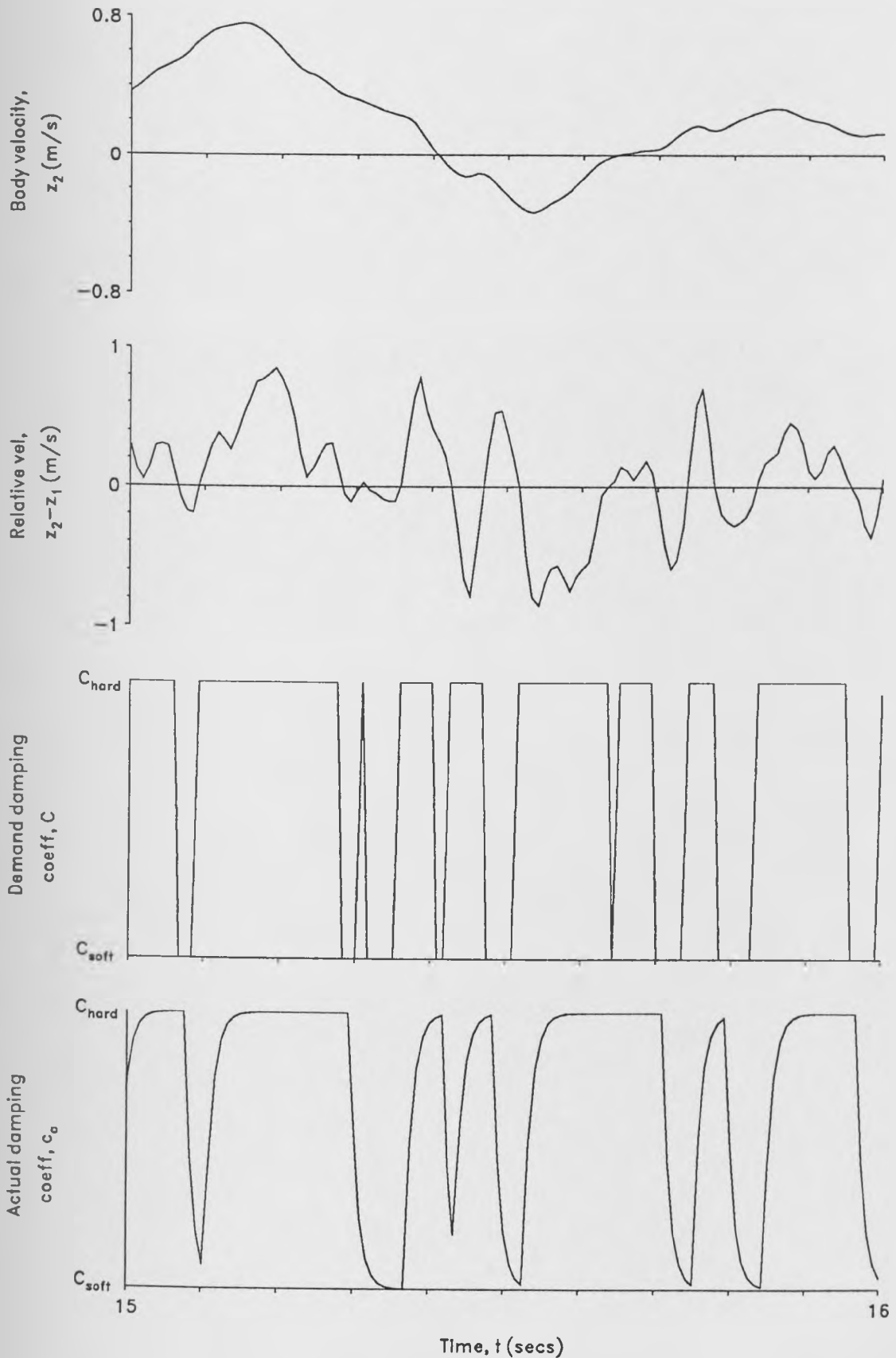


Figure 6.4: Switchable damper system - time histories of absolute and relative body velocity with associated demand and actual damping coefficients ( $T=10\text{ms}$ ,  $T_{th}=16\text{ms}$ ).

## 6.2.2 Damping Constraints

A very low demand force, or alternatively a demand for power input, will request the largest valve orifice size. This corresponds to some minimum value of damping coefficient,  $C_{min}$ . Similarly a maximum level,  $C_{max}$ , must also exist when the variable orifice is fully closed. This would typically be governed by standard control valves within the damper and would act as a safety measure should the proportional valve fail. Both the upper and lower limits of damping must be imposed on the vehicle model during simulation and can be seen clearly in Fig 6.5, where  $C_{min}=0.3\text{kNs/m}$  and  $C_{max}=2.5\text{kNs/m}$  are used as an example. This force/velocity plot is obtained, in the style of Fig 5.2, from the time histories of damper force and suspension velocity during a simulated run over the same road profile used in Chapter 5.

A flow chart outlining the modelling procedure of the continuously variable damper system, and showing the steps to include the time delay and damping constraints, is seen in Fig 6.6.

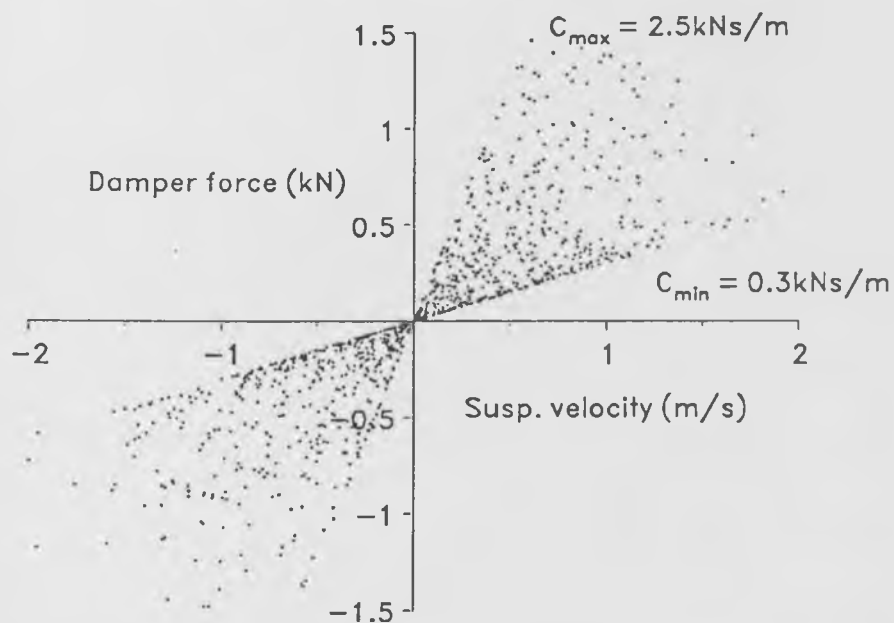


Figure 6.5: Force/velocity plot of the continuously variable damper showing damping constraints.

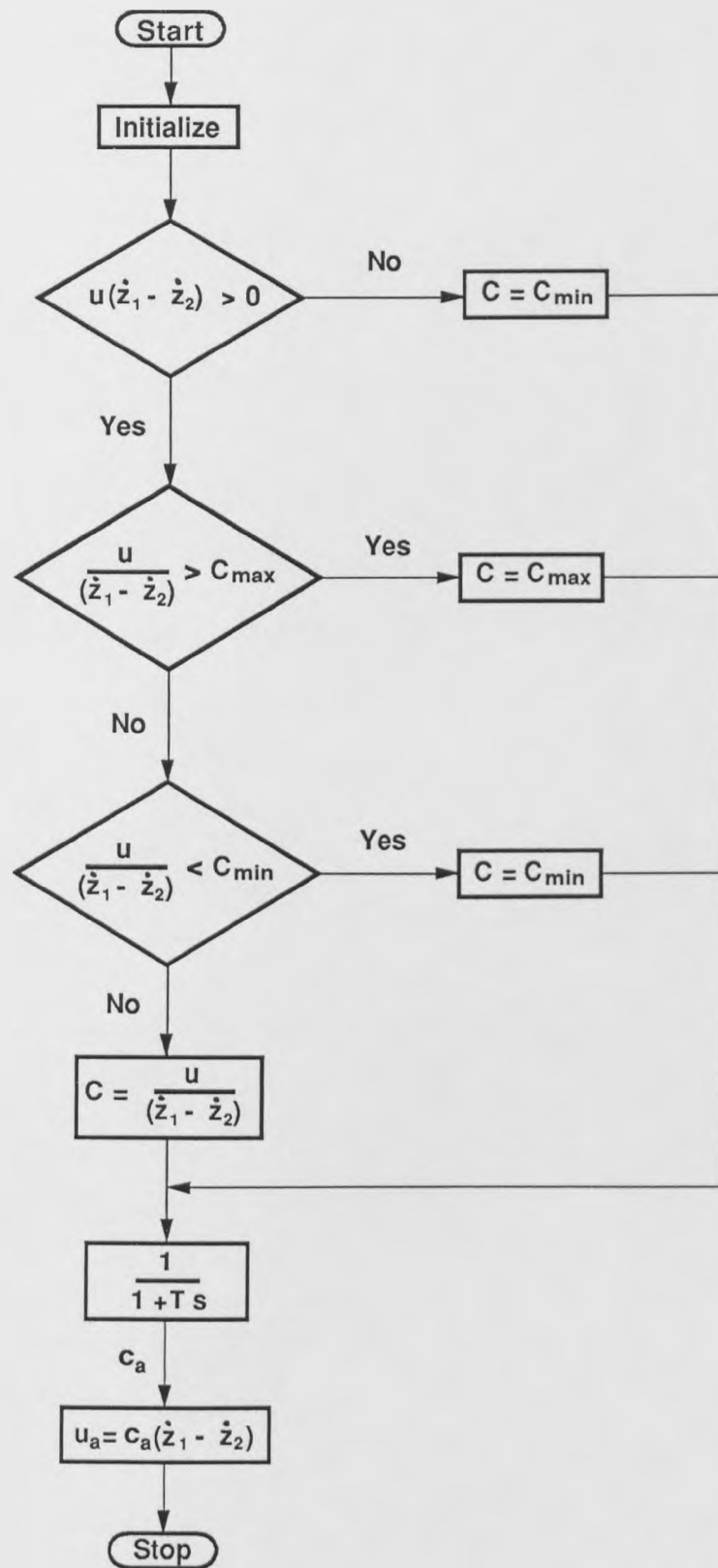


Figure 6.6: Computer simulation of the continuously variable damper system.

## 6.3 Results

### 6.3.1 Effect of Time Delays

Figs 6.7 and 6.8 examine the effect of the first order time delay only on the performance of the continuously variable and two-state switchable damper systems respectively. Both systems employ a spring stiffness equal to that of the passive system described in Table 3.1 (22kN/m), and delays having time constants ( $T$ ) of 5, 10 and 15ms are considered in each case. The performance of each system is compared against that of the passive and corresponding ideal controllable system, on an equal workspace basis (SWS=0.029m). The performance of the the passive design described in Table 3.1 is again shown by point P. The switchable system is studied further in Fig 6.9. The results here are more elaborate in that they cover a range of hard damper settings (1.32, 1.85 and 2.38kNs/m) and two spring stiffnesses (20kN/m and 30kN/m). Consequently they cannot be plotted on an equal workspace basis and are shown in the style of Fig 5.10. For a given combination of ( $C_{hard}$ ) and ( $K_s$ ), a set of three curves are shown, one for each time constant ( $T$ ). Although each set of curves uses a different amount of suspension working space, within each set the SWS value again remains constant to +1%.

Figs 6.10(a) and (b) show the effect of the first order time delay on the psd's of ISO weighted vertical body acceleration for selected continuously variable and switchable systems respectively. Points a, b, and c, on the continuously variable curves in Fig 6.7 are chosen for more detailed comparison in the psd curves on the basis that they have an equal tyre load performance. For a similar reason the switchable damper systems are chosen for psd analysis from Fig 6.8, with points d, e and f each having a  $C_{soft}/C_{hard}$  ratio of 0.3.

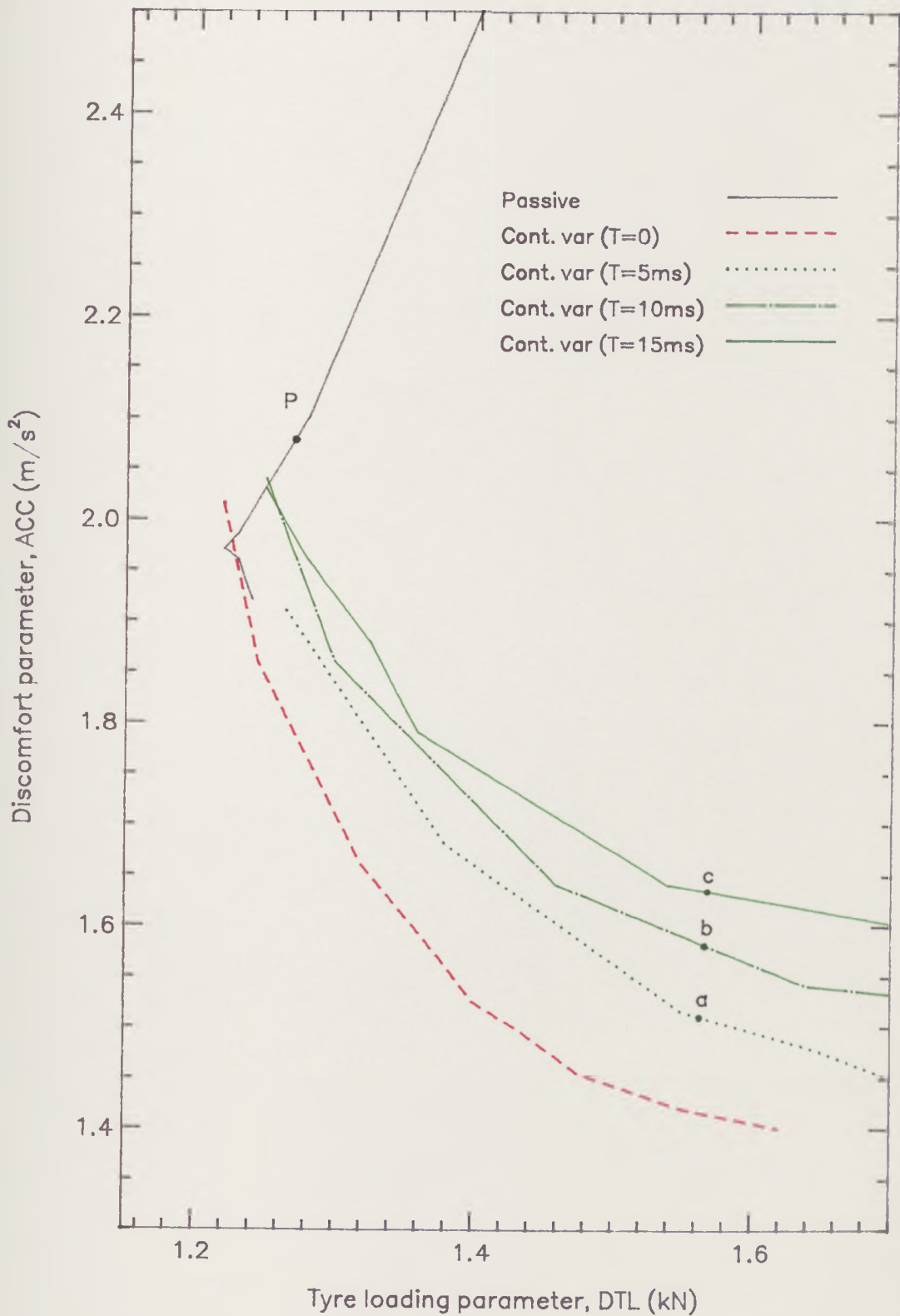


Figure 6.7: Continuously variable damper system - effect of variation in first order time constant,  $T$ , ( $K_s=22\text{kN/m}$ ,  $\text{SWS}=0.029\text{m}$ ).

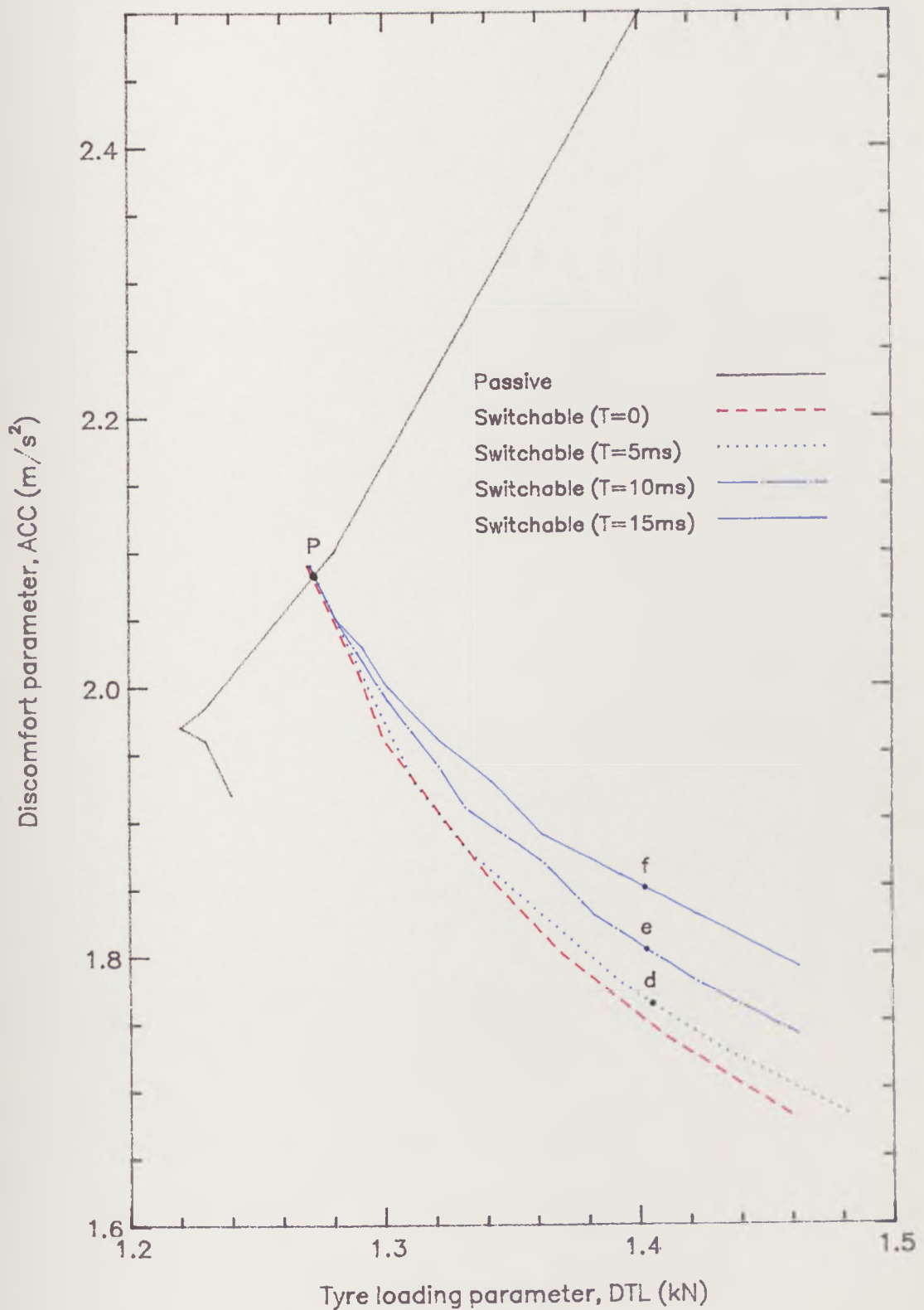


Figure 6.8: Two-state switchable damper system - effect of variation in first order time constant,  $T$ , ( $K_s=22\text{kN/m}$ ,  $C_{hard}=1.5\text{kNs/m}$ ,  $\text{SWS}=0.029\text{m}$ ).

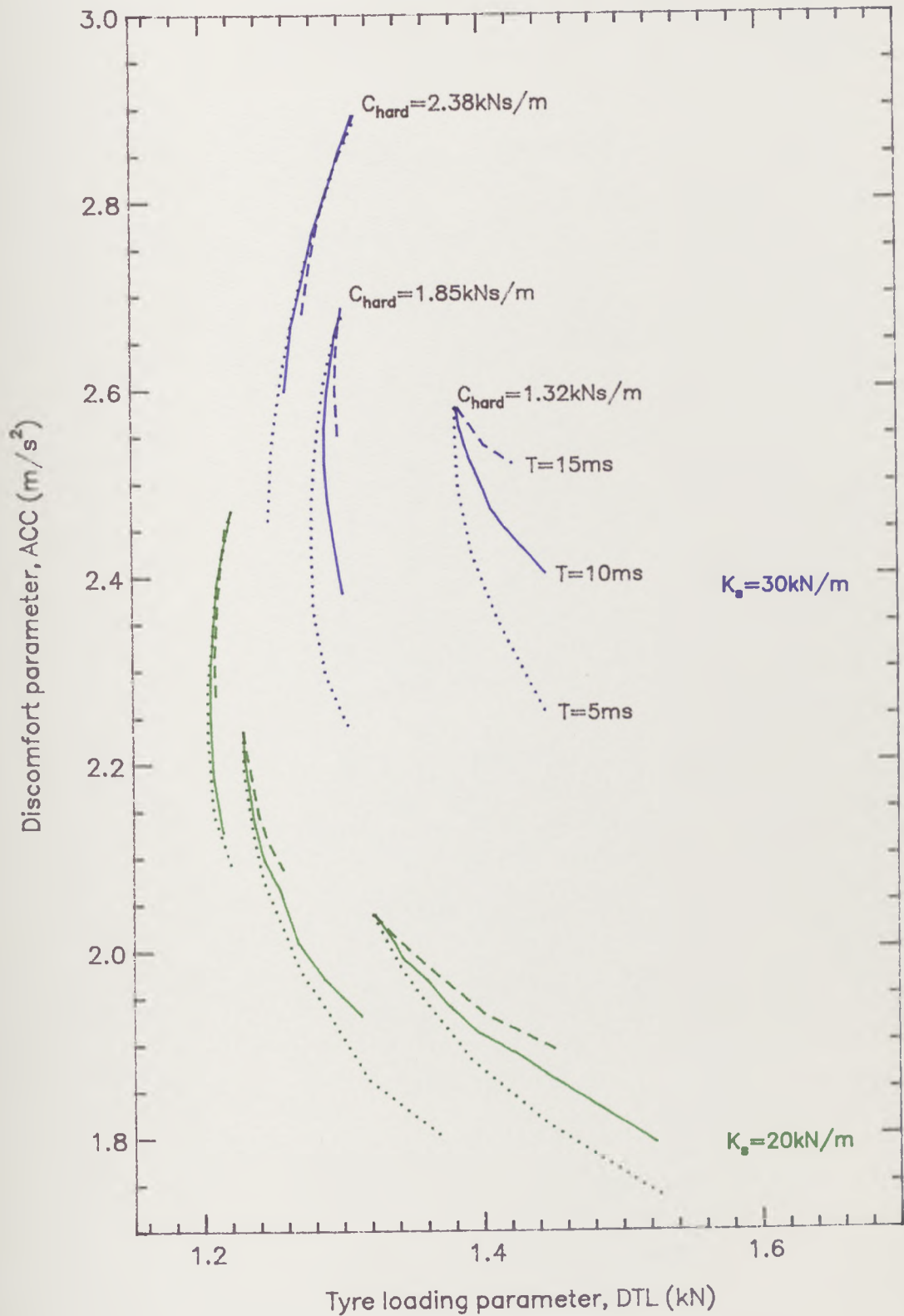


Figure 6.9: Two-state switchable damper system - variation in first order time delay at different suspension spring stiffnesses.

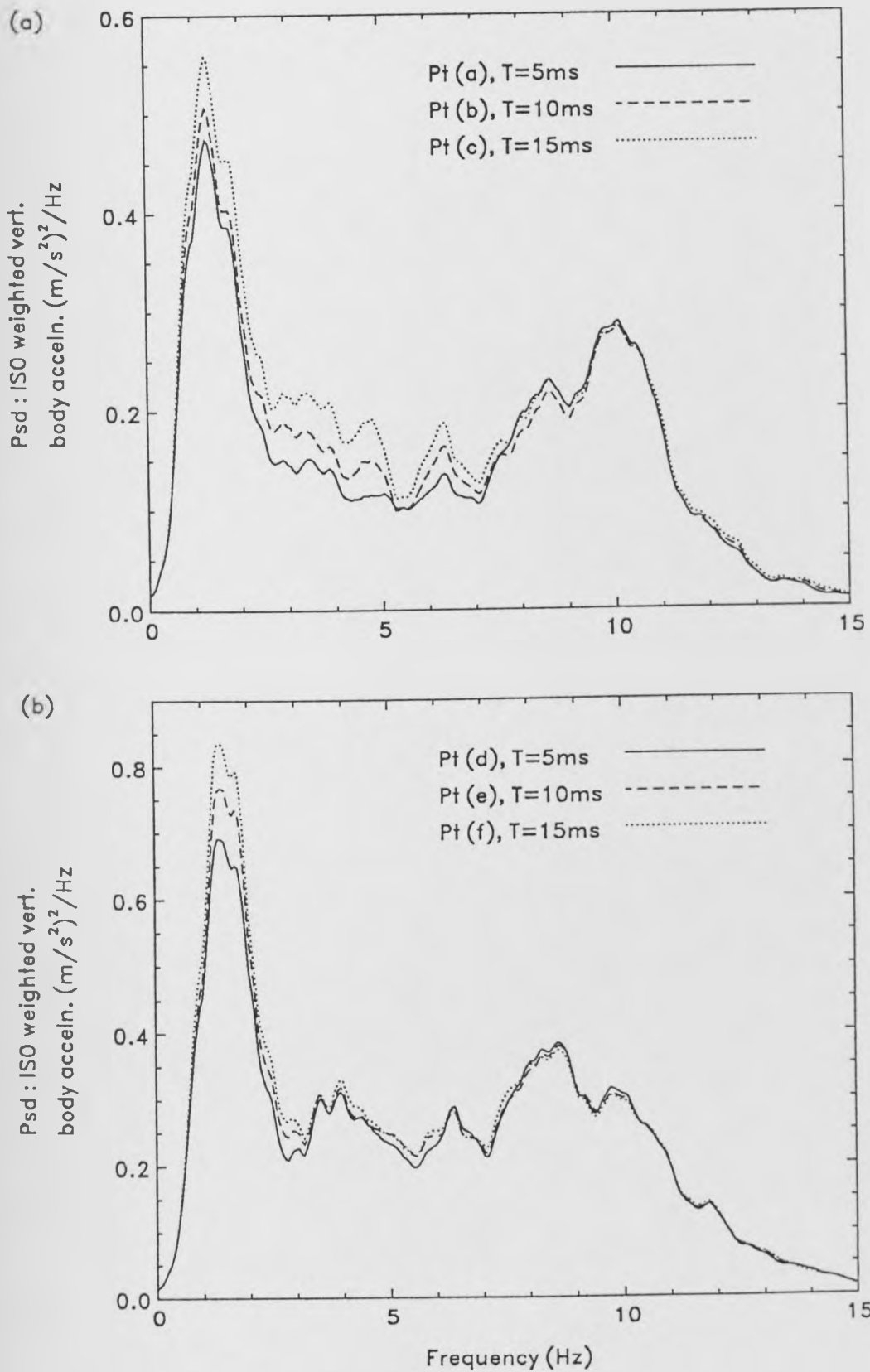


Figure 6.10: Psd's of ISO weighted vertical body acceleration showing the effect of variation in first order time delay of the continuously variable (a) and switchable damper systems (b).

Table 6.1 considers the effect of the threshold delay on the performance of the two-state switchable damper system. Two systems having  $T_{th}$  values of 8 and 16ms in addition to a first order lag ( $T=10$ ms), are compared against a switchable damper having a first order lag only.

$\frac{C_{soft}}{C_{hard}}$	First order lag only (10ms)			First order lag (10ms) + 8ms threshold delay			First order lag (10ms) + 16ms threshold delay		
	ACC (m/s <sup>2</sup> )	SWS (m)	DTL (kN)	ACC (m/s <sup>2</sup> )	SWS (m)	DTL (kN)	ACC (m/s <sup>2</sup> )	SWS (m)	DTL (kN)
1.0	2.30	0.0253	1.22	2.30	0.0253	1.22	2.30	0.0253	1.22
0.8	2.21	0.0252	1.22	2.22	0.0253	1.23	2.23	0.0255	1.23
0.6	2.12	0.0251	1.23	2.13	0.0252	1.24	2.17	0.0258	1.24
0.4	2.01	0.0252	1.26	2.05	0.0254	1.26	2.11	0.0263	1.28
0.2	1.91	0.0257	1.31	1.95	0.0258	1.32	2.05	0.0268	1.33

Table 6.1: Effect of the threshold delay on the switchable damper system ( $C_{hard} = 1.85$ kNs/m,  $K_s = 20$ kN/m).

### 6.3.2 Effect of Damping Constraints

The effect of the minimum ( $C_{min}$ ) and maximum ( $C_{max}$ ) damping constraints on the performance of the continuously variable damper system is considered in Figs 6.11 and 6.12 respectively. Initially, in Fig 6.11, no maximum damping level is set and the minimum damping level is given values of 0.1, 0.3, and 0.5 kNs/m. Then, taking the valve response time constant ( $T$ ) to be 10ms, the performance

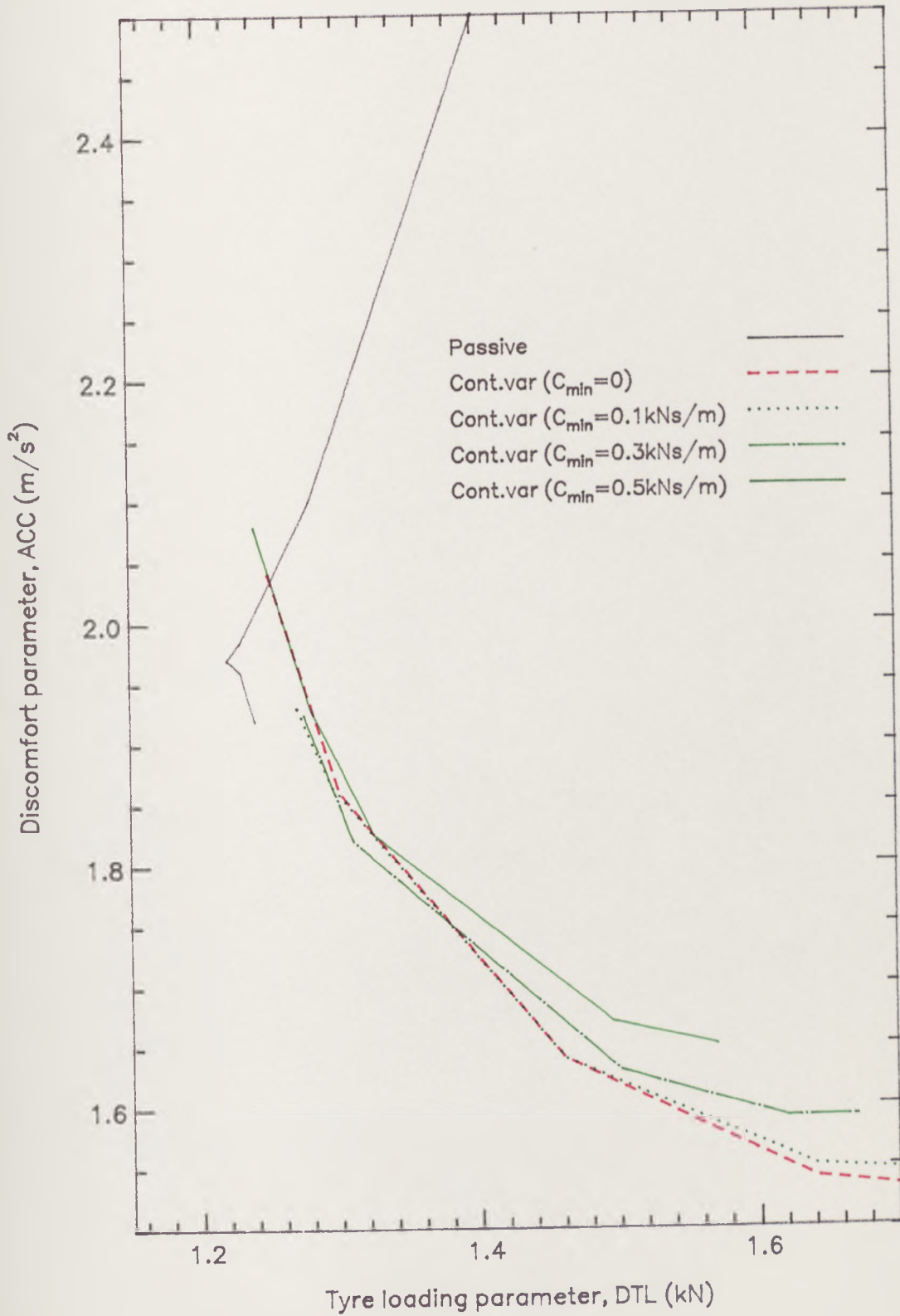


Figure 6.11: Continuously variable damper system - effect of the minimum damping coefficient,  $C_{min}$ , ( $K_s=22\text{kN/m}$ ,  $\text{SWS}=0.029\text{m}$ ).

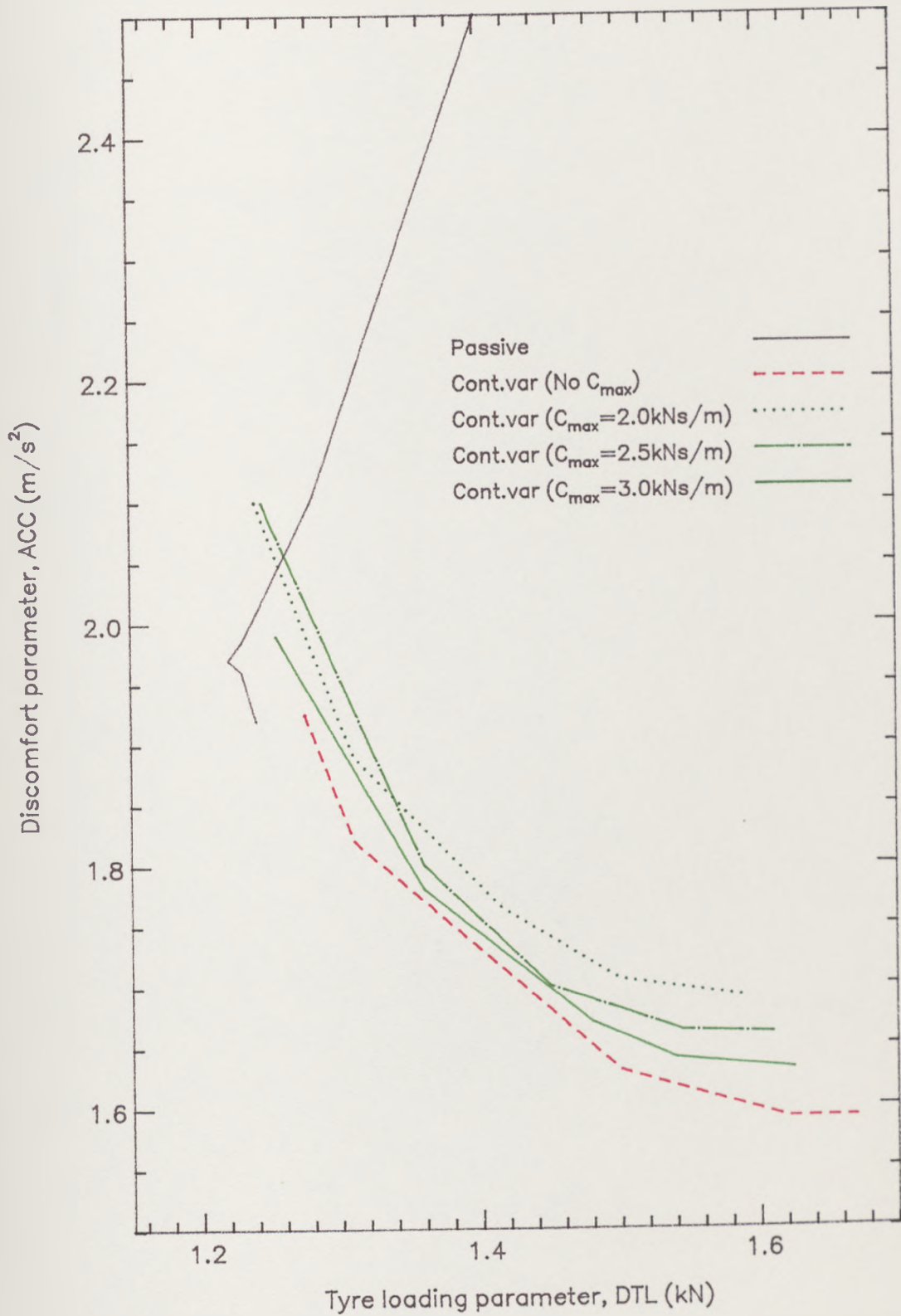


Figure 6.12: Continuously variable damper system - effect of the maximum damping coefficient,  $C_{max}$ , ( $K_s=22\text{kN/m}$ ,  $C_{min}=0.3\text{kNs/m}$ ,  $\text{SWS}=0.029\text{m}$ ).

of these three systems is compared against that of the unconstrained model. Taking the minimum damping level of 0.3kNs/m as an example, Fig 6.12 then examines the performance when the system is also given maximum damping constraints of 2.0, 2.5, and 3.0 kNs/m.

## 6.4 Discussion of Results

Figs 6.7 and 6.8 highlight the importance of short first order response times for the continuously variable and two-state switchable damper systems respectively. As the time constant ( $T$ ) is increased from zero to 15ms, the performance of both systems, in terms of ride comfort deteriorates significantly. Looking first at the continuously variable damper, Fig 6.7 shows that the adverse effect of an increase in  $T$  is more noticeable if the system is operating under a control law which is biased toward comfort. These systems, for a given tyre load performance, show an increase in discomfort parameter (ACC) of approximately 5% for every 5ms increase in  $T$ . On the other hand, for systems which are biased in favour of road holding and have approximately the same tyre load performance as the passive suspension (P), the increase in ACC is only 2% for every 5ms increase.

Similar performance losses can be seen for the switchable damper system in Fig 6.8. As expected, in this case the reduction in ride comfort due to the valve response is greater when the hard and soft settings are wider apart, ie. low values of  $C_{soft}/C_{hard}$ . For this particular system ( $K_s=22\text{kN/m}$ ,  $C_{hard} = 1.5\text{kNs/m}$ ), with a  $C_{soft}/C_{hard}$  value of 0.2, the increase in ACC is around 3% for a 5ms increase in time constant.

Concentrating further on the switchable damper system, it is clear in Fig 6.9 that the detrimental effect of the first order time delay becomes greater when

it is applied to systems which offer the greatest potential ride improvements, ie. stiff systems. At  $K_s=30\text{kN/m}$  and  $C_{soft}/C_{hard}=0.2$  the increase in ACC for every 5ms increase in time constant, is now approximately 6%. Nevertheless, even when the time constant  $T=15\text{ms}$ , providing the hard damping coefficient is set high (for example  $C_{hard}=2.38\text{kNs/m}$ ), ride comfort improvements of 15% are still possible over the equivalent hard passive design.

The deterioration in ride comfort for both the continuously variable and switchable damper systems can also be seen in the psd's of Figs 6.10(a) and (b). For both systems, the inclusion of a first order lag in the vehicle model is seen to result in an increase in vertical body acceleration across the frequency range 0 to 10Hz.

The threshold delay has not been included in the calculations to obtain the two-state switchable damper system results in Fig 6.8 or 6.9. The introduction of this limitation to the switchable model further affects performance in terms of comfort and tyre loading, and has the added effect of increasing the usage of suspension working space for a given value of  $C_{soft}/C_{hard}$ . For a system having  $K_s=22\text{kN/m}$  and  $C_{hard}=1.85\text{kNs/m}$ , Table 6.1 shows that this increase is only slight if the  $T_{th}=8\text{ms}$ . However, if  $T_{th}$  is increased to 16ms, there is a significant rise in SWS such that at  $C_{soft}/C_{hard}=0.4$  the usage of suspension working space has increased by approximately 4% over an equivalent passive system.

The effect of the maximum ( $C_{max}$ ) and minimum ( $C_{min}$ ) damping constraints imposed on the continuously variable damper system seen in Figs 6.11 and 6.12 respectively, is to further restrict the ride performance of the suspension. This only appears to be a problem if the system performance index has been biased towards comfort. The curves for various values of maximum and minimum damping tend to converge as the system tyre load performance is reduced, and there becomes little difference in their respective discomfort parameters.

In general though, it appears that the minimum damping constraint has the greatest adverse effect on ride and for a comfort biased design with a  $C_{min}$  value of 0.5kNs/m, the increase in ACC over a system with no damping constraints is around 5%. Recent prototype valves suggest that this value may be pessimistic and therefore  $C_{min}=0.3\text{kNs/m}$  is selected before the addition of maximum damping constraints in Fig 6.12.

From a ride comfort point of view it is obvious that the range of available damping should be as wide as possible. In the case of the maximum constraint, although it is practically possible to achieve any value of  $C_{max}$ , it must also be remembered that this higher limit provides the system damper setting during failure mode, or at any time the ride control law is overridden by the additional handling algorithm. During these modes it will still be necessary to maintain an acceptable level of comfort and this must be reflected in the final choice of  $C_{max}$ . Fortunately, Fig 6.12 shows that the maximum limit can be reduced as low as 3.0kNs/m before a significant effect on performance is seen. For such a system, the ACC value of a comfort biased system is increased by approximately 3% with the introduction of an upper limit of 3.0kNs/m. Further increases of 3% are also seen as the limit is reduced through 2.5 to 2.0kNs/m.

## 6.5 Concluding Remarks

In this chapter, some of the limitations present in realistic valve hardware are introduced into the vehicle model. In the case of the continuously variable damper system these consist of a valve response time delay, together with constraints on the available maximum and minimum damping settings. In the absence of any published test work, the proportional valve is assumed to respond according to first order lag dynamics. The valve response of the two-state switchable

and three-state adaptive damper systems are based on the results of practical testing, and consists typically of a “threshold” delay followed by a first order lag. In each case, the nature of the limitations are described and the modelling techniques are outlined. Using these more realistic models, the effect of the limitations on the performance of each system is determined. Following the assumption that switching times for the adaptive damper will be short in comparison to the length of time spent in each setting, results in this chapter concentrate on the continuously variable and two-state switchable damper systems. The conclusions to be drawn from these are ;

1. The ride improvements seen from the controllable damper systems in Chapter 5 are significantly impaired with the introduction of a first order time delay. In the case of the continuously variable damper the deterioration is greatest when the system is operating according to a comfort biased control law, where the increase in discomfort is approximately 5% for every 5ms increase in the time constant. The delay should obviously be as small as possible, but from a designers viewpoint, a time constant of 10 to 15ms is a reasonable target to aim for, achieving comfort gains of up to 20% over the conventional passive suspension.
2. As expected, the deterioration in performance due to the introduction of a first order time lag in the two-state switchable damper model is greater at low values of  $C_{soft}/C_{hard}$ . If the suspension has a spring stiffness equal to that of the standard passive system considered in Chapter 3 ( $K_s=22\text{kN/m}$ ) and a  $C_{soft}/C_{hard}$  value of 0.3, the increase in discomfort parameter is around 3% for every 5ms increase in the time constant. If a stiffer spring is used the performance losses are relatively greater, with an increase of approximately 5% for every 5ms increase in time constant at  $K_s=30\text{kN/m}$ . Nevertheless, worthwhile overall improvements may still

- be achieved, particularly if the hard setting,  $C_{hard}$ , is given a higher value than the damping coefficient of the standard passive system.
3. Psd's show that the deterioration in discomfort parameter of both systems is caused by an increase in ISO weighted vertical body acceleration in the frequency range 0 to 10Hz.
  4. The performance of the switchable system is compromised further by the presence of a threshold delay in the valve response. As well as affecting the ride and road holding performance of the suspension, this delay has the additional effect of increasing the usage of suspension working space. Typically, for a damper with a  $C_{soft}/C_{hard}$  value of 0.2, the discomfort parameter is increased by a further 2% for every 8ms increase in threshold delay, with the dynamic tyre load affected to a lesser extent with an increase of only 1% for every 8ms. The effect on suspension working space increases as the value of the threshold delay increases. At 8ms, the effect on SWS is negligible but at 16ms the increase is around 4%. In this respect the threshold delay becomes an important feature of the response, and to prevent excessive use of working space the delay must not be allowed to increase much beyond the values considered here.
  5. The ride performance of the continuously variable system is also limited by the introduction of maximum and minimum damping constraints to the damper model. In general the effect of these is greater if the system is operating according to a comfort biased control law. The minimum constraint,  $C_{min}$ , appears to be the most important with its effect becoming progressively worse as the value of  $C_{min}$  is increased. A value of 0.1kNs/m has very little effect on performance, but with  $C_{min}=0.5kNs/m$  the discomfort is typically increased by 5% over a system with no damping constraints. It is clear therefore, that the designer must aim to provide

a minimum setting which is as low as possible. The choice of maximum setting,  $C_{max}$ , is governed to a large extent by the handling and safety aspects of the suspension requirements. Fortunately, this constraint is not as detrimental to ride performance and, for a  $C_{min}$  of 0.3kNs/m, can be reduced as low as 2.0kNs/m with only a 6% increase in discomfort.

6. In a similar style to the switchable damper, the valve switching dynamics of the three-state adaptive damper also consist of a threshold delay followed by a first order lag. Since the switching times will be short in comparison with the length of time spent in each setting, they will have less effect on performance and therefore are not considered in detail here.

# Chapter 7

## Half-Vehicle Model Studies

### 7.1 Introduction

The quarter vehicle model has been used throughout previous chapters to establish the performance of the competing passive, active and controllable damper systems, and it is accepted that this model provides a sufficiently accurate insight into the basic ride performance of each system. In the case of the active and continuously variable damper (semi-active) systems, the model has also been used, in conjunction with linear optimal control theory, to generate various control laws. However, any control law derived using a single wheel station cannot take into account the correlations which occur between wheel inputs; (a) between left and right tracks, typically described by a coherence function, and (b) the correlation between front and rear inputs, arising from the fact that the rear wheel input is, as a first approximation, a delayed version of that at the front. Extension of the model, to represent a half or full vehicle, may prove to be beneficial if the control laws can take advantage of these correlations.

The possibility of incorporating this correlation information in the actuator control law has been considered by several authors in recent years. Although the inclusion of left/right coherency information in the control law has been proved by Abdel-Hady [1989] to have an insignificant effect on eventual predicted performance, more interesting results have been achieved in the case of control laws which account for front/rear correlation and take advantage of the fact

that the input to the rear wheel is a delayed version of that at the front. The physical idea of this effect, referred to throughout the work here as “wheelbase preview” is that the control law used to drive the rear actuator/damper can take advantage of the preview information obtained from the front suspension.

Two methods have been suggested for representing the delay between front and rear wheels. The first, presented by Louam *et al* [1988] and based on discrete optimal control theory, obtains a control law for a half vehicle model in which the wheelbase preview information occurs naturally in the optimisation process, providing substantial performance improvements. Although this method is optimal, it is also rather elaborate and implies that the system must be optimised at each time step. The calculations required to perform such operations are time consuming and may present significant practical difficulties. Another approach is presented by Fruhauf [1986] and later Abdel-Hady [1989], who, using a full vehicle model, transform the system with time delay into an equivalent linear one without time delay. A Pade approximation is used to simulate the delay between front and rear wheel inputs, and although this approximation results in a sub-optimal control law, both studies recorded significant improvements in performance over a system using an uncorrelated control law.

All work so far has concentrated on fully active systems. This chapter, using a half vehicle model and the Pade approximation technique, extends the work by Abdel-Hady [1989] to examine the effect of including wheelbase preview on the semi-active continuously variable damper system.

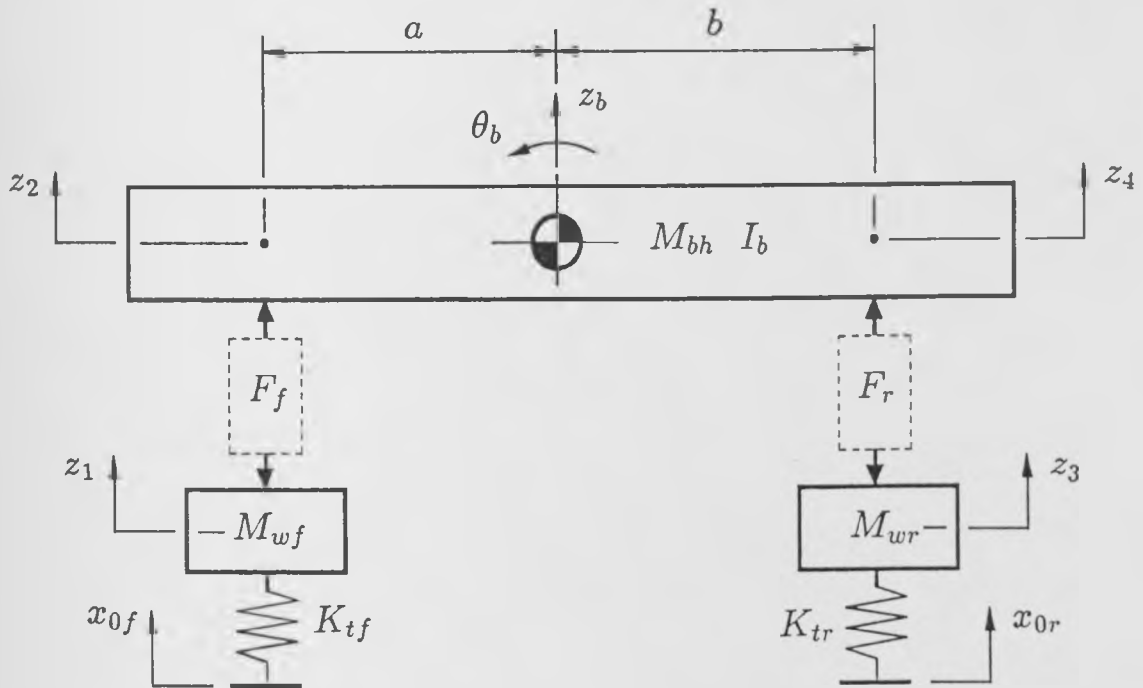


Figure 7.1: The half vehicle model.

## 7.2 Equations of motion

The basic half vehicle model used throughout this chapter was introduced briefly in Chapter 2 and is shown in more detail in Fig 7.1. The vehicle body itself is assumed to be rigid and has degrees of freedom in the vertical and pitch directions. The body mass and pitch inertia are represented by  $M_{bh}$  and  $I_b$  respectively, whereas the notation used for wheel masses, suspension elements and tyre stiffnesses is consistent with previous chapters except for an additional suffix,  $f$  or  $r$ , to denote front and rear respectively. The equations of motion can be written in two ways. In terms of body bounce ( $z_b$ ) and pitch ( $\theta_b$ ) at the centre of gravity they are ;

$$M_{wf}\ddot{z}_1 = K_{tf}(x_{0f} - z_1) - F_f \quad (7.1)$$

$$M_{wr}\ddot{z}_3 = K_{tr}(x_{0r} - z_3) - F_r \quad (7.2)$$

$$M_{bh}\ddot{z}_b = F_f + F_r \quad (7.3)$$

$$I_b\ddot{\theta}_b = -aF_f + bF_r \quad (7.4)$$

where  $F_f$  and  $F_r$  are general terms representing the front and rear suspension force respectively, of any system.

Since the output variables of interest are concerned with events at each end of the vehicle, it is more convenient to define the system using  $z_1$ ,  $z_2$ ,  $z_3$  and  $z_4$  as the state variables.

For small  $\theta_b$  ;

$$\ddot{z}_2 = \ddot{z}_b - a\theta_b \quad (7.5)$$

$$\ddot{z}_4 = \ddot{z}_b + b\theta_b \quad (7.6)$$

Allowing the equations of motion to be rewritten as :

$$\ddot{z}_1 = \frac{1}{M_{wf}} [K_{tf}(x_{0f} - z_1) - F_f] \quad (7.7)$$

$$\ddot{z}_2 = \left[ \frac{1}{M_{bh}} + \frac{a^2}{I_b} \right] F_f + \left[ \frac{1}{M_{bh}} - \frac{ab}{I_b} \right] F_r \quad (7.8)$$

$$\ddot{z}_3 = \frac{1}{M_{wr}} [K_{tr}(x_{0r} - z_3) - F_r] \quad (7.9)$$

$$\ddot{z}_4 = \left[ \frac{1}{M_{bh}} - \frac{ab}{I_b} \right] F_f + \left[ \frac{1}{M_{bh}} + \frac{b^2}{I_b} \right] F_r \quad (7.10)$$

### 7.2.1 Passive case

In the case of the passive system the front and rear suspension forces are :

$$F_f = K_{sf}(z_1 - z_2) + C_{sf}(\dot{z}_1 - \dot{z}_2) \quad (7.11)$$

$$F_r = K_{sr}(z_3 - z_4) + C_{sr}(\dot{z}_3 - \dot{z}_4) \quad (7.12)$$

Substitution of Eqns 7.11 and 7.12 into Eqns 7.7 to 7.10 allows the equations to be written in the form of the general matrix equation (2.11) ;

$$MXDD\ddot{z} + MXD\dot{z} + MXz = MUx_0 + MUD\dot{x}_0 + MFf$$

where for the half vehicle  $z = [z_1 \ z_2 \ z_3 \ z_4]^T$  and  $x_0 = [x_{0f} \ x_{0r}]^T$ . Using the suffix *hp* to denote the passive system, the coefficient matrices are as follows ;

$$\begin{aligned}
 MXD_{hp} &= \begin{bmatrix} \frac{C_{sf}}{M_{wf}} & -\frac{C_{st}}{M_{wf}} & 0 & 0 \\ -C_{sf}s_1 & C_{sf}s_1 & -C_{sr}s_2 & C_{sr}s_2 \\ 0 & 0 & \frac{C_{sr}}{M_{wr}} & -\frac{C_{sr}}{M_{wr}} \\ -C_{sf}s_2 & C_{sf}s_2 & -C_{sr}s_3 & C_{sr}s_3 \end{bmatrix}, MU_{hp} = \begin{bmatrix} 1 & 0 \\ 0 & 0 \\ 0 & 1 \\ 0 & 0 \end{bmatrix} \\
 MX_{hp} &= \begin{bmatrix} \frac{K_{tf}+K_{sf}}{M_{wf}} & -\frac{K_{st}}{M_{wf}} & 0 & 0 \\ -K_{sf}s_1 & K_{sf}s_1 & -K_{sr}s_2 & K_{sr}s_2 \\ 0 & 0 & \frac{K_{tr}+K_{sr}}{M_{wr}} & -\frac{K_{sr}}{M_{wr}} \\ -K_{sf}s_2 & K_{sf}s_2 & -K_{sr}s_3 & K_{sr}s_3 \end{bmatrix} \quad (7.13)
 \end{aligned}$$

where

$$s_1 = \frac{1}{M_{bh}} + \frac{a^2}{I_b}, \quad s_2 = \frac{1}{M_{bh}} + \frac{ab}{I_b}, \quad s_3 = \frac{1}{M_{bh}} + \frac{b^2}{I_b} \quad (7.14)$$

In this case  $MXDD_{hp}$  is an identity matrix and  $MUD_{hp}$  and  $MF_{hp}$  are both null matrices.

## 7.2.2 Active case

In the fully active case the actuator is the only suspension element and the suspension forces become :

$$F_f = u_1, \quad F_r = u_2 \quad (7.15)$$

Using the suffix *ha* to denote the active half vehicle, the coefficient matrices are given by ;

$$MX_{ha} = \begin{bmatrix} \frac{K_{tf}}{M_{wf}} & 0 & 0 & 0 \\ 0 & 0 & 0 & 0 \\ 0 & 0 & \frac{K_{tr}}{M_{wr}} & 0 \\ 0 & 0 & 0 & 0 \end{bmatrix} \quad (7.16)$$

$MXDD_{ha}$  is now an identity matrix,  $MXD_{ha}$  and  $MUD_{ha}$  are null matrices, while the matrix  $MU_{ha} = MU_{hp}$ . The active control forces  $u$  can now be included in Eqn (2.11) using the vector of functions  $f$ , such that  $f = [u_1 \ u_2]^T$ . The matrix  $MF_{ha}$  becomes :

$$MF_{ha} = \begin{bmatrix} -1 & 0 \\ s_1 & s_2 \\ 0 & -1 \\ s_2 & s_3 \end{bmatrix} \quad (7.17)$$

### 7.2.3 Semi-active case

In the case of the semi-active continuously variable damper system the suspension forces are given by :

$$F_f = K_{sf}(z_1 - z_2) + u_1, \quad F_r = K_{sr}(z_3 - z_4) + u_2 \quad (7.18)$$

To describe a practical system, a further two equations are required to represent the valve responses according to the first order dynamics described in Section 6.2.1. In matrix form these are ;

$$T\dot{c}_a + c_a = C \quad (7.19)$$

where for the half vehicle  $c_a = [c_{af} \ c_{ar}]^T$  is a vector containing the actual front and rear damping coefficients,  $C = [C_f \ C_r]^T$  is a vector of demand damping coefficients and  $T$  is a matrix containing the front and rear time constants :

$$T = \begin{bmatrix} T_f & 0 \\ 0 & T_r \end{bmatrix} \quad (7.20)$$

The actual damping forces, in the vector  $u_a = [u_{af} \ u_{ar}]^T$  are then given by :

$$u_{af} = c_{af}(\dot{z}_1 - \dot{z}_2), \quad u_{ar} = c_{ar}(\dot{z}_3 - \dot{z}_4) \quad (7.21)$$

In a similar style to the controllable damper quarter car model (Section 6.2.1), the demand damping coefficients and actual damping forces are both represented in Eqn (2.11) by elements of the vector  $f$ , such that  $f = [C \ u_a]^T$ . Eqn (7.19) can then be combined with Eqns (7.7) to (7.10) by defining a new vector of state variables  $z_{hs} = [z \ c_a]^T$ . The resulting coefficient matrices of the semi-active half vehicle are related to those of the passive and active half vehicles by :

$$\begin{aligned} MXDD_{hs} &= \begin{bmatrix} I & 0 \\ 0 & 0 \end{bmatrix}, MXD_{hs} = \begin{bmatrix} 0 & 0 \\ 0 & T \end{bmatrix}, MU_{hs} = \begin{bmatrix} MU_{hp} \\ 0 \end{bmatrix} \\ MX_{hs} &= \begin{bmatrix} MX_{hp} & 0 \\ 0 & I \end{bmatrix}, MF_{hs} = \begin{bmatrix} 0 & MF_{ha} \\ I & 0 \end{bmatrix} \end{aligned} \quad (7.22)$$

## 7.3 Control Laws

### 7.3.1 First order equations

The generation of linear optimal control laws for active systems first requires the transformation of Eqns (7.7) to (7.10) into the first order format of Eqn (2.19). Using the procedure outlined in Section 2.3.2 the equation for the half vehicle can be written in the first order format of Eqn (2.19) :

$$\dot{x} = Ax + Bu + B_1x_0$$

Again  $x = [z \ \dot{z}]^T$  and in this case  $A$ ,  $B$  and  $B_1$  are related to  $MX_{ha}$ ,  $MU_{ha}$  and  $MF_{ha}$  by :

$$A = \begin{bmatrix} 0 & I \\ -MX_{ha} & 0 \end{bmatrix}, B = \begin{bmatrix} 0 \\ MF_{ha} \end{bmatrix}, B_1 = \begin{bmatrix} 0 \\ MU_{ha} \end{bmatrix} \quad (7.23)$$

Similarly the equations for the semi-active continuously variable damper system also require reduction to first order format. In this case, following the results in Section 5.3, it is necessary to include the passive spring in the model used to obtain the control gains. Using the same procedure, the controlled damper forces become system states via two first order equations, which in matrix form are ;

$$T_u \dot{x}_u + x_u = u \quad (7.24)$$

where  $x_u = [x_{uf} \ x_{ur}]^T$  is the state vector of damper forces, and  $T_u$  is a diagonal matrix containing the time constants,  $T_{uf}$  and  $T_{ur}$ , both of which are set at 0.001s. Defining a new vector  $x_b = [x \ x_u]^T$  the first order equation of motion for the semi-active system is described by Eqn (5.5) ;

$$\dot{x}_b = A_b x_b + B_b u + B_{b1} x_0$$

where the coefficient matrices are given by :

$$A_b = \begin{bmatrix} 0 & I & 0 \\ -MX_{hp} & 0 & MF_{ha} \\ 0 & 0 & -T^{-1} \end{bmatrix}, B_b = \begin{bmatrix} 0 \\ 0 \\ T^{-1} \end{bmatrix}, B_{b1} = \begin{bmatrix} 0 \\ MU_{hp} \\ 0 \end{bmatrix} \quad (7.25)$$

### 7.3.2 Uncorrelated Case

The procedure for generating a control law which ignores the correlation between front and rear wheel input is the same as described in Chapter 4. This chapter concentrates on the limited state feedback case, with the gradient search routine being used to find the feedback gains.

The ground inputs at each wheel are assumed to be filtered white noise and in matrix form can be described by ;

$$\dot{x}_0 = F_w x_0 + Iw \quad (7.26)$$

where

$$F_w = \begin{bmatrix} -2\pi V\alpha & 0 \\ 0 & -2\pi V\alpha \end{bmatrix} \quad (7.27)$$

and  $w = [v_f \ v_r]^T$  is a vector containing the front and rear white noise inputs. For the fully active system this equation is then combined with Eqn (2.19) using the extended state vector  $x_a = [x \ x_0]^T$  to give Eqn (4.9) ;

$$\dot{x}_a = A_a x + B_a u + B_{aw} w$$

where

$$A_a = \begin{bmatrix} A & B_1 \\ 0 & F_w \end{bmatrix}, B_a = \begin{bmatrix} B \\ 0 \end{bmatrix}, B_{aw} = \begin{bmatrix} 0 \\ I \end{bmatrix} \quad (7.28)$$

The connection matrix  $D$ , required by the performance index (Eqn (4.13)), becomes ;

$$D = \begin{bmatrix} -1 & 0 & 0 & 0 & 0 & 0 & 0 & 0 & 1 & 0 \\ 1 & -1 & 0 & 0 & 0 & 0 & 0 & 0 & 0 & 0 \\ 0 & 0 & -1 & 0 & 0 & 0 & 0 & 0 & 0 & 1 \\ 0 & 0 & 1 & -1 & 0 & 0 & 0 & 0 & 0 & 0 \end{bmatrix} \quad (7.29)$$

defining the controlled outputs in the performance index to be tyre and suspension deflection at both ends of the vehicle. The body accelerations are controlled via the actuator force terms in Eqn (4.13).

The first order matrix equation for the semi-active continuously variable damper system (Eqn (5.9)) can be obtained by combining Eqns (4.9) and (7.26) using the vector  $x_c = [x_b \ x_0]^T$  ;

$$\dot{x}_c = A_c x_c + B_c u + B_{cw} w$$

where

$$A_c = \begin{bmatrix} A_b & B_{b1} \\ 0 & F_w \end{bmatrix}, B_c = \begin{bmatrix} B_b \\ 0 \end{bmatrix}, B_{cw} = \begin{bmatrix} 0 \\ I \end{bmatrix} \quad (7.30)$$

For the reasons discussed earlier, in the case of the continuously variable damper system it is preferable to include the spring stiffness in the optimisation procedure and  $D$  has to be modified to include body acceleration :

$$D = \begin{bmatrix} -1 & 0 & 0 & 0 & 0 & 0 & 0 & 0 & 1 & 0 & 0 & 0 \\ 1 & -1 & 0 & 0 & 0 & 0 & 0 & 0 & 0 & 0 & 0 & 0 \\ K_{sf}s_1 & -K_{sf}s_1 & K_{sr}s_2 & -K_{sr}s_2 & 0 & 0 & 0 & 0 & 0 & 0 & s_1 & s_2 \\ 0 & 0 & -1 & 0 & 0 & 0 & 0 & 0 & 0 & 1 & 0 & 0 \\ 0 & 0 & 1 & -1 & 0 & 0 & 0 & 0 & 0 & 0 & 0 & 0 \\ K_{sf}s_2 & -K_{sf}s_2 & K_{sr}s_3 & -K_{sr}s_3 & 0 & 0 & 0 & 0 & 0 & 0 & s_2 & s_3 \end{bmatrix} \quad (7.31)$$

The measured variables in both cases are suspension deflection, body velocity, and wheel velocity for each end of the vehicle, resulting in the following control laws ;

$$u_1 = -[K_2(x_1 - x_2) + K_4(x_3 - x_4) + K_5x_5 + K_6x_6 + K_7x_7 + K_8x_8] \quad (7.32)$$

$$u_2 = -[K_{10}(x_1 - x_2) + K_{12}(x_3 - x_4) + K_{13}x_5 + K_{14}x_6 + K_{15}x_7 + K_{16}x_8] \quad (7.33)$$

where  $u_1$  and  $u_2$  are the demand forces for the front and rear controlled elements respectively. To find the vector of limited state feedback gains  $K_L$ , the gradient search routine requires a set of initial guesses to use as a starting point for its calculations. The increased terms in the control law make this a more difficult proposition than in the quarter car case. However, since the vehicle is approximately decoupled ( $I_b \approx M_{bhab}$ ), it can be assumed that the front and rear actuators will operate independently and that the terms in Eqs (7.32) and (7.33) which transfer information from front to rear and vice-versa will consequently be very small. This alleviates the problem by allowing the initial guesses for  $K_4$ ,  $K_7$ ,  $K_8$ ,  $K_{10}$ ,  $K_{13}$ , and  $K_{14}$  to be set to zero, while the remaining gains can be estimated in a similar style to the quarter car model.

### 7.3.3 Correlated Case

#### Representation of wheelbase time delay

The correlation between front and rear wheels is incorporated in the linear optimal control model using a Pade approximation. The method, covered in detail by Abdel-Hady [1989], is summarised below :

1. The time delay between the front and rear white noise inputs ( $v_f$  and  $v_r$ ) is regarded as a transportation lag which can be represented mathematically by ;

$$\frac{v_r(s)}{v_f(s)} = e^{-\tau s} \quad (7.34)$$

where the time delay  $\tau = \text{wheelbase/vehicle speed}$ .

2. The Pade approximation simulates the lag by expanding the exponential as a ratio of two polynomials ;

$$\frac{v_r(s)}{v_f(s)} = \frac{\alpha_0 - \alpha_1 s + \alpha_2 s^2 - \alpha_3 s^3 + \dots + \alpha_N s^N}{\alpha_0 + \alpha_1 s + \alpha_2 s^2 + \alpha_3 s^3 + \dots + \alpha_N s^N} \quad (7.35)$$

where  $N$  is the order of the approximation. For  $N = 2$ , the constants are ;

$$\alpha_0 = 12/\tau^2, \quad \alpha_1 = 6/\tau, \quad \alpha_2 = 1 \quad (7.36)$$

while for  $N = 4$  they are :

$$\alpha_0 = 1072/\tau^4, \quad \alpha_1 = 536/\tau^3, \quad \alpha_2 = 120/\tau^2 \quad (7.37)$$

$$\alpha_3 = 13.55/\tau, \quad \alpha_4 = 1$$

3. Eqn (7.35) is then converted into state space representation, resulting in the matrix equation ;

$$\dot{\eta}(t) = A_\eta \eta(t) + B_\eta v_f(t) \quad (7.38)$$

where  $\eta$  is vector of delay states with size dependent on the order of the approximation.

The output is then defined by :

$$v_r = v_f(t - \tau) = D_\eta \eta(t) + v_f \quad (7.39)$$

4. The matrices  $A_\eta$ ,  $B_\eta$  and  $D_\eta$  depend on the time delay  $\tau$  and the order of the approximation  $N$ . For example, if  $N = 2$ , they are written as follows ;

$$A_\eta = \begin{bmatrix} 0 & 1 \\ -\alpha_0 & -\alpha_1 \end{bmatrix}, B_\eta = \begin{bmatrix} 0 \\ 1 \end{bmatrix}, D_\eta = \begin{bmatrix} 0 & -12/\tau \end{bmatrix} \quad (7.40)$$

while for a fourth order approximation they become :

$$A_\eta = \begin{bmatrix} 0 & 1 & 0 & 0 \\ 0 & 0 & 1 & 0 \\ 0 & 0 & 0 & 1 \\ -\alpha_0 & -\alpha_1 & -\alpha_2 & -\alpha_3 \end{bmatrix}, B_\eta = \begin{bmatrix} 0 \\ 0 \\ 0 \\ 1 \end{bmatrix}$$

$$D_\eta = \begin{bmatrix} 0 & -2\alpha_1 & 0 & -2\alpha_3 \end{bmatrix} \quad (7.41)$$

## Equations

The equation describing the white noise ground inputs (7.26) can be rewritten as :

$$\dot{x}_0 = F_w x_0 + b_1 v_f + b_2 v_r \quad (7.42)$$

where  $b_1 = [1 \ 0]^T$  and  $b_2 = [0 \ 1]^T$ . The rear input term can then be eliminated from the problem by substituting Eqn (7.39) into (7.42) ;

$$\dot{x}_0 = F_w x_0 + b_2 D_\eta \eta + (b_1 + b_2) v_f \quad (7.43)$$

For the fully active case, Eqn (4.9) can be combined with Eqn (7.38) using the vector  $x_d = [x_a \ \eta]^T$  to give ;

$$\dot{x}_d = A_d x_d + B_d u + B_{dw} v_f \quad (7.44)$$

The matrices  $B_d = [B_a \ 0]^T$ ,  $B_{dw} = [B_{aw} \ B_\eta]^T$   
and

$$A_d = \begin{bmatrix} A_a & B_3 \\ 0 & A_\eta \end{bmatrix} \quad (7.45)$$

where  $B_3 = [0 \ b_2 D_\eta]^T$

Similarly, the semi-active first order equation (5.9) can be combined with Eqn (7.38) using the vector  $x_e = [x_c \ \eta]^T$  giving :

$$\dot{x}_e = A_e x_e + B_e u + B_{ew} v_f \quad (7.46)$$

The coefficient matrices are this time given by  $B_e = [B_c \ 0]^T$ ,  $B_{ew} = [B_{cw} \ B_\eta]^T$   
and

$$A_e = \begin{bmatrix} A_c & B_3 \\ 0 & A_\eta \end{bmatrix} \quad (7.47)$$

The correlated equations (7.44) and (7.46) are now in the same form as the uncorrelated equations and can be solved using the same techniques.

If a full state feedback solution to the problem is obtained, (discussed in detail by Abdel-Hady [1989]) the correlation information is included in the control law using additional feedback gains which are associated with the delay states  $\eta$ , while for a given set of weightings in the performance index, the gains associated with the vehicle states remain unchanged from the uncorrelated case. Due to the inability to measure the delay states directly and also the practical difficulty in measuring the ground inputs, it is again appropriate to employ the limited state feedback described in Chapter 4. This method allows the unobservable delay states to be omitted from the measured variables, resulting in control laws which are the same as in the uncorrelated case (Eqns (7.32) and (7.33)).

The gradient search routine outlined in Chapter 4 is again used in an attempt to generate the feedback gains. However, in this case the NAG library routine,

EO4KCF, is not as effective and is often unable to reach a minimum. This is probably due to the increased complexity of the correlated model and also, since the preview information is now hidden within the original feedback gains, a difficulty in providing the routine with a set of initial guesses.

For the fully active case the problem can be eased by recognising that only the rear of the vehicle will benefit from a correlated control law, and that any information which is passed from the rear of the vehicle to the front actuator/damper can be omitted from the control laws with little effect on performance. The appropriate terms in Eqn (7.32) can then be set to zero. This results in a reduction in the number of iterations required by the gradient search routine and ultimately provides a sub-optimal active control law. The technique works well for the almost decoupled vehicle described by Table 7.1, but may not be appropriate for a vehicle having  $I \neq M_{bh}ab$  since the cross-coupling terms become important. The stability of the system equations during the search for a minimum can also be improved if a 4th order, rather than a 2nd order Pade approximation is used.

The correlated semi-active system described by Eqn (7.46) is further complicated by additional state variables which represent the damper forces (Eqn 7.24), and the techniques used to generate feedback gains for the correlated active model are inadequate. It now becomes virtually impossible to generate the gains directly using routine EO4KCF and it is necessary to employ the second method of finding semi-active control laws, as described in Section 5.2.1. In this method the passive spring is initially omitted from the calculations and the gains can be generated using the same procedure as the fully active system. The spring force is then subtracted from the control force to provide the force required at each damper.

## 7.4 Results

The vehicle data used in this chapter is shown in Table 7.1. Additional parameters are included to describe the front of the vehicle and weight distribution while the rear data is consistent with that used throughout the quarter car modelling work.

<u>Masses and Inertias</u>		
$M_{bh}$	0.690	Body mass (tonnes)
$I_b$	1.222	Pitch inertia (tonnes.m <sup>2</sup> )
$M_{wf}$	0.0405	Front wheel mass (tonnes)
$M_{wr}$	0.0454	Rear wheel mass (tonnes)
<u>Stiffness and Damping</u>		
$K_{tf}$	192	Front tyre stiffness (kN/m)
$K_{tr}$	192	Rear tyre stiffness (kN/m)
$K_{sf}$	17	Front susp. stiffness (kN/m) (passive and semi-active)
$K_{sr}$	22	Rear susp. stiffness (kN/m) (passive and semi-active)
$C_{sf}$	1.5	Front damping coeff. (kNs/m) (passive only)
$C_{sr}$	1.5	Rear damping coeff. (kNs/m) (passive only)
<u>Geometry</u>		
$a$	1.25	Dist. from cg to front wheel station (m)
$b$	1.51	Dist. from cg to rear wheel station (m)
$l$	2.76	Wheelbase (m)

Table 7.1: Half vehicle parameters.

The performance of fully active and continuously variable damper systems using both correlated and uncorrelated control laws is compared in Fig 7.2. The results are generated using Eqns (7.15) to (7.17) for the active and Eqns (7.18) and (7.22) for the semi-active systems respectively, and in line with previous chapters the comparison is again based on an equal usage of suspension workspace. For an rms suspension working space of 0.029m, the figure shows the discomfort parameter (ACC) and the tyre loading parameter (DTL) of a range of possible systems. Only results at the rear of the vehicle are considered, since it is here where the benefits of a correlated control law will be greatest. Two groups of semi-active system curves are shown, one for systems fitted with ideal components and the other for systems in which practical limitations have been modelled ie. a first order time lag ( $T=10\text{ms}$ ) and maximum and minimum damping constraints ( $C_{max}=2.5\text{kNs/m}$ ,  $C_{min}=0.3\text{kNs/m}$ ). The active system curves are generated for suspensions fitted with ideal components only. In the active case, systems AC and AU on the correlated and uncorrelated curves respectively are selected for further analysis. The systems are chosen on the basis that they have a similar tyre load performance. Their performance index weightings and gain matrices are ;

1. Uncorrelated system (AU)

Weightings :

$$q_1, q_3 \text{ (front and rear tyre deflection)} = 4700$$

$$q_2, q_4 \text{ (front and rear susp. deflection)} = 300$$

$$\rho \text{ (body accelerations)} = 1$$

Gain matrix :

$$K_{AU} = \begin{bmatrix} -21.11 & 0.18 & -0.94 & 4.55 & 0 & 0.05 \\ 0.17 & -22.94 & 0 & 0.05 & -0.97 & 4.31 \end{bmatrix} \quad (7.48)$$

## 2. Correlated system (AC)

Weightings :

$$q_1, q_3 \text{ (front and rear tyre deflection)} = 5000$$

$$q_2, q_4 \text{ (front and rear susp. deflection)} = 400$$

$$\rho \text{ (body accelerations)} = 1$$

Gain matrix :

$$K_{AC} = \begin{bmatrix} -18.58 & 0 & -0.84 & 3.60 & 0 & 0 \\ -0.63 & -22.90 & 0.45 & -1.38 & -0.60 & 4.89 \end{bmatrix} \quad (7.49)$$

The psd's of rear vertical body acceleration and dynamic tyre load for these systems are shown in Fig 7.3(a) and (b). For the correlated case it is also of interest to look at the response to special features; in this case, a step input of 0.1m is taken to represent a discontinuity such as a severe bump or pot-hole in the road. Using systems AC and AU a comparison between the correlated and uncorrelated responses in terms of body acceleration, dynamic tyre load and suspension deflection at the rear of the vehicle is shown in Figs 7.4(a),(b), and (c). For the results shown, the front wheel contacts the step input at  $t = 0$  and the rear wheel at  $t = 0.14$  seconds (wheelbase/vehicle speed).

In a similar style, points SC and SU from the semi-active systems which include practical limitations are also analysed. Their performance index weightings and gain matrices are :

## 1. Uncorrelated system (SU)

Weightings :

$$q_1, q_4 \text{ (front and rear tyre deflection)} = 5750$$

$$q_2, q_5 \text{ (front and rear susp. deflection)} = 50$$

$$q_3, q_6 \text{ (front and rear body acceleration)} = 0.1$$

Gain matrix :

$$K_{SU} = \begin{bmatrix} 2.50 & -0.18 & -0.76 & 1.96 & -0.01 & 0.01 \\ -0.24 & 5.53 & -0.01 & 0.02 & -0.73 & 1.98 \end{bmatrix} \quad (7.50)$$

## 2. Correlated system (SC)

Weightings :

$$q_1, q_3 \text{ (front and rear tyre deflection)} = 1500$$

$$q_2, q_4 \text{ (front and rear susp. deflection)} = 100$$

$$\rho \text{ (body accelerations)} = 1$$

Gain matrix :

$$K_{SC} = \begin{bmatrix} -8.65 & 0 & -0.57 & 2.79 & 0 & 0 \\ -0.28 & -9.19 & 0.41 & -1.66 & -0.25 & 4.13 \end{bmatrix} \quad (7.51)$$

Note :

To obtain the force required at each damper, the front and rear spring forces,  $K_{sf}(x_1 - x_2)$  and  $K_{sr}(x_3 - x_4)$ , must be subtracted from the control forces which are generated using matrix (7.51)

The psd's and step responses of each system are shown in Figs 7.5(a),(b) and Figs 7.6(a), (b) and (c) respectively.

## 7.5 Discussion

The comparative results between uncorrelated fully active and semi-active continuously variable systems shown in Fig 7.2 generally agree with those reported in the previous chapters based on quarter modelling. Therefore, for control laws which ignore the correlation between inputs at each wheel, the quarter car provides an reasonable representation of the full vehicle behaviour. The

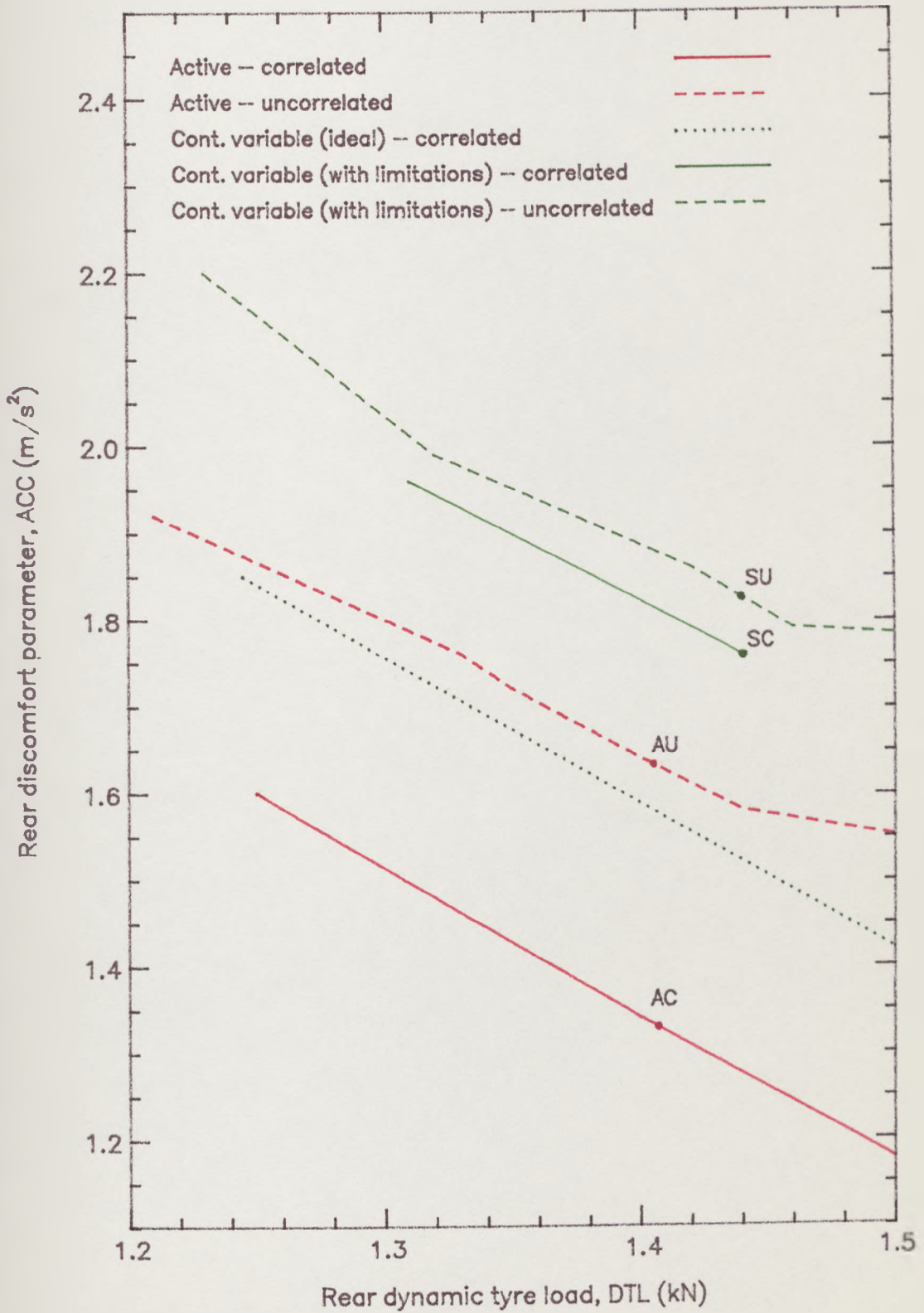


Figure 7.2: Effect of wheelbase preview on the performance of active and continuously variable damper systems (SWS=0.029m).

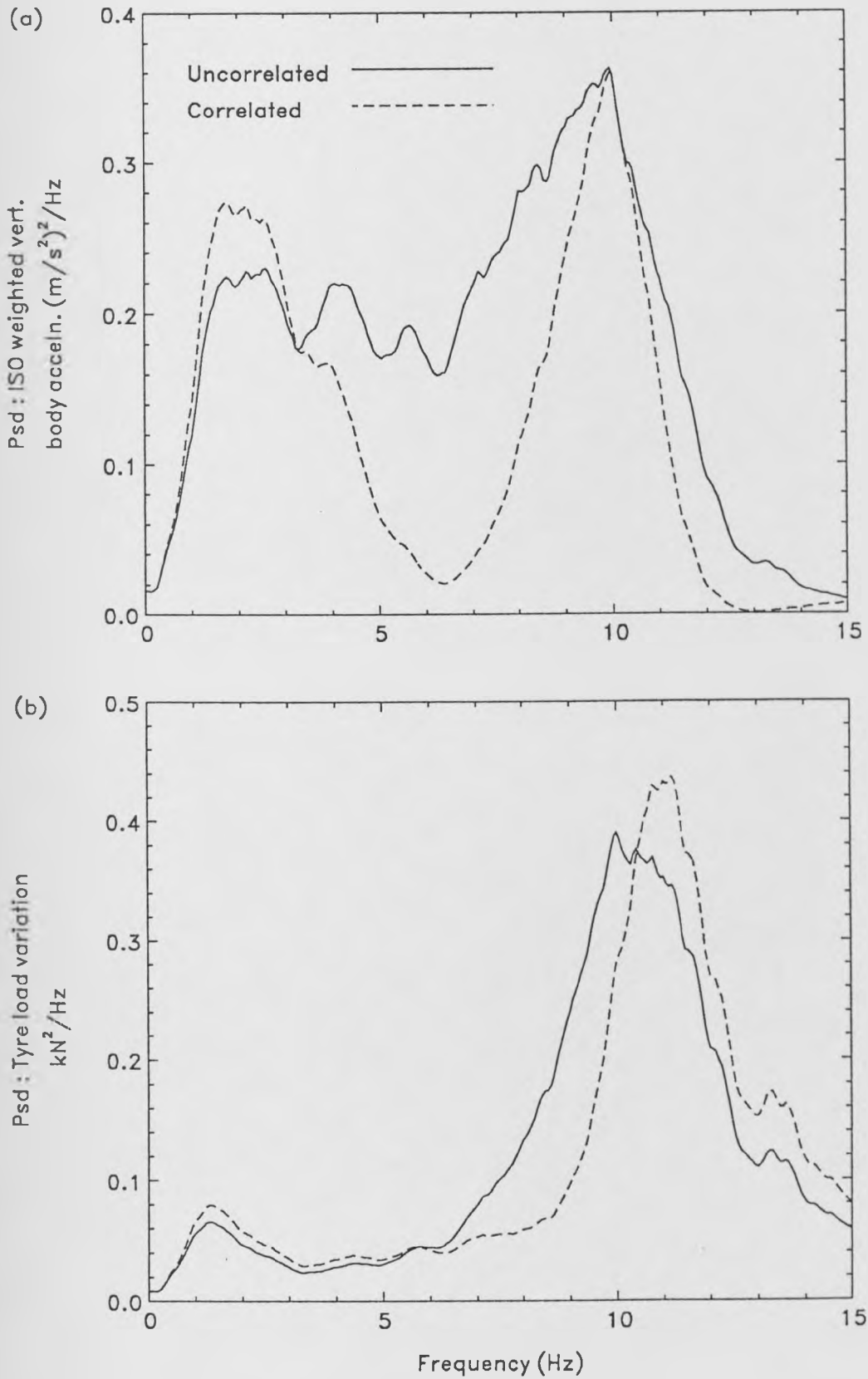


Figure 7.3: Psds of rear ISO weighted vertical body acceleration and dynamic tyre load - active system (half vehicle).

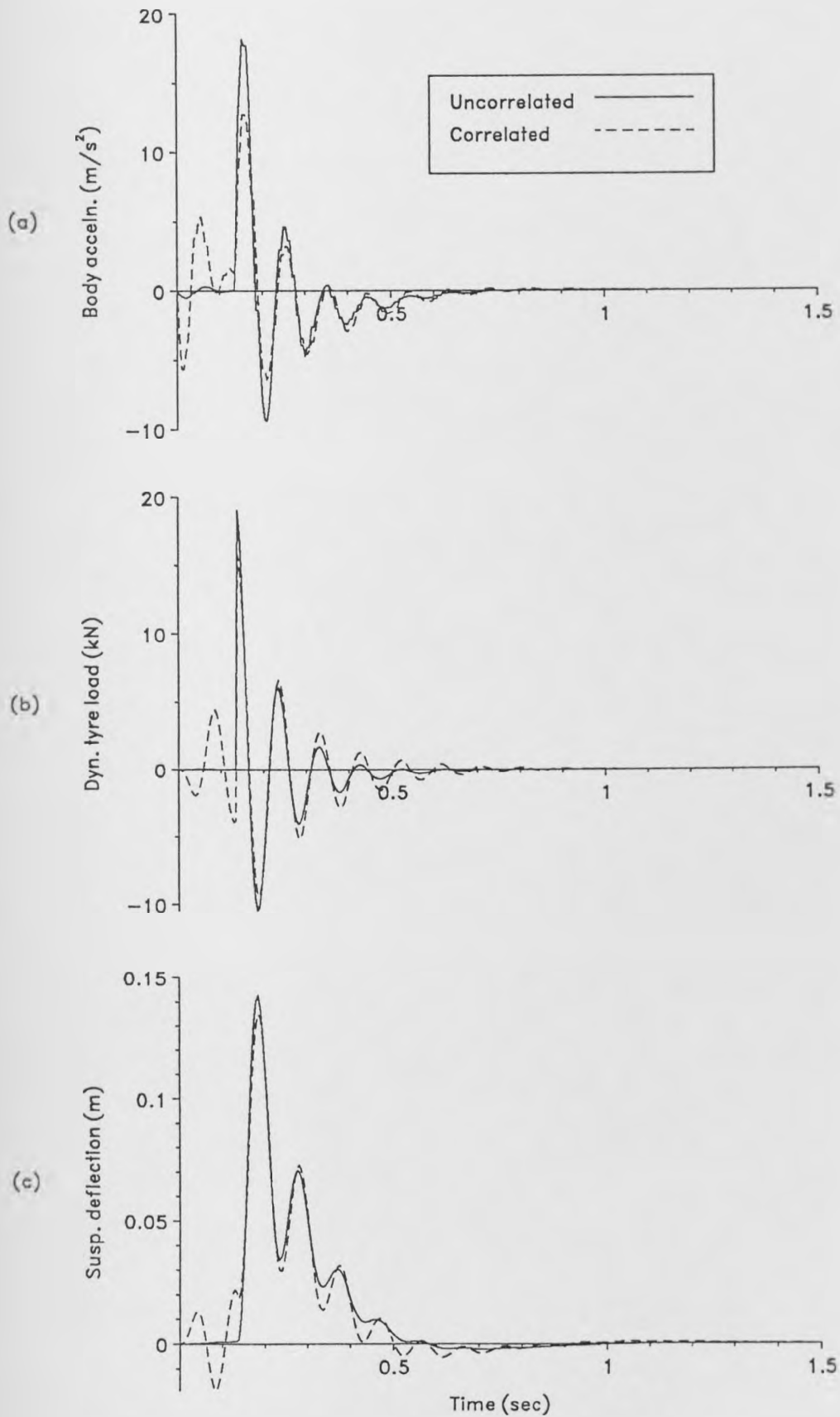


Figure 7.4: Active systems - response at the rear of the vehicle to a step input of 0.1m.

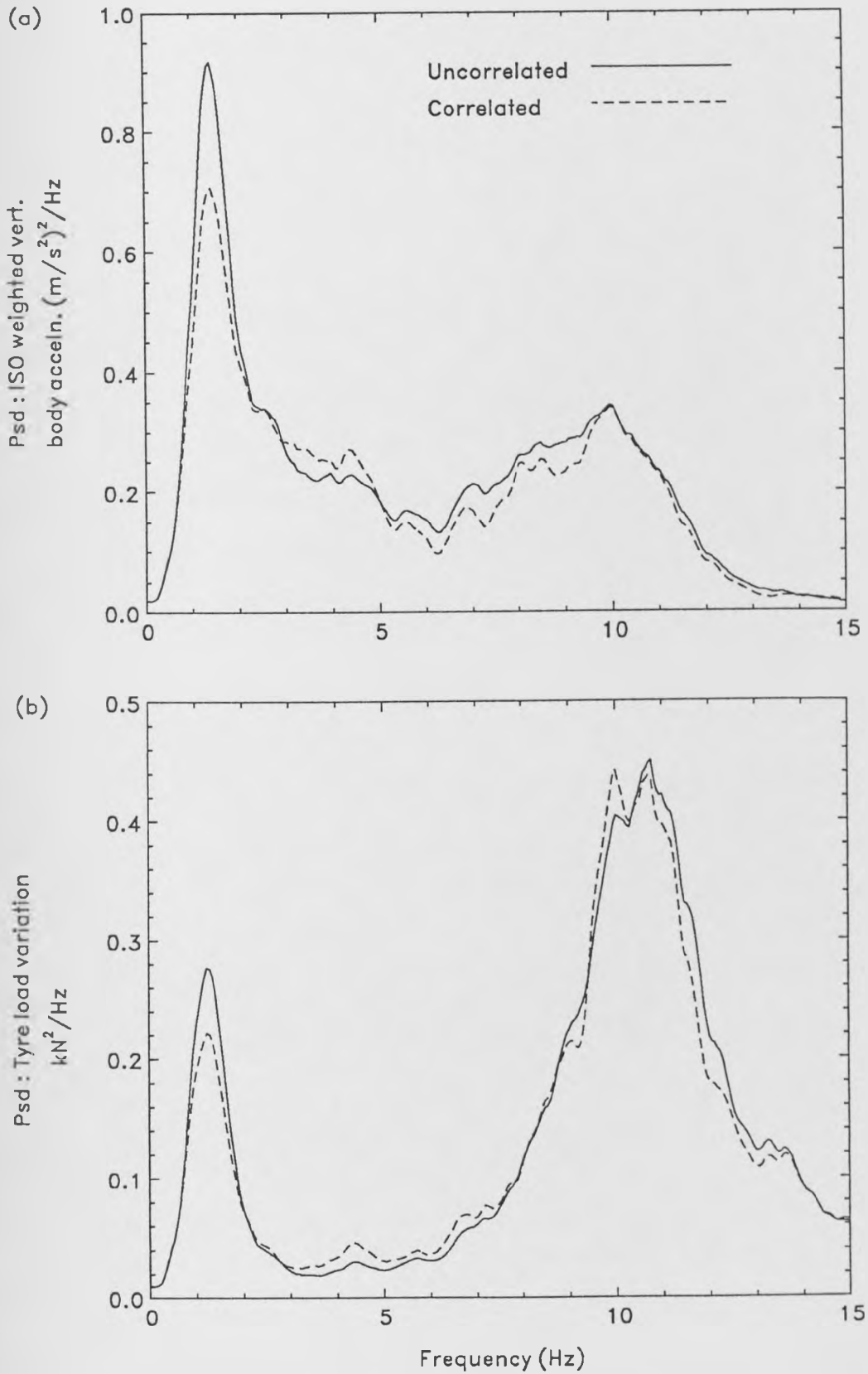


Figure 7.5: Psd's of rear ISO weighted vertical body acceleration and dynamic tyre load - continuously variable damper system (half vehicle).

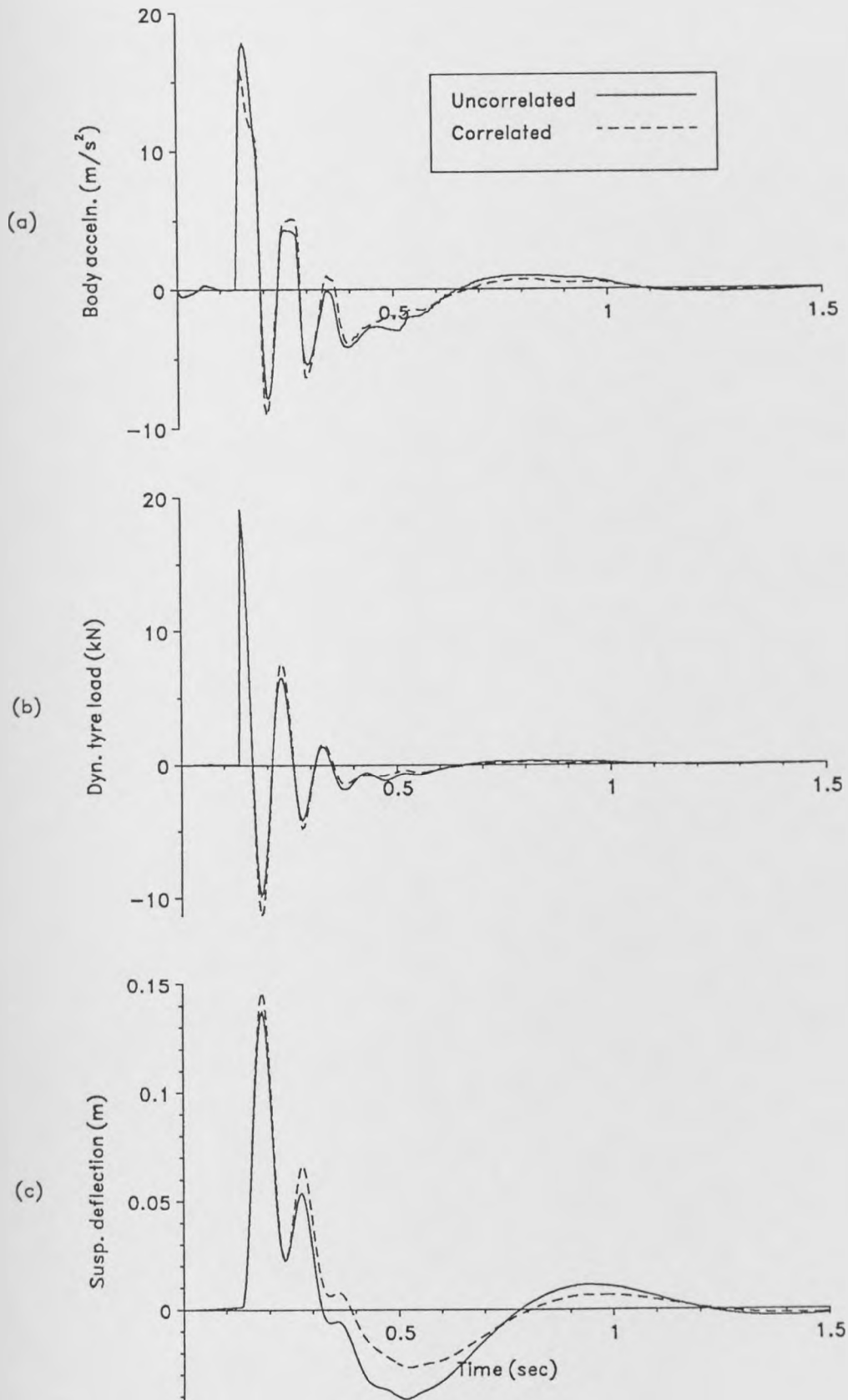


Figure 7.6: Continuously variable damper systems - response at the rear of the vehicle to a step input of 0.1m.

most interesting results in Fig 7.2 refer to the inclusion of wheelbase preview information in the control law. For the fully active system, the improvements obtained using a correlated control law are substantial, ie. approximately a 20% improvement in comfort for a given tyre load performance. Also, in the case of semi-active suspensions, it can be seen that an ideal continuously variable damper system with correlated control law actually performs better than a fully active system with uncorrelated law. However, when realistic response limitations are included in such a system the results for the correlated control law are less striking and improvements in comfort of approximately 5% are obtained over a similar uncorrelated system. These performance gains are still worthwhile since they are achieved using the existing hardware and therefore with no extra cost over the uncorrelated system.

Examination of the gain matrices for the uncorrelated systems ( $K_{AU}$ ) and ( $K_{SU}$ ) reveals that any gains which are associated with passing information from the front of the vehicle to the rear actuator and vice versa are small, confirming that the two ends of the model are almost decoupled. As expected, the coupling terms in the correlated gain matrices  $K_{AC}$  and  $K_{SC}$  become more significant. This leads to difficulties in providing an initial estimate of the gains for the gradient search routine and subsequently an increase in the computing time required. The problem can be eased to some extent by assuming that the front of the vehicle cannot benefit from information passed from the rear, and therefore the corresponding terms in matrices (7.49) and (7.51) have been set to zero.

The psd's of rear ISO weighted body acceleration and dynamic tyre load for the selected systems AU, AC, SU and SC, provide a further insight into how the performance of the correlated systems is achieved. In Fig 7.3(a) the substantial ride comfort improvements of the correlated active system appear clearly as a reduction in accelerations in the frequency range between the body and wheel

resonant frequencies. Significant reductions are also seen at frequencies beyond “wheelhop” but the resonant peaks themselves remain approximately equal to those of the uncorrelated system. Except for a slight shift in the wheel resonant frequency, the psd’s of dynamic tyre load for the uncorrelated and correlated active systems in Fig 7.3(b) are approximately equal. Perhaps this is to be expected since the systems AU and AC were selected on the basis of having similar tyre load performances. The smaller performance gains achieved by the correlated semi-active system (SC) appear more conventionally in Fig 7.5(a) as a reduction in the body acceleration resonance peak. For the same reason as the active systems, the psd’s of dynamic tyre load for systems SU and SC are approximately equal.

Additional information is provided by Figs 7.4 and 7.6 showing the response of AU, AC, SU and SC to a step input of 0.1m. A comparison of both sets of curves reveals that in general a fully active system (correlated or uncorrelated) is able to control the transient accelerations and deflections more quickly than a semi-active system. This is because the active system has the ability to supply power to the actuator. If the active system has the benefit of some preview information, further improvements are possible. The rear actuator is now able to respond by jacking up the body before the rear wheel hits the disturbance. This can be seen in Figs 7.4(a), (b) and (c) where activity at the rear of the vehicle is clearly evident before the rear wheel contacts the step at  $t = 0.14$  seconds. The advantage of this, shown in Fig 7.4(a), is a noticeable reduction in peak body accelerations when the rear wheel eventually hits the step. The semi-active suspension is unable to do this and so for this class of input, the inclusion wheelbase preview information appears to be only marginally advantageous. The response of the correlated system (SC) shows only slight improvements in body accelerations and suspension deflections (Figs 7.6(a) and (c)) over the uncorrelated case (SU).

## 7.6 Concluding Remarks

Using a two-dimensional half-vehicle model, correlated control laws have been generated which take advantage of the fact that the rear wheel input is actually a delayed version of that at the front. A fourth order Pade approximation is used to represent the “wheelbase preview” between front and rear wheels resulting in four extra system states and equations. To avoid measurement of these unobservable delay states a limited state feedback solution is employed throughout, and the control law feedback gains are again found via a gradient search routine. The work, which is essentially an extension of the work by Abdel-Hady [1989] compares the performance of both fully active and continuously variable damper (semi-active) systems when the actuators/ dampers are driven by uncorrelated and correlated control laws. The conclusions are as follows :

1. Predicted results for fully active systems show that inclusion of the “wheelbase preview” in the control law is very significant. For a given dynamic tyre load performance, reductions in rms weighted body accelerations of up to 20% are possible over the uncorrelated case.
2. The results of the ideal semi-active system, ie. no response limitations, with correlated control law are also encouraging. The overall performance of this system is actually better than a fully active suspension with uncorrelated control law.
3. Performance improvements obtained from using wheelbase preview on a semi-active suspension which includes practical limitations are relatively small, for example, a 5% improvement in comfort for a given tyre load performance. Since the damper is driven by a correlated control law using limited state feedback, no additional hardware is required and there are

therefore no extra costs. Consequently, any performance improvements over the uncorrelated law are worthwhile.

4. A power spectral density comparison of uncorrelated and correlated fully active suspensions shows that the substantial ride improvements are largely due to a reduction in accelerations in the mid range (3 to 8Hz) and beyond the “wheelhop” frequency. The correlated law does not appear to affect activities around the resonance peaks. For semi-active systems the improvements appear as a reduction in the body resonance peak.
5. Step responses show that a fully active correlated control law is effective at reducing transient body accelerations, but also that, for this class of input, a semi-active correlated law is only marginally advantageous.

The possibility of active and semi-active suspensions adapting to suit the prevailing running conditions is introduced in Chapter 4. In this chapter, since the time delay between front and rear inputs is a function of speed, it becomes clear that any control strategy employing the wheelbase preview effect must be able to adapt to the vehicle speed as well as the road quality. A further practical consideration is that in the event of a large steer input, the rear wheels do not follow the same track as the front, and to counter this the the control strategy may need to incorporate an algorithm which overrides the preview information. However, a large steer input implies a low vehicle speed, and therefore the problem may not be practically important. In the case of the continuously variable damper system it is probably even less important, since it has already been suggested in Chapter 5 that the suspension will switch to passive damping during manoeuvring. Finally, it is recognised that all the work here concerns the rear of vehicle and that performance improvements toward the front will be less marked. If the system has a facility for preview ahead of the front wheels, for example, a body-to-road sensor mounted on the bumper, it is anticipated

that the techniques used in this chapter may be employed to generate correlated control laws from which the front, as well as the rear, of the vehicle will benefit.

# Chapter 8

## Measurements

### 8.1 Introduction

In this chapter the vertical body and suspension wishbone acceleration, together with the suspension displacement of a passively suspended production saloon car, are measured during actual runs over three road surfaces. The objective is to use the measurements to estimate the value of the parameters in Eqn (2.2), i.e. the roughness coefficient ( $G$ ) and exponent ( $p$ ), thus providing a surface description of each road.

The conventional and most accurate method of obtaining road surface descriptions is by using surveying techniques, or through extensive measurements using some form of profilometer. This latter method has been employed by a number of workers including, for example, La Barre *et al* [1970] who conducted a study of roads throughout Europe, and Healey *et al* [1977] who used the measured profile description as input to a mathematical vehicle model. Although these methods are accurate, they are also time consuming and costly.

A different approach is taken by Aurell and Edlund of the Volvo Truck Corporation [1989], who use a road simulator to excite the vehicle with random inputs corresponding to various known road-spectra, and then work out their frequency response functions from the resulting accelerations. The vehicle is then traversed over the test surface in question and spectra for the front axle acceleration is obtained. From the measured psd's and corresponding frequency

response functions the road surface spectra can be calculated and the parameters  $G$  and  $p$  can be found. Their results, from an extensive range of conditions, found that the slope ( $p$ ) of the log input psd could be set to -3 for normal roads and -2.5 for severe operating conditions. Use of the actual vehicle to obtain the frequency response functions, ensures that the method remains relatively accurate even if the system is non-linear.

The work in this chapter attempts to determine three road roughness and speed conditions which are representative of the typical operational range of the vehicle. Without the equipment required for direct measurement and in the absence of a road simulator, the spectra of the surfaces considered here can only be estimated from the measured acceleration psd's using a linear quarter vehicle model. A crude but practical correlation is still established between the three actual surfaces used for testing and the three idealised surfaces, which are then used for further performance comparisons in Chapter 9.

## 8.2 Instrumentation

The vehicle used throughout the measurements was a Ford Scorpio 2.8 (EFI) V6 Ghia (see Fig 8.1), the rear suspension unit of which can generally be described by the quarter car parameters used in previous chapters (see Table 3.1). The vehicle was fitted with Monroe ASC type dampers, which, rather than switch adaptively, were modified to allow the rear damper setting to be changed manually from inside the vehicle. This enabled measurements to be repeated for two passive settings; soft (0.8kNs/m) and normal (1.5kNs/m). The data was collected in analogue form using two accelerometers, an LVDT and three channels of a TEAC R-71 data recorder. To measure body accelerations, one accelerometer (Setra Systems, model 141) was mounted on the body, at the suspension



Figure 8.1: Ford Scorpio 2.8 (EFI) V6 Ghia.

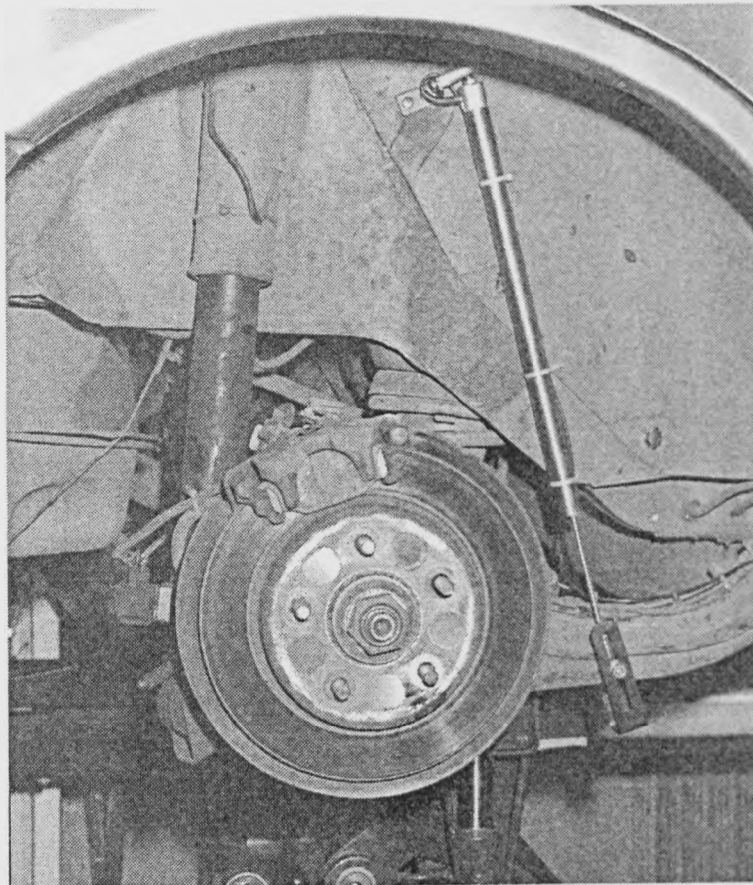


Figure 8.2: Mounting of LVDT inside rear wheel arch.

housing directly above one rear wheel. To measure wheel accelerations, a similar accelerometer should ideally be mounted on the wheel hub itself. On the test vehicle this proved to be impractical and for ease of mounting and access, the wheel accelerometer was mounted on the corresponding suspension arm. The LVDT (RDP Electronics, series D5/500-8000), was mounted inside the same rear wheel arch, alongside the damper, to measure suspension displacement (see Fig 8.2).

The analogue data from the tape recorder is converted to digital form using a data acquisition system developed at Leeds University by Alstead[1985]. The system, developed for the collection of data from a high speed tractor, is based on a Motorola 68000 microprocessor which controls a 16 channel multiplexer and 10 bit analog to digital converter (ADC). In this case, rather than collecting data itself, the system uses the tape recorder signal as the input. Using a sampling rate of 100Hz, the incoming data from the three analogue channels is stored in memory and transferred to floppy disk at the termination of each run. Once in digital form the measured data can be transferred to the VAX 8600 mainframe computer for further analysis. Using the calibration data for each transducer, together with associated programs on the VAX, ie. CALFILE, ENGUNITS, and TIMEPLOT (Alstead [1985]), the raw binary data can be converted into separate channels of data in appropriate engineering units, and ultimately into time histories of each measured variable. Fourier analysis of the data using the VDAS package (Horton [1991]) then enables power spectral densities to be calculated.

### 8.3 Results

The surfaces under consideration were chosen from roads in the vicinity of Monroe (UK) Ltd's production and research facility near York to represent typical smooth, minor and poor minor roads:

- York ring road (smooth)
- Wiggington-Skelton road (minor)
- Back Wiggington road (poor minor)

Vehicle speeds over the three roads were 70, 50 and 40 mph (31.3, 22.4 and 17.9m/s) respectively.

Using the minor road as an example, time histories of vertical body acceleration, suspension arm acceleration and suspension displacement for each damper setting are shown in Figs 8.3 and 8.4 (a), (b) and (c).

For efficient operation, the NAG library routine (G13CBF), used in VDAS for the calculation of power spectral densities, requires the number of sample points to be a power of two. With this in mind, 4096 data points are selected from each run, which, with a sampling rate of 100Hz, translates to around 41 seconds of each recorded signal being analysed. The sampled length of each road is approximately 1300m, 950m, and 750m for the smooth, minor and poor minor surfaces respectively. The psd's of body and suspension arm acceleration, obtained from the measured data over the smooth, minor, and poor minor road are shown in Figs 8.5, 8.6 and 8.7 respectively. The corresponding rms values are shown in Table 8.1.

These psd's can now be used to estimate the surface roughness properties of the three roads using the following procedure. First, it is assumed that the sur-

Condition	Damper setting	Rms value (unweighted)		
		Body acceleration (m/s <sup>2</sup> )	Suspension arm acceleration (m/s <sup>2</sup> )	Suspension displacement (m)
(A)	soft	0.444	1.130	0.0059
	normal	0.399	0.655	0.0042
(B)	soft	1.150	1.210	0.0156
	normal	0.938	0.943	0.0108
(C)	soft	0.918	1.370	0.0134
	normal	0.868	1.390	0.0113

Table 8.1: Measured rms values.

faces are random processes and can therefore be characterised in the frequency domain by an equation of the form (2.2):

$$S_{x_0}(n) = Gn^{-p}$$

The next step is to generate a quarter car model of the test vehicle. This is essentially the passive model used in Chapter 3 and described by the parameters in Table 3.1. Since the work involves comparison with measured data, a number of modifications can be made to the theoretical model to increase its accuracy, namely the introduction of damping to the tyre model (0.1kNs/m) and adjustment of the body mass (340kg) to account for the operator sitting in the rear of the vehicle. The comparisons also require the theoretical model to include suspension wishbone acceleration as one of the output variables. The road roughness parameters,  $G$  and  $p$ , are then estimated empirically by adjusting the input to the theoretical model until the output psd's and rms values

from this model match those of the measured data. The roughness coefficient  $G$  sets the amplitude of the input across the whole frequency range, while the exponent  $p$  dictates the frequency content of the input. The following values of  $G$  and  $p$  provided the best fit to the measured data ;

- Smooth  $G = 7 \times 10^{-9}$
- Minor  $G = 8 \times 10^{-8}$
- Poor minor  $G = 2 \times 10^{-7}$

while the slope of the input psd was estimated at -3 in each case.

The theoretical psd's of the soft and intermediate passive systems using these estimated road surface descriptions can be seen in Figs 8.8 to 8.10. To enable a direct comparison with the measured psd's the accelerations here are unweighted.

## 8.4 Discussion

Looking first at the psd's from measured results in Figs 8.5 to 8.7 the body accelerations are in each case dominated by the body bounce peak at just over 1 Hz, with the harder damper setting having the expected effect of reducing this resonant peak. The results measured by the accelerometer on the rear suspension arm represent a combination of wheel and body acceleration, and this can be seen in the psd's where peaks occur at both the body and wheel resonant frequencies. The size ratio of these peaks depends on the suspension geometry and exact position of the transducer. (In this case the ratio of body acceleration to wheel acceleration is 2:1, since the accelerometer was mounted one third of the way from the body to the wheel). A comparison of these

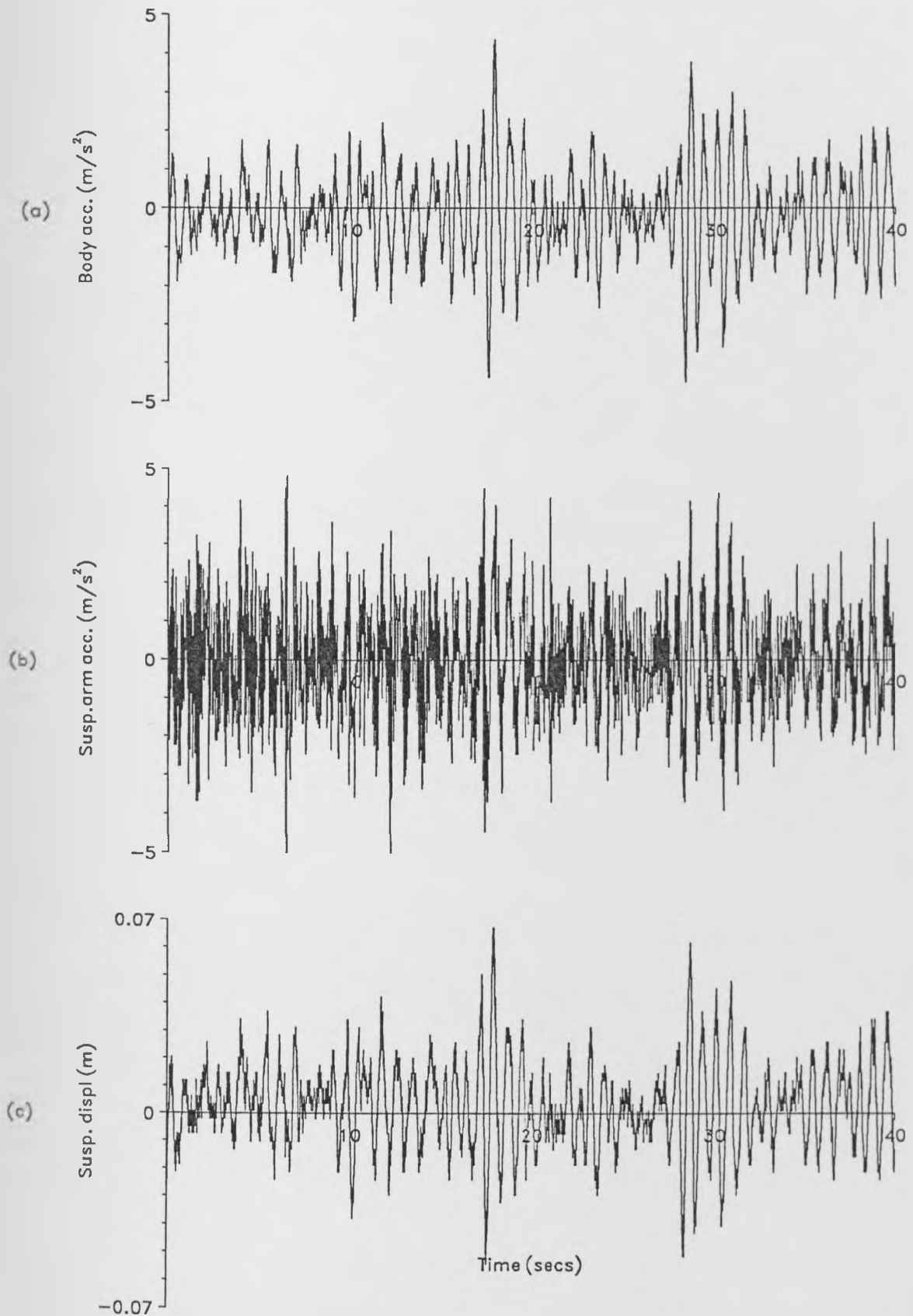


Figure 8.3: Measured body acceleration, suspension arm acceleration and suspension displacement - (Ford Scorpio over minor road at 50mph, damping =  $0.8kN_s/m$ ).

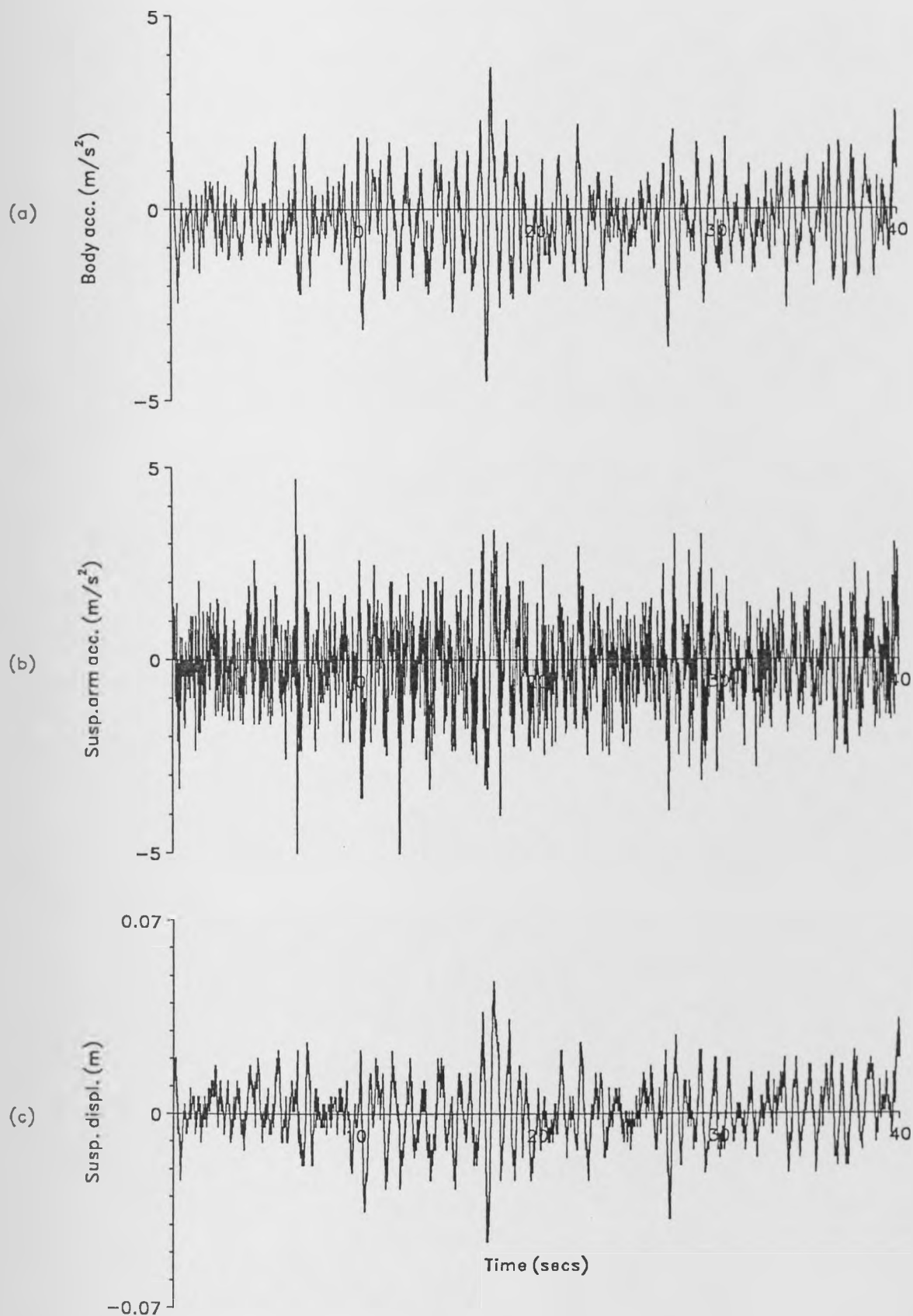


Figure 8.4: Measured body acceleration, suspension arm acceleration and suspension displacement - (Ford Scorpio over minor road at 50mph, damping = 1.5kNs/m).

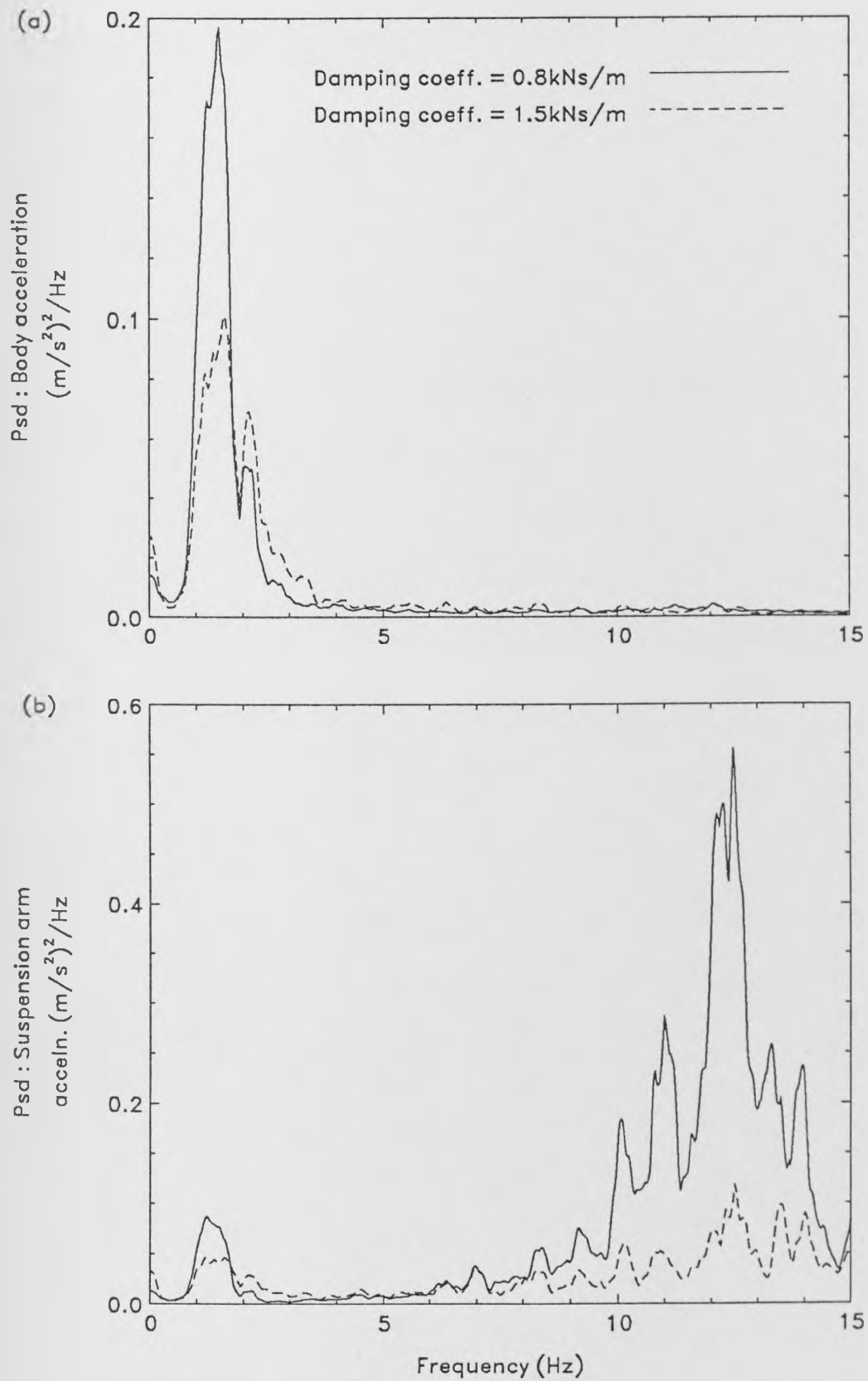


Figure 8.5: Psd's of measured body and suspension arm acceleration - York ring road (A1237) at 70mph.

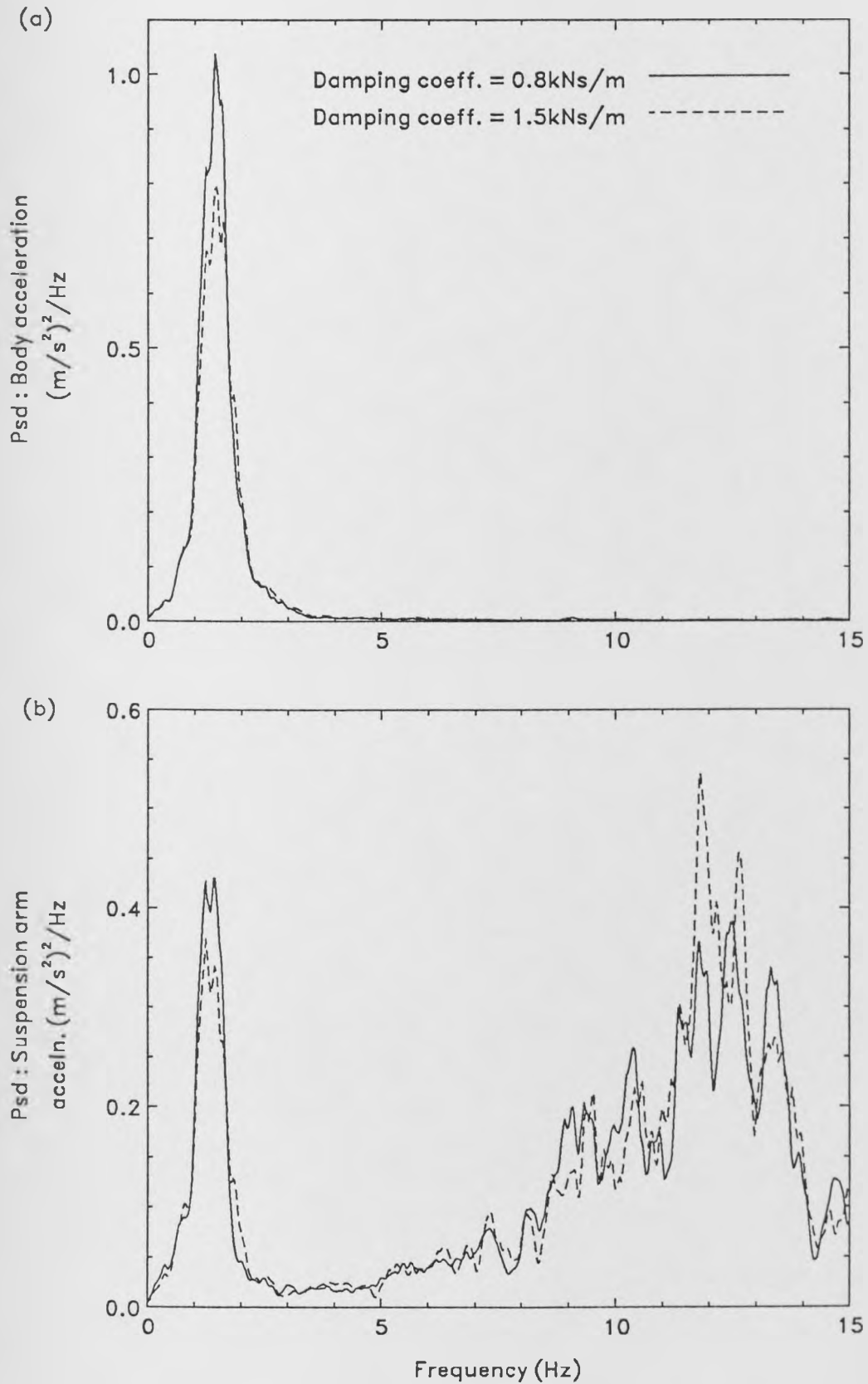


Figure 8.6: PsD's of measured body and suspension arm acceleration - Wiggington to Skelton road at 50mph.

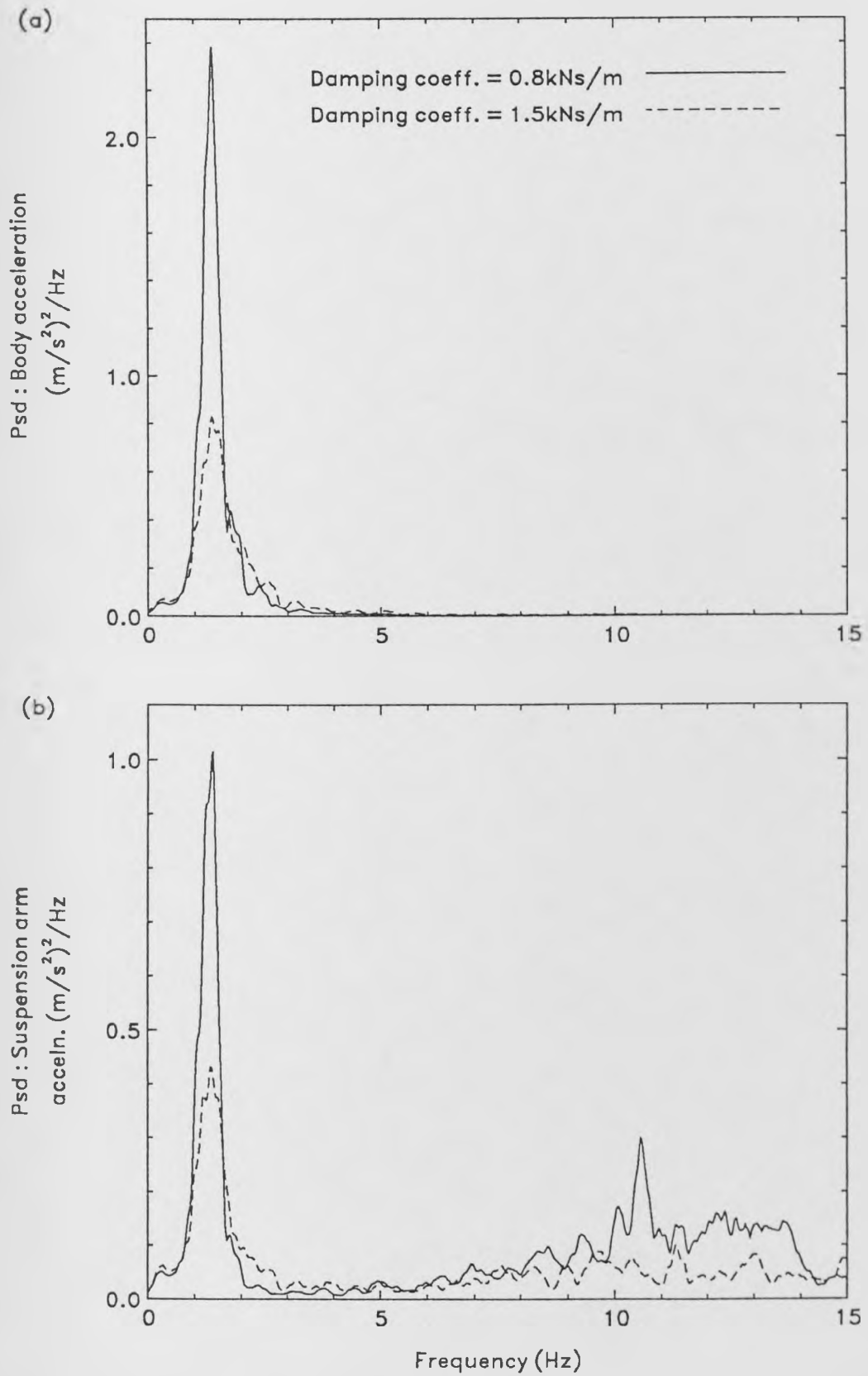


Figure 8.7: PsD's of measured body and suspension arm acceleration - Back Wiggington road at 40mph.

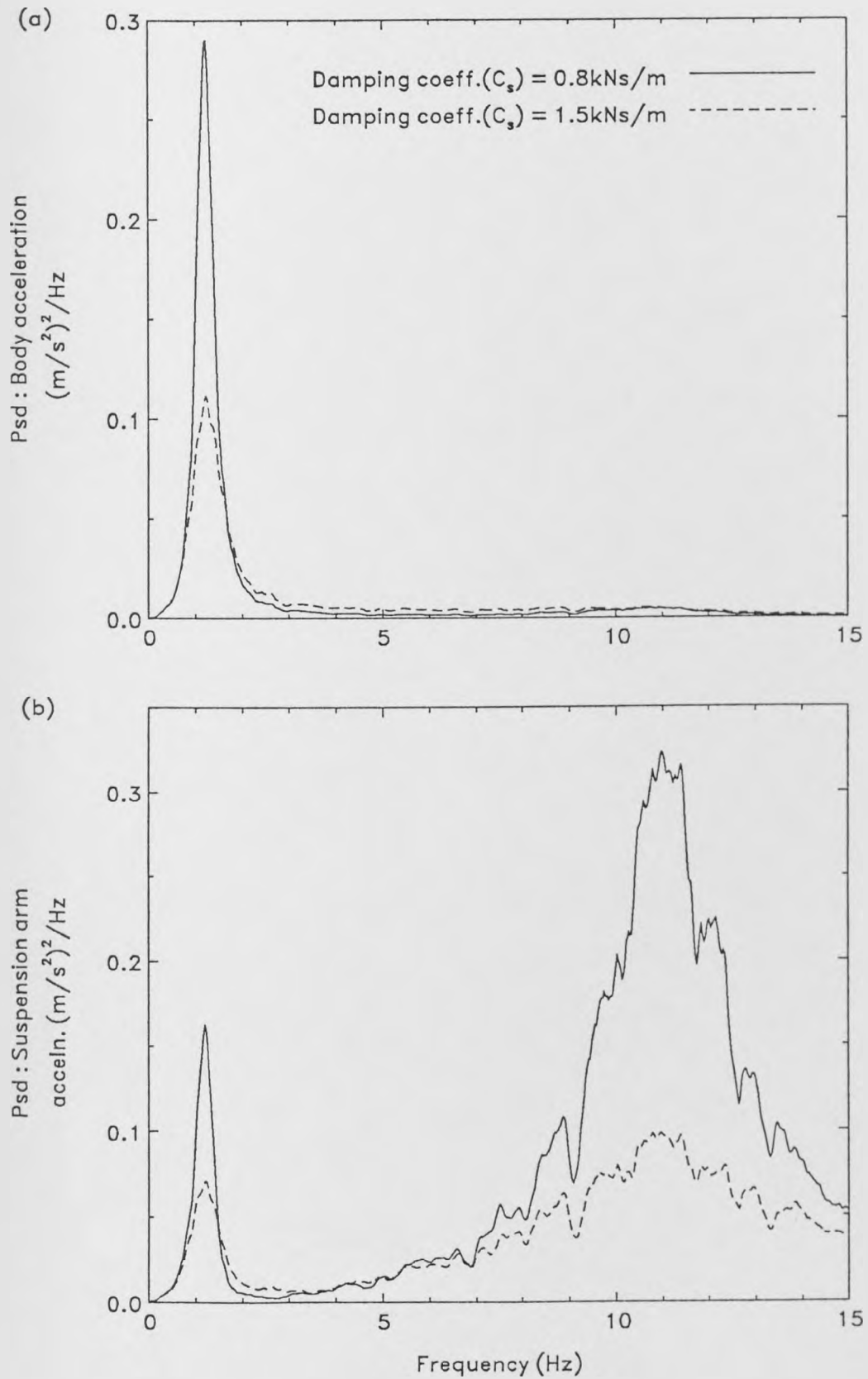


Figure 8.8: Theoretical psd's of body and suspension arm acceleration - Condition (A). (Compare with Fig 8.5)

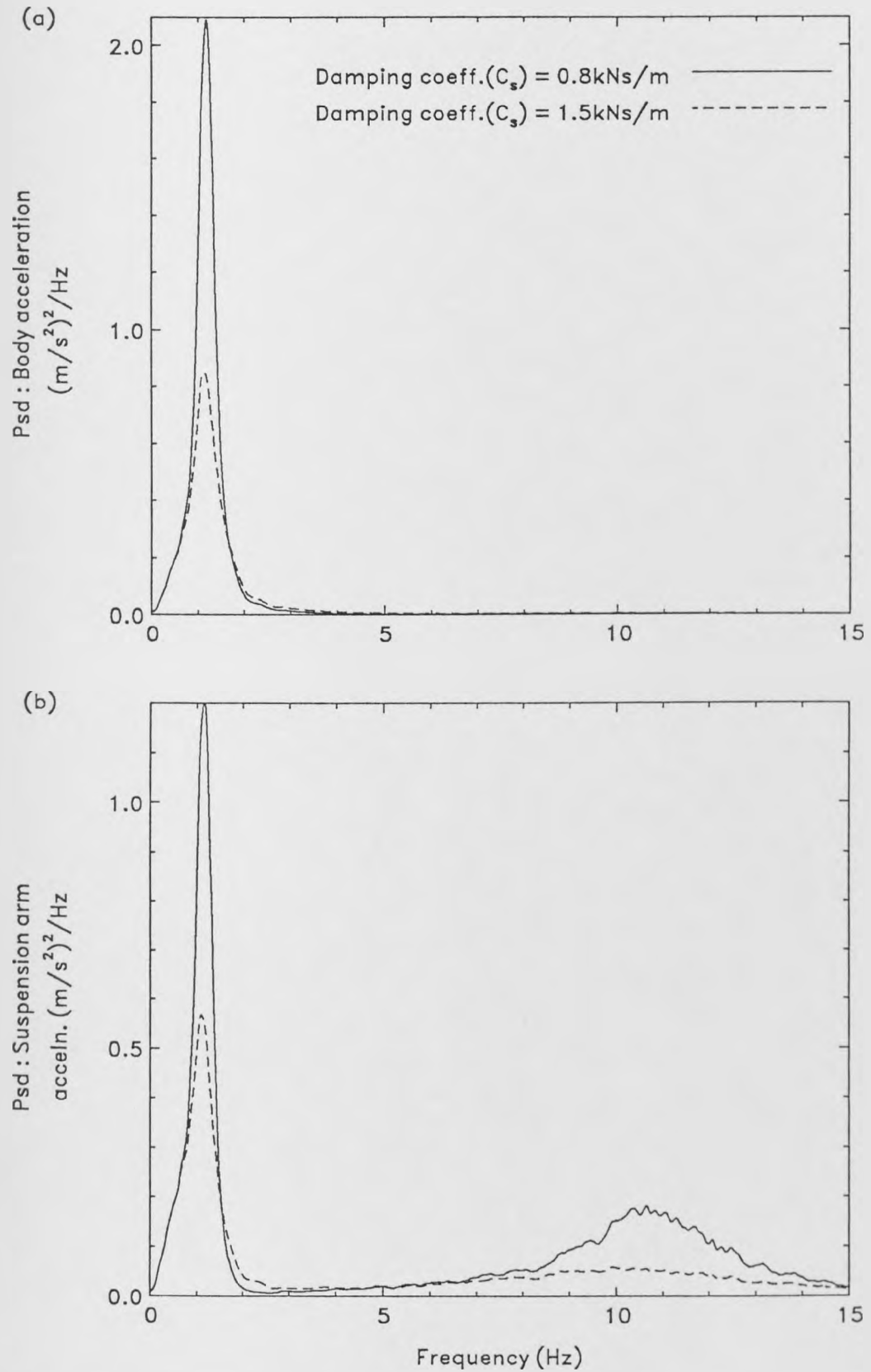


Figure 8.9: Theoretical psd's of body and suspension arm acceleration - Condition (B). (Compare with Fig 8.6)

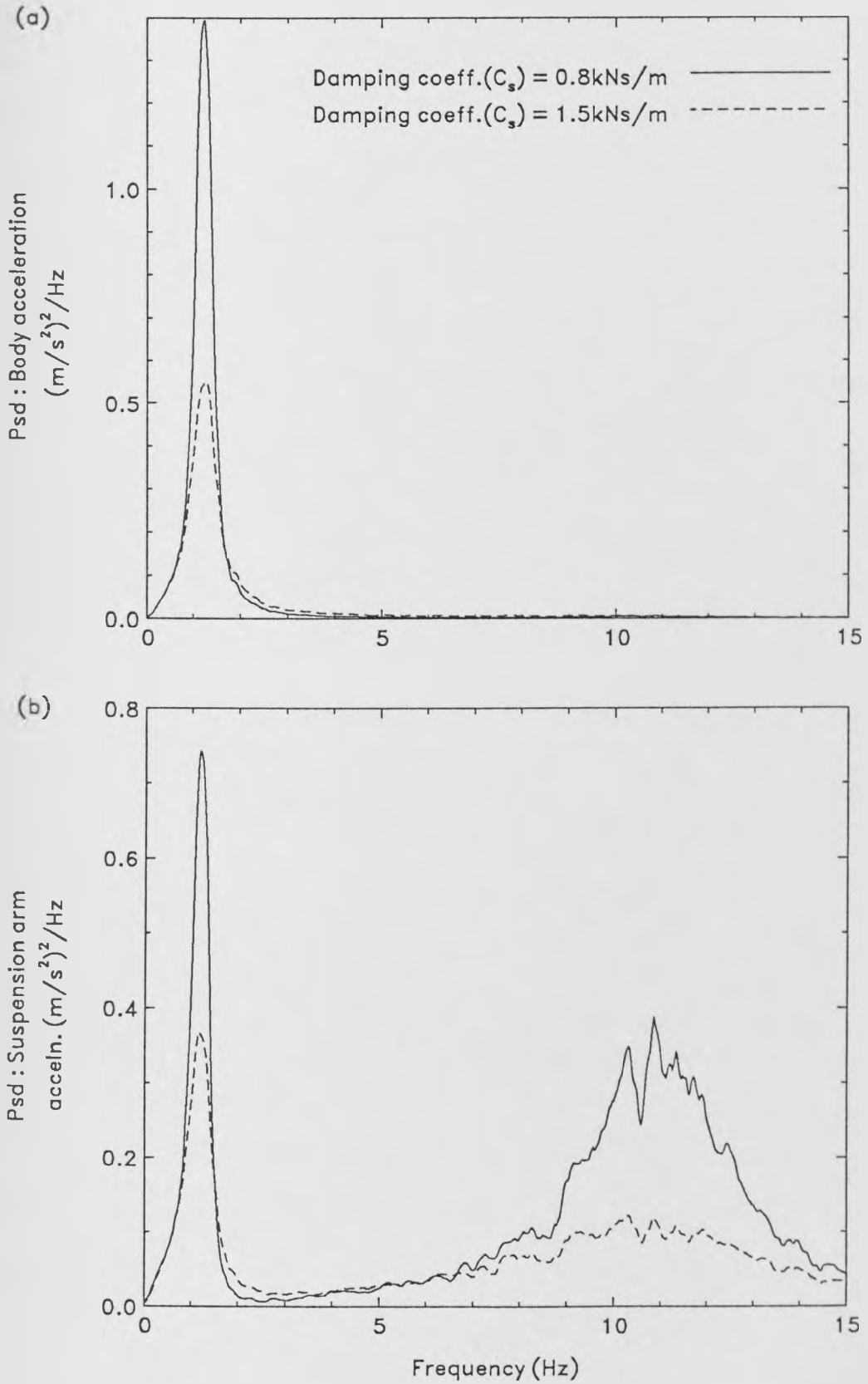


Figure 8.10: Theoretical psd's of body and suspension arm acceleration - Condition (C). (Compare with Fig 8.7)

measured psd's and the theoretical psd's in Figs 8.8 to 8.10 reveal two features. First the shape of the psd curves are encouragingly similar and second, the effects of the changes in damping are also similar. Although this is in part due to the adjustment of the theoretical input to estimate the surface roughness parameters, both features support the approach of using the quarter car model as a basis for suspension design studies.

It is accepted that the technique described in this chapter for obtaining the surface roughness parameters is very approximate. For the method to be correct, the model must be an accurate representation of the real vehicle. The single wheel station model used here has obvious limitations, and it is almost certain that some of the measured data is a result of excitations from, for example, wheel imbalance or engine vibration, which cannot be accounted for in such a simple vehicle model. Furthermore the model does not include any detail of suspension mountings and neglects any non-linearities which may occur in the suspension elements. Nevertheless, the estimated parameters are all within the range of figures quoted in the literature.

The exponent  $p$  is essentially the slope of the log psd curve for the ground input. As discussed in Chapter 2, Robson [1973] shows the psd of a typical road to have a dual slope characteristic, with a slope of -3.15 at low wavenumbers and -2.32 at higher wavenumbers. All three input psd's here were estimated to have a slope of -3. These are somewhat higher than the -2.5 used in earlier theoretical comparisons in Chapters 3 to 7 but correlate strongly with the values quoted by Aurell and Edlund [1989] and still lie within the range quoted by Robson. The estimated values of roughness coefficient  $G$  also fall within the ranges quoted by Robson.

The "standardisation" of three typical surfaces in this manner, enables a comparison of competing suspensions over a range of conditions, rather than the

single surface comparisons of previous chapters.

## 8.5 Concluding Remarks

In this chapter, the body acceleration, suspension arm acceleration and suspension displacement at the rear of a passively suspended saloon car are measured during actual runs over three typical road surfaces. By comparing the resulting psd's with theoretical psd's obtained from simulated runs over a series of idealised inputs, the surface roughness parameters ( $G$  and  $p$  in Eqn 2.2) of the test surfaces have been estimated. They have been found to lie within the range of values quoted in the literature. Although this empirical approach to characterising road surfaces is not a rigorous scientific procedure, the work does serve to provide a range of idealised surfaces which are associated with known roads. Using these surfaces, the next chapter will provide theoretical results of a more practical nature by comparing suspension performance over each of the three "roads".

# Chapter 9

## Comparison of Systems

### 9.1 Introduction

Although the results generated in Chapters 3 to 7 have concentrated on the ride performance of vehicles fitted with various suspensions when they traverse a single road surface, it is clear that in practice, the suspension must be designed to operate over a wide range of surface conditions. It is suggested in Chapter 2 that, using the factors  $\sqrt{G}$  and  $\sqrt{V^{p-1}}$ , the results of a system from a single surface can be scaled to determine the behaviour at other operating conditions. However, this technique strictly applies to results which are obtained for linear systems only and therefore may not work for results of the controllable damper with its time varying coefficient. This chapter compares the performance of selected controllable damper systems with that of the standard passive and ideal active suspensions, over a typical range of operating conditions. Using realistic suspension parameters and the three road surface descriptions established in Chapter 8, the aim is to produce theoretical comparisons which this time have a more practical flavour.

In Chapter 7 the benefits of using a half vehicle model, enabling the employment of control laws which include information about the correlation between ground inputs, were highlighted. In the process a number of problems were encountered, particularly with regard to finding an optimal solution using the NAG library gradient search routine. Therefore, while these improvements are acknowledged,

in the interest of reduced computing time this comparison returns to using the more manageable quarter vehicle model.

## 9.2 Selected designs

The passive suspension parameters used here are as described in Table 3.1, ie.  $K_s=22\text{kN/m}$  and  $C_s=1.5\text{kNs/m}$ , while the active system operates according to the limited state feedback control law shown in Eqn (4.29). For the controllable damper systems it is assumed that the spring rate is fixed and that, for both static and dynamic attitude control purposes, this should be equal to that of the standard passive system ( $22\text{kN/m}$ ). All the systems chosen for comparison are intended to represent “practical” suspensions and therefore the constraints identified in Chapter 6 are all described using realistic data, where possible from the results of practical testing. The details of these response limitations and the remaining suspension parameters are summarised as follows :

### 9.2.1 Continuously variable damper

Like the active system, the continuously variable damper operates according to the limited state control law given by Eqn (4.29) ;

$$u = -[K_2(x_1 - x_2) + K_3x_3 + K_4x_4]$$

where the feedback gains  $K$  are found using the gradient search routine described in Chapter 4.

Following the reasoning in Section 6.4, a realistic value for the minimum damping constraint is taken to be  $0.3\text{ kNs/m}$ , while the maximum constraint, which is governed by standard control valves within damper is set at  $2.5\text{ kNs/m}$ .

The proportional valve is assumed to respond according to first order lag dynamics with a time constant ( $T$ ) of 10ms.

### 9.2.2 Switchable damper

Unlike the semi-active system which has the ability to continually change its damper setting within the available limits, this system switches between two fixed settings. From the results in Fig (5.9) it is clear that, for a given suspension stiffness, the performance of the switchable damper system can vary widely depending on the choice of hard and soft settings. With this in mind, two possible systems are considered here; the first (1) has a hard damper setting equal to that of the passive system, while the second (2) has a hard setting equal to the maximum available damping of the continuously variable damper level. The minimum settings in both cases are such that the ratio of soft to hard is 0.3 .

System (1) :

Hard damper setting,  $C_{hard} = 1.5$  kNs/m

Soft damper setting,  $C_{soft} = 0.45$  kNs/m

System (2) :

Hard damper setting,  $C_{hard} = 2.5$  kNs/m

Soft damper setting,  $C_{soft} = 0.75$  kNs/m

The response of the two-state valve is assumed to consist of a threshold delay ( $T_{th}$ ) of 10ms, followed by a first order lag with time constant ( $T$ ) also 10ms. These times are based on measured valve responses of the currently available Monroe ASC adaptive damper, which has a similar mode of operation. Fig 9.1 shows the total response times, ie. threshold delay + first order lag, of the

valve to be a function of suspension velocity and damper setting. The soft to-intermediate and soft-to-hard curves are most applicable to the switchable systems (1) and (2) respectively and from these the time of 20ms is selected as an average response across the range of suspension velocities.

### 9.2.3 Adaptive damper

The selected adaptive damper is based on a prototype Monroe ASC system fitted to the rear suspension of a Ford Scorpio and has soft, intermediate, and hard settings of 1.0 kNs/m, 1.5 kNs/m and 2.0 kNs/m respectively. The limits of suspension travel in each setting depends on the vehicle speed and for each of the three conditions can be determined from Fig 5.4 ;

At 70 mph : soft to intermediate =  $\pm 0.020\text{m}$   
intermediate to hard =  $\pm 0.058\text{m}$

At 50 mph : soft to intermediate =  $\pm 0.025\text{m}$   
intermediate to hard =  $\pm 0.068\text{m}$

At 40 mph : soft to intermediate =  $\pm 0.031\text{m}$   
intermediate to hard =  $\pm 0.071\text{m}$

The actual valve response times for this system are shown in Fig 9.1. A threshold delay and first order lag of 10ms each are included in the model to represent an average response, although in this case the times are small compared to the minimum duration of each setting change (0.5 seconds), and consequently will have little effect on performance.

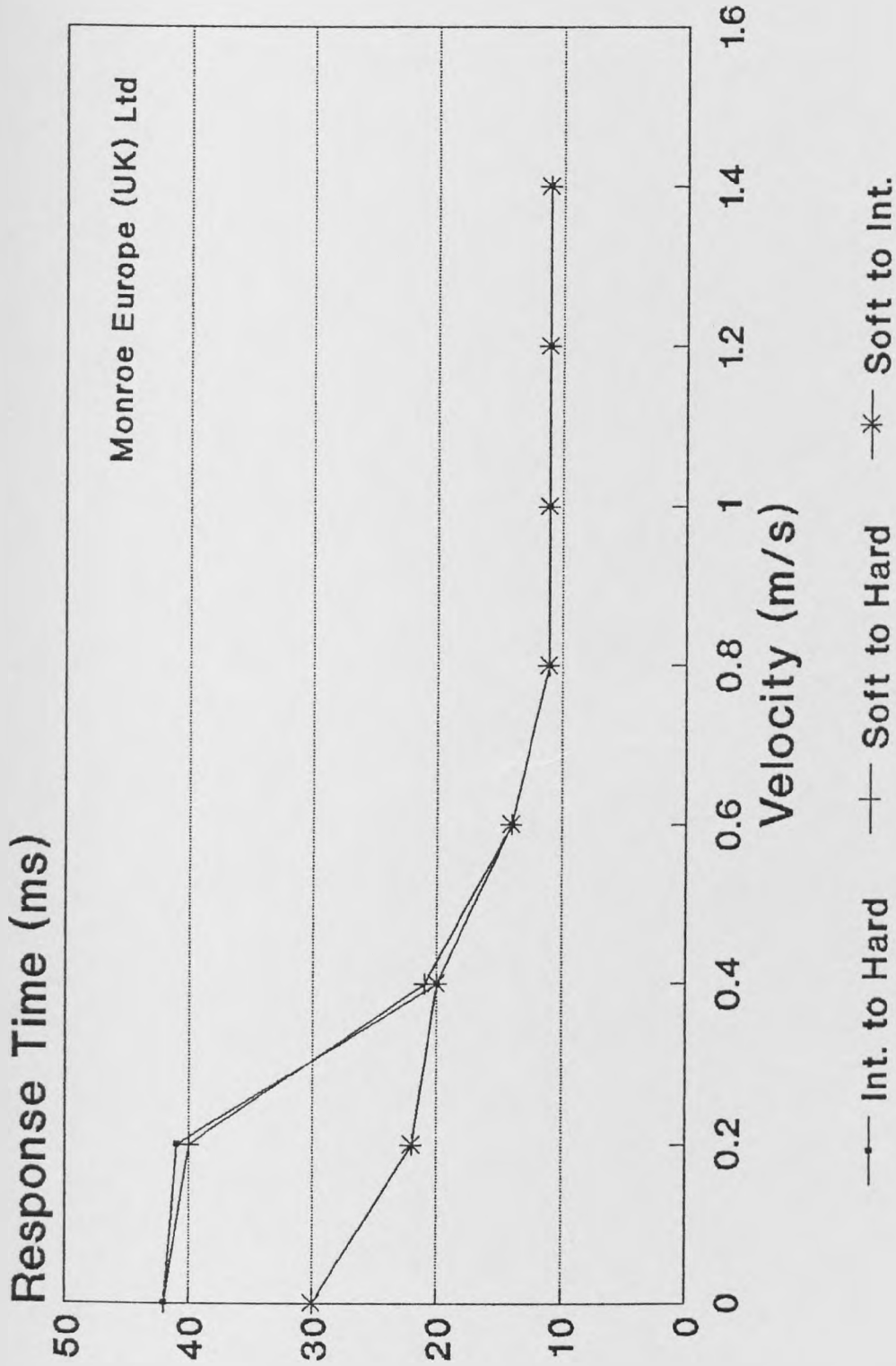


Figure 9.1: Measured total valve response times of the Monroe ASC system.

### 9.3 Results

The three conditions used in the comparison are ;

- (A) Smooth road at 70 mph (31.3 m/s) :  $G = 7 \times 10^{-9}$ ,  $p = 3$
- (B) Minor road at 50 mph (22.35 m/s) :  $G = 1 \times 10^{-7}$ ,  $p = 3$
- (C) Poor minor road at 40 mph (17.9 m/s) :  $G = 2 \times 10^{-7}$ ,  $p = 3$

Profiles representing each surface are generated from the above descriptions using the procedure outlined in Section 2.2.

The comparisons of competing systems in previous chapters have generally been based on an equal usage of suspension workspace. Whilst this method provides a useful starting point for analysis, in reality it perhaps places an unfair restriction on the active and controllable damper systems. These systems can adapt to the prevailing running conditions with a simple adjustment to the control law, and are therefore able to use the available working space more effectively than a fixed passive suspension. For example, the surface description used in Chapters 3 to 7 is such that the rms suspension working space used by the passive system is 0.029m. On the same surface, adaptation of the active or semi-active control law will allow these systems to use up to the maximum allowable rms (0.0365m) with a corresponding improvement in ride comfort.

To increase the practical nature of the results in this chapter, the constraint of equal workspace usage is relaxed, allowing the active and controllable damper systems to use any amount of suspension travel providing it is within the available limits. A comparison on this basis is shown in Table 9.1.

The active system compared here is driven by a control law described by Eqn (4.29) and has feedback gains;  $K_2 = -7.239$ ,  $K_3 = -0.444$  and  $K_4 = 2.356$ ,

Running condition	System	Rms - ISO weighted vert. body accn ( $m/s^2$ )	Rms - tyre load variation (kN)	Rms - susp. working space (m)
(A)	Passive	0.204	0.115	0.0034
	Active	0.081	0.128	0.0055
	Cont.variable	0.168	0.125	0.0035
	Switchable (1)	0.189	0.115	0.0035
	Switchable (2)	0.202	0.105	0.0027
	Adaptive	0.207	0.130	0.0042
(B)	Passive	0.553	0.310	0.0091
	Active	0.175	0.410	0.0170
	Cont.variable	0.453	0.342	0.0100
	Switchable (1)	0.512	0.312	0.0094
	Switchable (2)	0.547	0.287	0.0073
	Adaptive	0.543	0.335	0.0106
(C)	Passive	0.622	0.351	0.0103
	Active	0.228	0.425	0.0200
	Cont.variable	0.517	0.420	0.0120
	Switchable (1)	0.580	0.356	0.0106
	Switchable (2)	0.620	0.327	0.0083
	Adaptive	0.615	0.385	0.0122

Table 9.1: Performance of Competing Systems over Three Surface/Speed Conditions

generated using a performance index with weighting coefficients;  $q_1 = 750$ ,  $q_2 = 75$  and  $\rho = 1$ . While it is possible to find control laws which use more of the workspace and provide further improvements in comfort, such systems have a poor performance in terms of dynamic tyre load. The system in Table 9.1 is therefore a compromise, chosen to provide a road holding performance which is reasonably close to that of the passive system.

The continuously variable damper system is selected on a similar basis. Using performance index weightings of  $q_1 = 0$ ,  $q_2 = 0$ ,  $q_3 = 0.1$  and  $\rho = 1$ , the feedback gains in Eqn (4.29) are as follows ;  $K_2 = 8.659$ ,  $K_3 = -0.147$  and  $K_4 = 1.536$ .

The results from Table 9.1 can be interpreted more clearly in Fig 9.2, a plot of discomfort parameter (ACC) against tyre loading parameter (DTL). Unlike similar graphs in previous chapters the comparison is not based on equal workspace usage and the SWS values for each system are as shown in the table. In the case of the active and continuously variable damper systems, a range of possible systems are plotted to highlight the potential change in performance as their control laws respond to a change in performance index weighting between comfort and road holding. On these curves, points ACT and CV represent the performance of the active and continuously variable systems selected in Table 9.1.

For condition (B), psd's of ISO weighted vertical body acceleration and dynamic tyre load for the passive system are compared with those of the continuously variable damper system in Figs 9.3(a),(b), the switchable damper system in Figs 9.4(a),(b), and finally the adaptive damper system in Figs 9.5(a),(b).

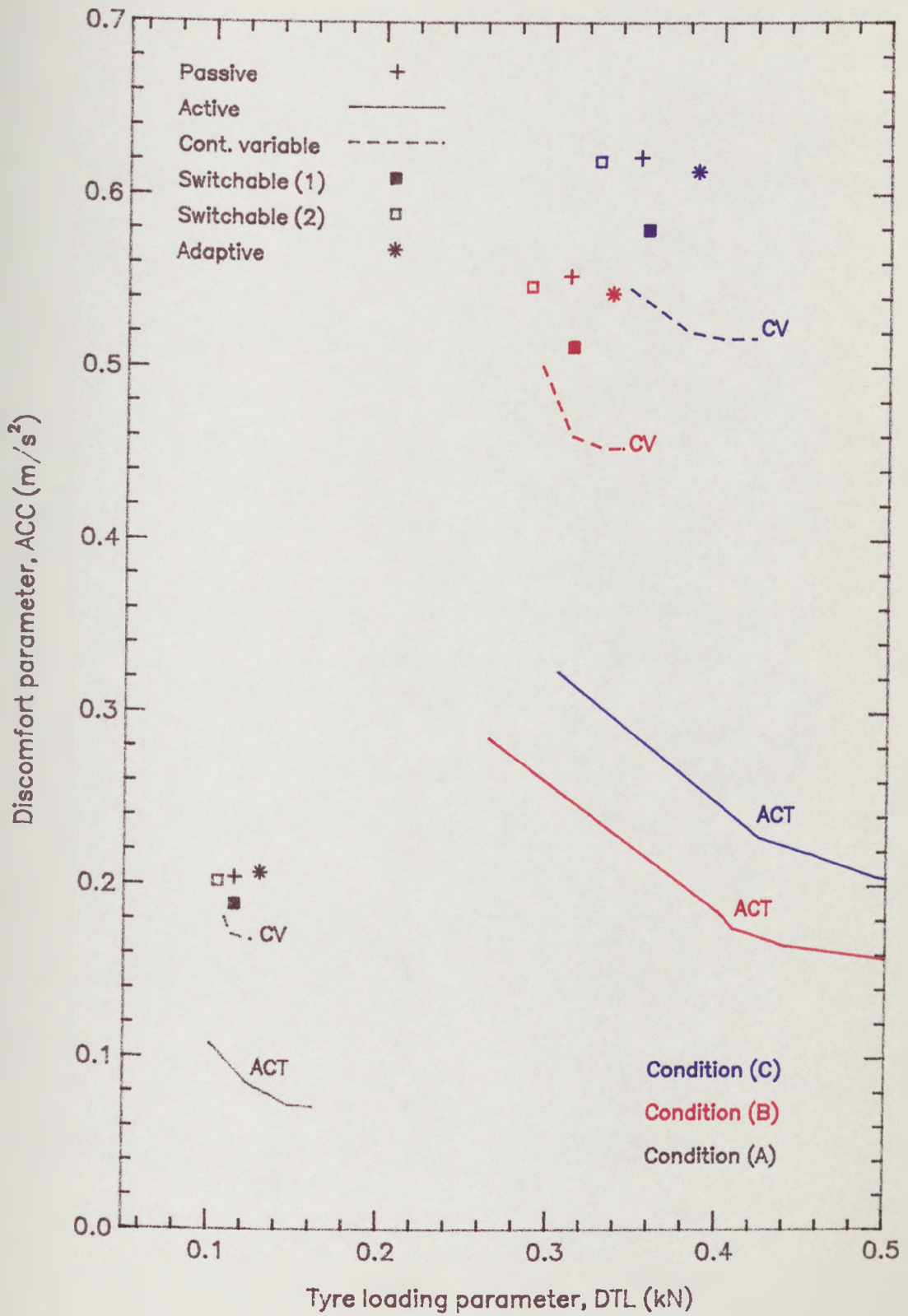


Figure 9.2: Comparison of systems over three idealised surfaces.

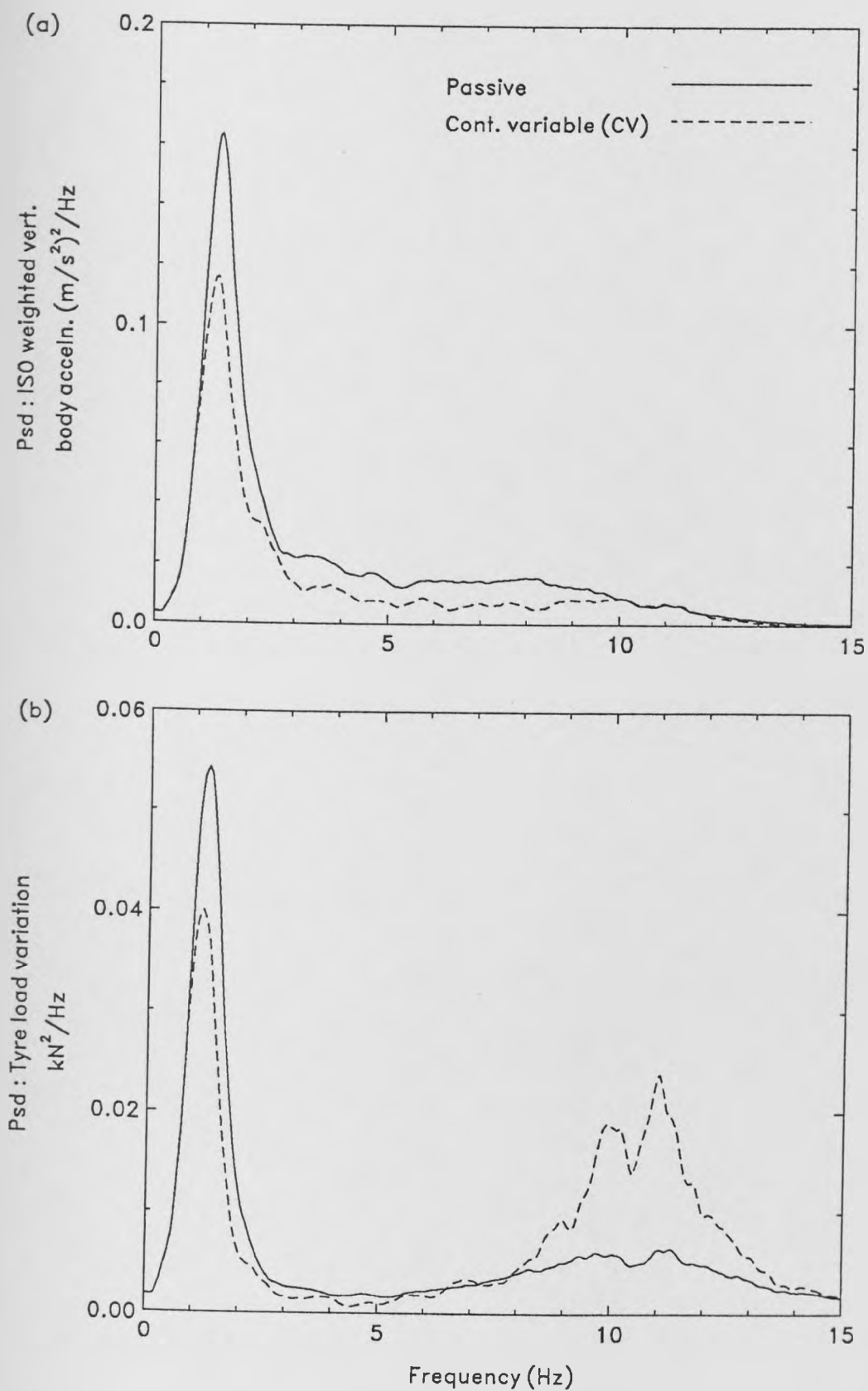


Figure 9.3: Psd's of ISO weighted vertical body acceleration and dynamic tyre load - continuously variable damper system at condition (B).

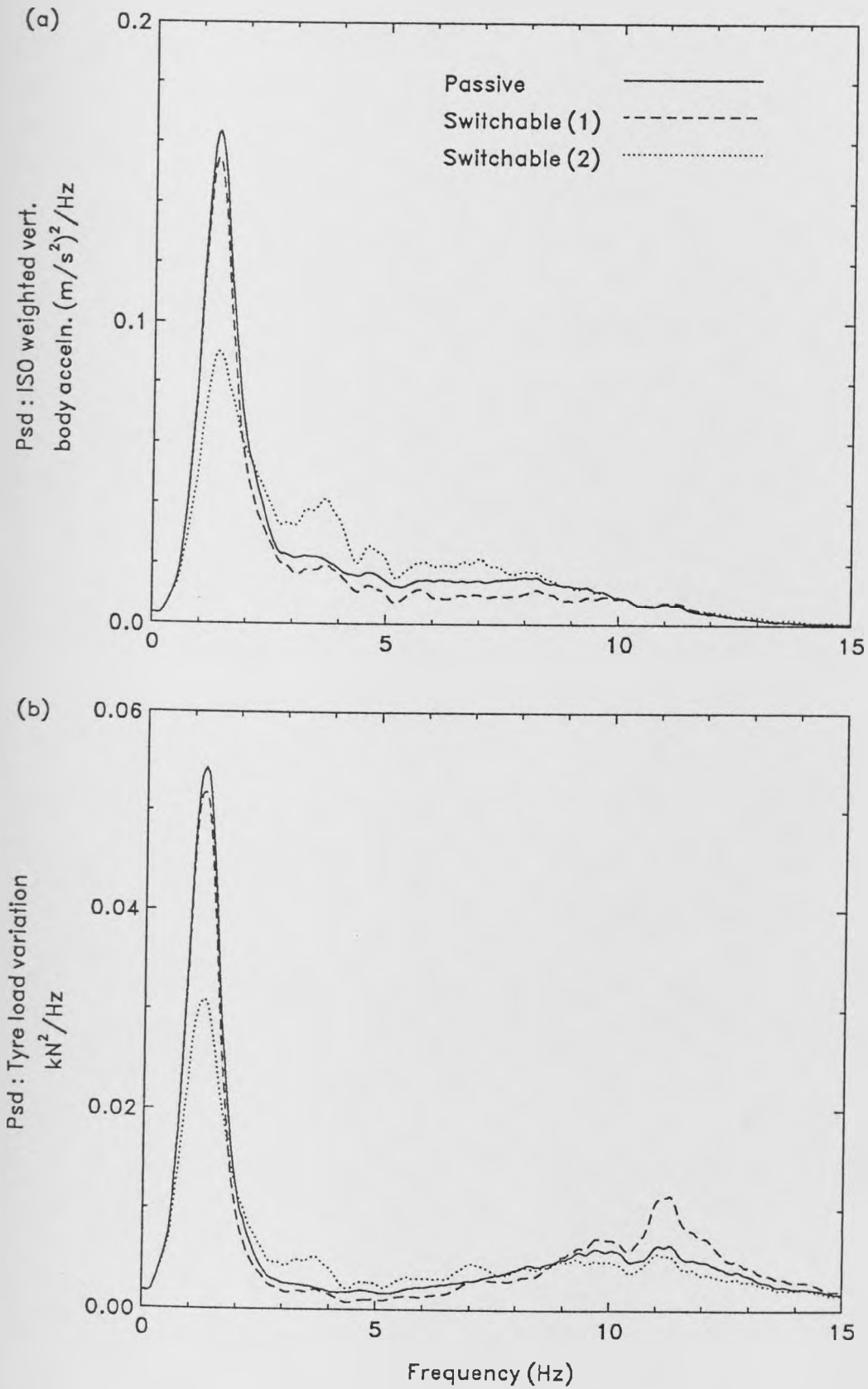


Figure 9.4: Psd's of ISO weighted vertical body acceleration and dynamic tyre load - two-state switchable damper system at condition (B).

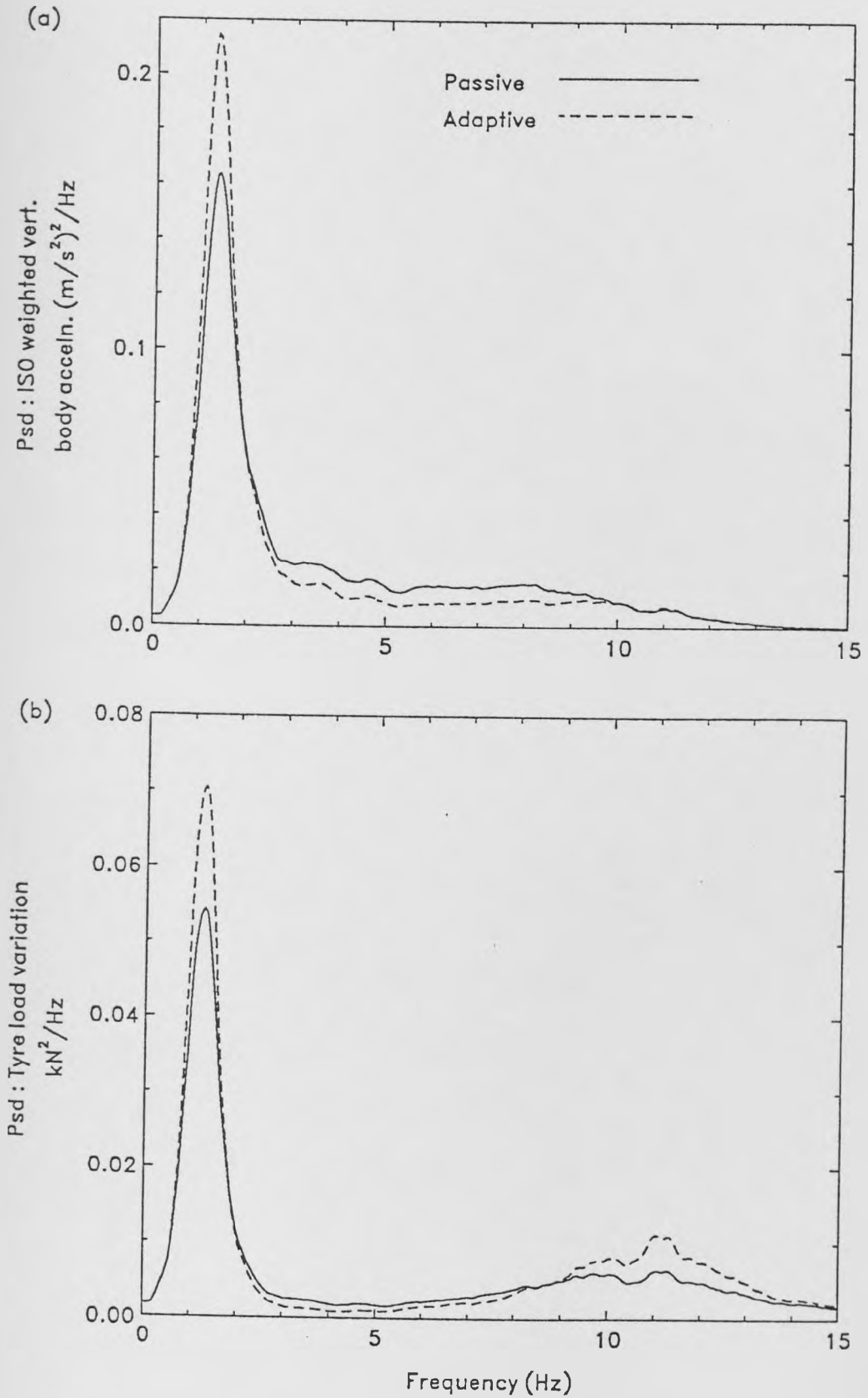


Figure 9.5: Psd's of ISO weighted vertical body acceleration and dynamic tyre load - three-state adaptive damper system at condition (B).

## 9.4 Discussion

### 9.4.1 Scaling effect

The first point of interest in Fig 9.2 is the effect a change in running conditions has on the general performance level of all systems. The scaling effect mentioned in Section 2.4.2 is clearly visible and appears to apply not only to the results of the linear passive and active suspensions but also those of the time varying continuously variable and switchable damper systems. Taking the continuously variable damper system as an example, the predicted performance at condition (A) is  $ACC=0.168\text{m/s}^2$ ,  $DTL=0.125\text{kN}$  and  $SWS=0.0034\text{m}$ . To find the performance at condition (B) these results can be scaled using the factor ;

$$\sqrt{\frac{G_B}{G_A}} \cdot \sqrt{\frac{V_B^2}{V_A^2}} = 2.7 \quad (9.1)$$

giving ACC, DTL and SWS figures of  $0.454\text{m/s}^2$ ,  $0.338\text{kN}$  and  $0.0092\text{m}$  respectively, which are close to the results obtained using non-linear analysis in Table 9.1.

The switching strategy of the adaptive damper system is based on the amount of suspension travel, which in turn depends on the road roughness/speed condition. In contrast to the other controllable damper systems, which are constantly changing their damper setting, this system selects a damper setting to suit the operating conditions and is likely to remain in this setting for much longer periods. Consequently, this is the only system compared in Fig 9.2 which does not lend itself to scaling between operating conditions.

### 9.4.2 Comparison of results

At any of the three conditions the ride improvements of the active system over the fixed passive system are dramatic. If the road holding ability of the passive system is maintained the improvement in ride is approximately 55%, while if a comfort biased control law is used, reductions in discomfort parameter of up to 75% are possible. This is a marked improvement on previous comparisons, for example in Fig 4.4, where using similar systems an improvement of only 45% is available. The main reason behind this is the removal of the workspace restriction, allowing the active system, with its ability to provide power input, to utilise the available space much more effectively than the equivalent passive suspension. Another reason lies with the choice of road surface descriptions used in this chapter, or more precisely, the use of an exponent 3 in Eqn (2.2) rather than the 2.5 of previous chapters. This is discussed in more detail later, when the psd's of the results are examined.

At each condition the continuously variable damper system is the best performing version of the controllable damper system. This suspension is purely dissipative and therefore cannot adapt to use the workspace as effectively as the active suspension. Suspension travel is now governed to a large extent by the stiffness of the parallel mounted spring, which in this case is equal to the passive design, and therefore its performance curve lies closer to the passive than active results. Despite this, the improvements in ride comfort are significant, with reductions in discomfort parameter of between 12 and 18% over the passive suspension, depending on how the performance index has been weighted. Again these are better results than seen in previous chapters. For example, Fig 6.12 includes a performance curve for a continuously variable damper system with the same response limitations as in this chapter. At the same tyre loading parameter as the passive system, the improvements in comfort are small

(approximately 3%). Percentage ride improvements similar to those in Fig 9.2 are possible but in Fig 6.12 they can only be achieved at the expense of a 20% increase in tyre loading parameter. Since the passive and continuously variable damper systems in Table 9.1 use a similar amount of workspace, it becomes clear that the difference between the relative results here and those in Chapter 6 is caused entirely by the difference in road surface description.

The performance of switchable system (1) lies approximately halfway between that of the continuously variable and passive systems, giving around an 8% improvement in ride with no deterioration in road holding. In view of the reduced complexity of the hardware and the relatively simple control strategy, these gains may still be considered worthwhile. Switchable system (2) is an alternative design which is biased toward improved road holding rather than ride. This is reflected in Fig 9.2 where for the same or slightly better comfort as the passive suspension, this system can improve on the tyre loading parameter by around 8 to 10%. Both switchable systems use damper settings with a soft to hard ratio of 0.3. For the running conditions here  $C_{soft}/C_{hard}$  could be reduced further to use more workspace and increase comfort, however, at more severe conditions this may result in excessive suspension travel.

Despite being modelled on an existing prototype, the selected adaptive system appears to offer only marginal comfort gains over the passive system for the range of conditions considered here. At condition (A) the discomfort parameter is actually worse than that of the passive, while at conditions (B) and (C) the improvement in ride is less than 5%. If these results are compared to those of the switchable damper, a system of similar complexity and hardware, it becomes questionable whether the improvements are worthwhile.

In the style of Chapter 5 the results for the controllable damper systems are analysed further by comparing their psd's of body acceleration and dynamic tyre

load with those of the passive system. The most important point to emerge is a general one concerning the effect an adjustment to the road surface description has on the relative performance of competing systems. The use of an exponent  $p = 3$  in this chapter, instead of the  $p = 2.5$  in previous chapters, has the effect of changing the frequency content of the input. For a given roughness coefficient  $G$ , the lower wavenumber content is increased whilst the high wavenumber content is decreased. The subsequent effect on vehicle response can be seen by comparing, for example, the passive psd's in Fig 9.3 with those of the same passive system in Fig 5.6. Looking at the psd's of dynamic tyre load in particular, there is a clear shift in emphasis in the response, with the activity around the body resonance peak becoming relatively more important than activity at the "wheelhop" frequency. The change in input will similarly affect the response of the controllable damper systems, and will also affect how these systems are judged in relation to the passive system. As discussed in Chapter 5, the continuously variable system operates primarily by controlling events around the body resonance peak, reducing both body accelerations and dynamic tyre load in this region. It is less effective at controlling events around wheelhop and in this region generally performs worse than the passive suspension. The same trend is seen in the psd's of this chapter (Figs 9.3(a)(b)), although here the importance of the "wheelhop" peak has been reduced by the change of input and consequently each continuously variable system will show more favourably in terms of rms tyre load variation. This has the effect of shifting the rms performance curve to the left in relation to the passive performance providing increased comfort for a given tyre load. The same argument can be applied to the fully active and switchable damper systems and is the reason behind the higher percentage ride improvements seen in this chapter.

The psd's in Fig 9.4(a) and (b) highlight the difference in performance of the two selected switchable damper systems. The ride improvements of system (1) are

achieved through a reduction in body accelerations in the frequency range up to 10Hz. System (2) is more effective at reducing the body resonance peak but the response between 2 and 10Hz is worse. This increase in “harshness” results in a discomfort parameter which is close to that of the passive suspension. From Fig 9.4(a) it is seen that the improved rms tyre load variation of system (2) is almost entirely due to a reduction in response around the body resonance frequency, the response at wheelhop being little better than passive response.

The psd of body acceleration for the adaptive system in Fig 9.5(a) shows an improved response in the frequency range 2 to 10Hz, but also an increase in the body resonance peak. The psd for tyre load variation (Fig 9.5(b)) shows the body and wheel resonance peaks to be greater than the standard passive suspension with a small improvement at frequencies inbetween. As discussed earlier, the choice of surface description in this chapter has increased the importance of the response around body resonance. In contrast to the other switchable systems, the adaptive suspension does not control events in this frequency range and consequently its rms value, relative to other competing suspensions, will suffer. For the duration of the simulation the effect of the adaptive strategy is a net reduction in damping level and therefore the response of the adaptive system is similar to that of a lightly damped fixed passive system.

### 9.4.3 Control law adaptation

The continuously variable damper has a further advantage over the switchable and adaptive damper systems ie. the ability to adjust its control law to suit the conditions. However, since the results in Fig 9.2 scale in the manner discussed earlier, it follows that any control law which is designed to use as much working space as possible at one condition, can be used to similar effect at any other condition. In this respect, only when the SWS figure exceeds the maximum

available will adjustment of the control law be required, in to order to limit the amount of suspension travel and prevent excessive bump stop contact. For the conditions used here, the SWS figure is always below the limit, and therefore any control law adaptation is more likely to involve a change in emphasis between comfort and road holding. Such a change will probably be initiated by higher level algorithms requiring, for example, better road holding for manoeuvring, and result in a shift along the performance curves shown in Fig 9.2.

## 9.5 Concluding Remarks

Using the three surface conditions established in Chapter 8, this chapter provides a comparison of competing systems over a range of typical operating conditions. Each controllable damper system is intended to represent a “practical” system and is modelled using realistic data to describe the response limitations suggested in Chapter 6. The equal workspace restriction of previous comparisons is now relaxed, allowing the fully active and controllable damper systems to use the available workspace to greater effect. The result is a theoretical comparison with a practical feel, from which the following conclusions are drawn :

1. In a similar way to the results of the linear passive and active systems, the results of the continuously variable and switchable damper systems can be scaled between operating conditions. The adaptive suspension is the only controllable damper system which does not behave in this manner.
2. A judgement on the relative performances of competing systems is influenced by the value assumed for the slope of the ground input psd. Even though the slope used in this chapter (-3) and the one used in previous chapters (-2.5) are both within the range of measured values quoted by Robson [1973] and [1979], the relative comparisons vary significantly.

The steeper slope used here results in less input at higher wavenumbers and, in turn, alters the relative importance associated with the suspension response around the body and wheel resonance peaks. Consequently, suspensions which are more effective at controlling body rather than wheel movement show more favourably in terms of rms tyre load variation. For the active and continuously variable systems this results in a shift to the left of any DTL vs. ACC performance curves and therefore improved comfort for any given tyre load.

3. At these conditions, the fully active system offers dramatic improvements in comfort (up to 75%) over the passive system. This is due in part to the use of a ground input psd with slope -3, but mainly to the active systems ability to use the available workspace more efficiently than the passive system.
4. The best performing controllable damper suspension is the continuously variable system, with a possible improvement in comfort of around 18% over the passive design. The large difference between these results and those of the fully active system is due to the purely dissipative nature of the continuously variable system, and also the fixed rate passive spring, which restricts the usage of workspace to around that of the passive system.
5. The switchable damper operating according to the Karnopp strategy offers more modest performance improvements and these in turn depend on the choice of hard and soft settings. In view of the relatively simple strategy and required hardware, these gains may still be considered worthwhile.
6. The three-state adaptive damper studied here appears to offer only marginal improvements in terms of ride comfort. The system behaves in a similar way to a lightly damped passive system ie. a reduction in accelerations

in the frequency range 2 to 10Hz, but an increase in activity around the body and wheel resonance peaks.

The linear optimal control theory used to generate the active and continuously variable control laws assumes the road surface input to be a filtered white noise signal, ie. the input spectra has a slope of -2. Since the road surface descriptions used in this chapter have a slope of -3 it is clear that the generated laws are optimal for conditions which are different to the ones of interest here, and further improvements may be possible if the input for the optimisation procedure is filtered to suit the actual running conditions.

Once again it must be remembered that the results in this chapter concentrate mainly on ride. It is taken for granted that the overall controller design will include a handling algorithm to override the ride strategy during cornering, braking and accelerating manoeuvres. This will probably mean a simple switch to a harder setting although, in the case of the continuously variable damper, this may involve the use of separate handling control laws with lateral acceleration, yaw rate etc. as the feedback variables.

# Chapter 10

## Conclusions

This chapter attempts to summarise the concluding remarks given in each of the previous chapters.

The modelling and analysis techniques required by the subsequent chapters are outlined in Chapter 2. Reduction from the full vehicle to a more manageable two degree of freedom, quarter car model is discussed, together with an idealised road surface description based on the shape of the amplitude squared spectral density curve. Linear and non-linear analysis methods are reviewed and three performance criteria are established.

In Chapter 3, the quarter car model is used to present a brief performance analysis of the passive suspension. The choice of passive elements having fixed characteristics involves a compromise, due to several conflicting requirements. One of these is between ride comfort and suspension working space usage, with very soft springs providing the best comfort but also an impractically large suspension travel. For a given suspension working space the best performing systems in terms of ride comfort and road holding ability are identified using an equal workspace contour. However, this analysis only addresses the ride problem. The final choice of system is further complicated by the handling aspect, and a requirement of the suspension to be stiff enough to provide adequate attitude control during manoeuvring, accelerating and braking. Similar passive system studies have been undertaken by several authors but the aim in Chapter 3 is simply to; (a) establish the comparison techniques, and (b) quantify the performance of a typical passively suspended saloon car which can be then used

as a baseline figure in subsequent comparisons.

“Intelligent” suspensions, fitted with controllable elements are able to improve on the fixed characteristic passive suspension by avoiding some of the design compromises. The active suspension is an extreme case in which the conventional elements of the passive system are replaced with a hydraulic or pneumatic actuator. A quarter car model of such a system is described in Chapter 4. The actuator is assumed to be ideal and driven by one of a number of control law which are based on linear optimal control theory. A performance comparison of active systems driven by various control laws is carried out on an equal workspace basis. This reveals that, although a full state feedback control law provides the best performance, the more practical limited state feedback case is almost as effective. In either case, comfort gains of up to 45% are possible over the passive system. These are achieved largely through an effective control of events around body resonance. At the “wheelhop” frequency an active system can perform little better than a well designed passive suspension.

Despite the potential of the active system, the added cost and system complexity has left their commercial viability in some doubt. The majority of vehicle manufacturers have therefore turned their attention to finding a more practical alternative. In Chapter 5, three controllable damper systems are selected for comparison against the passive and ideal active systems. In order of increasing complexity, the dampers used in each system are; a three-state adaptive damper which responds to suspension displacement, a two-state switchable damper which operates according to the Karnopp strategy, and a continuously variable damper which is driven by a limited state feedback optimal control law. At this stage the valve switching dynamics are assumed to be ideal. The performance of the continuously variable system is predictably closest to that of the active system but is seen to deteriorate as the suspension stiffness is increased. The two-state switchable damper provides worthwhile improvements

in ride comfort and is seen to be most effective when employed on stiff suspensions. In both cases it is possible to achieve the ride comfort of the standard passive suspension at higher spring stiffnesses, offering potential improvements in terms of body attitude control. The benefits of the adaptive damper system do not appear in this chapter since the comparisons are only concerned with a single surface.

The majority of theoretical studies in the literature, relating to active and semi-active suspensions, have assumed ideal components. Some have included a notional time delay in the response but the effect of this is not dealt with in any detail. In Chapter 6 the limitations present in realistic hardware are introduced into the controllable damper models. These consist of valve response time delays and, in the case of the continuously variable damper system, limits on the range of damping. Their effect on performance is quantified and design targets are established. The continuously variable system is assumed to respond according to a first order time delay. The effect of this delay on system performance, depends to some extent on the suspension stiffness and control law weighting, but typically a 5ms increase in time constant results in a 5% increase in discomfort parameter for a given tyre load performance. A time constant of 10 to 15ms seems a reasonable target for the suspension designer. Restrictions on the range of damping, in particular the lower limit, also affect performance. The minimum setting should be as low as possible, while the maximum setting will be governed by handling and safety requirements of the suspension. The switchable system response is based on test work which suggests a “threshold” delay followed by a first order lag. The first order lag has a similar effect to the one seen on the continuously variable system, while the threshold delay further compromises the ride and tyre load performance and also increases the usage of suspension working space. The adaptive damper is modelled in a similar way to the switchable damper but in this case the switching times are short in

comparison to the length of time spent in each setting, and are consequently of less importance.

While the quarter car model is adequate for the basic ride problem, it does not take into account the correlations which occur between ground inputs. For the more advanced suspensions this becomes important, since they have the potential to take advantage of the fact that the rear wheel input is simply a delayed version of that at the front. In Chapter 7 a two dimensional, half-vehicle model is used to generate correlated control laws. Following the work of Abdel-Hady [1989], a Pade approximation is used to represent the time delay between inputs and the resulting control law is applied to the active system. Extending this, the work here also covers the continuously variable damper systems. If ideal systems are used the improvements over systems using uncorrelated control laws are significant, with a 20% reduction in discomfort parameter for a given dynamic tyre load. If practical limitations are included in the continuously variable model, the improvement is reduced to around 5% but this is still a worthwhile gain since it is obtained with no additional hardware and therefore no extra cost.

In Chapter 8, the body acceleration, suspension arm acceleration and suspension displacement at the rear of a passively suspended saloon car are measured during runs over three roads. The surfaces and speeds are selected to represent a typical range of operation for the vehicle. The resulting psd's are compared with similar psd's obtained from theoretical analysis using the quarter car model and several idealised inputs. An empirical approach is then used to estimate the surface roughness parameters of the three test roads. Although the procedure is rather crude, the parameters obtained were all within the range of values quoted in the literature, and it does provide a range of idealised surfaces which can be associated with known roads.

In Chapter 9, the three conditions are used to compare competing systems over a range of typical operating conditions. The controllable damper systems considered are intended to represent practical systems and are modelled using realistic data to describe their suspension parameters and response limitations. Although the continuously variable and switchable damper systems are non-linear, the comparison reveals that their results can generally be scaled between operating conditions. The adaptive system is the only system in which the results do not behave in this manner. The surface descriptions used in Chapter 9 each have a log-log psd slope of -3, while the one used in Chapters 3 to 7 has a slope of -2.5. Both values are within the range quoted in the literature but the difference appears to have an important effect on the relative comparisons. A steeper slope (-3) results in less input at higher wavenumbers, which in turn will improve the rating of systems which are effective at controlling body rather than wheel movement. A relaxation of the equal workspace restriction in Chapter 9 allows the fully active systems to improve on the ride comfort of the passive system by up to 75%. This is justified by the argument that on smoother roads, adaptation of the control law will allow the active suspension to utilise the available working space more effectively than the passive system. The best performing controllable damper system is the continuously variable system which can improve on the comfort of the passive system by around 18%. The two-state switchable system is less effective, but the hardware costs are also less and therefore may still be worth considering. For the three surfaces considered in Chapter 9, the adaptive damping strategy offers only marginal improvements in terms of rms vertical body acceleration.

Overall, the previous level of understanding of controlled suspension systems has been increased in four areas ; (a) new results have been generated for a variety of controllable damper systems, (b) the effect of realistic response limitations present in the hardware have been quantified, (c) the effect of wheelbase time

delay on the performance of the semi-active suspension has been predicted, and (d) the idea of system adaptation has been investigated, using a range of idealised surfaces which are derived from measurements over actual roads.

## References

- ABDEL HADY, M.B.A [1989]** “The effect of active suspension control on vehicle ride behaviour”. PhD. Thesis, University of Leeds, (Dept. of Mechanical Engineering).
- ACKER, B; DARENBERG, W; GALL, H [1989]** “Active suspensions for passenger cars”. Proc. 11th IAVSD Symposium on Dynamics of Vehicles on Roads and on Tracks, (Ed. R. Anderson), Kingston, Ont, pp.15-26.
- ALANOLY, J; SANKAR, S [1987]** “A new concept in semi-active vibration isolation”. Trans. of the ASME J. of Mechanisms, Transmissions and Automation in Design, 109, pp242-247.
- ALSTEAD, C.J [1985]** “Programmable data acquisition system : User Manual”. Ref. No. DAC/14, University of Leeds, (Dept. of Mechanical Engineering).
- AOYAMA, Y; KAWABATA, K; HASEGAWA, S; KOBARI [1990]** “Development of the full active suspension by Nissan”. SAE paper 901747.
- AURELL, J; EDLUND, S [1989]** “Operating severity distribution”. Proc. 11th IAVSD Symposium on Dynamics of Vehicle on Roads and on Tracks, (Ed. R. Anderson), Kingston, Ont, pp.42-56.
- BAKKER, E; NYBORG, L; PACEJKA, H.B [1987]** “Tyre modelling studies for use in vehicle dynamic studies”. SAE paper 870421.
- CEBON, D; NEWLAND, D.E [1983]** “The artificial generation of road surface topography by the inverse FFT method”. Proc. 8th IAVSD Symposium on Dynamics of Vehicles on Roads and on Tracks (Ed. J.K Hedrick), Cambridge, MA, pp.29-42.

- CHALASANI, R.M [1986 a]** "Ride performance potential of active suspension systems - Part 1 : Simplified analysis based on a quarter-car model". ASME Symposium on Simulation and Control of Ground Vehicle and transportation Systems (Eds L. Segel, J.Y. Wong, E.H. Law and D. Hrovat), AMD-Vol.80, DSC-Vol.2, pp.187-204.
- CHALASANI, R.M [1986 b]** "Ride performance of active suspension systems - Part 2 : Comprehensive analysis based on a full-car model". ASME Symposium on Simulation and Control of Ground Vehicle and transportation Systems (Eds L. Segel, J.Y. Wong, E.H. Law and D. Hrovat), AMD-Vol.80, DSC-Vol.2, pp.187-204.
- CITROEN [1989]** "Hydractive suspension system". Technical leaflet.
- CROLLA, D.A; ABOUL NOUR A.M.A [1988]**, "Theoretical comparisons of various active suspension systems in terms of performance and power requirements". Proc. I.Mech.E, International Conference on Advanced Suspensions, pp.1-9.
- CROLLA, D.A; FIRTH, G.R; HINE, P.J; PEARCE, P.T [1989]** "The performance of suspensions fitted with controllable dampers". Proc. 11th IAVSD Symposium on Dynamics of Vehicle on Roads and on Tracks, (Ed. R. Anderson), Kingston, Ont, pp.149-165.
- DODDS, C.J; ROBSON, J.D [1973]** "The description of road surface roughness". J. of Sound and Vibration, 31(2), pp.175-183.
- DOI, S; YASUDA, E; HAYASHI, Y [1988]** "An experimental study of optimal vibration adjustment using adaptive control methods". Proc. I.Mech.E, International Conference on Advanced Suspensions, pp.119-124.
- FOAG, W [1988]** "A practical control concept for passenger car active suspensions with preview". Proc. I.Mech.E, International Conference on Ad-

vanced Suspensions, pp.43-50.

**FRUHAUF, F; KASPER, R; LUCKEL, J [1985]** "Design of an active suspension for a passenger vehicle model using input processes with time delays". Proc. 9th IAVSD Symposium on the Dynamics of Vehicles on Roads and on Tracks (Ed. O. Nordstrom), pp.126-136.

**GOODALL, R.M; KORTUM, W [1983]** "Active controls in ground transportation - a review of the state of the art and future potential". Vehicle System Dynamics, 12, pp.225-257.

**HAC, A [1985]** "Suspension optimisation of a 2-dof vehicle model using a stochastic optimal control technique". J. of Sound and Vibration, 100(3), pp.343-357.

**HALL, B.B; GILL, K.F [1987]** "Performance evaluation of motor vehicle active suspension systems". Proc. I.Mech.E, 201(D2), pp.135-148.

**HASSAN, S.A [1986]** "Fundamental studies of passive, active and semi-active automotive suspension systems". PhD. Thesis, University of Leeds, (Dept. of Mechanical Engineering).

**HEALEY, A.J; NATHMAN, E; SMITH, C.C [1977]** "An analytical and experimental study of automobile dynamics with random roadway inputs". Trans. of the ASME, J. of Dynamic Systems, Measurement, and Control, December 1977, pp.284-292.

**HEDRICK, J.K; WORMLEY, D.N [1975]** "Active suspension for ground transportation vehicles - A state of the art review". Mechanics of Transportation Systems, ASME, AMD, Vol.15. pp.21-40.

**HENNECKE, D; ZIEGLEMEIER, F.J [1988]** "Frequency dependent variable suspension damping - theoretical background and practical success".

- Proc. I.Mech.E, International Conference on Advanced Suspensions, pp.101-112.
- HINE, P.J; PEARCE, P.R [1988]** "A practical intelligent damping system". Proc. I.Mech.E, International Conference on Advanced Suspensions, pp.141-148.
- HORTON, D.N.L [1986]** "An introduction to ride analysis in vehicle dynamics". Research report DAC/12, University of Leeds, (Dept. of Mechanical Engineering).
- HORTON, D.N.L [1991]** "VDAS - Vehicle dynamic analysis software". Version 3.2, University of Leeds, (Dept. of Mechanical Engineering).
- INTERNATIONAL STANDARD - ISO 2631 [1974],[1985]** "Guide for the evaluation of human exposure to whole-body vibrations". International Standards Organization.
- KARNOPP, D;CROSBY, M.J;HARWOOD, R.A [1974]** "Vibration control using semi-active force generators". J. of Engineering for Industry, May, pp.619-626.
- KAMASH, K.M.A; ROBSON, J.D [1978]** "The application of isotropy in road surface modelling". J. of Sound and Vibration, 57(1), pp.89-100.
- KONISHI, J; SHIRAISHI, Y; KATADA, K; ITO, H [1988]** "Development of electronically controlled air suspension system". SAE paper 881770.
- LA BARRE, R.P; FORBES, R.T; ANDREW, S [1970]** "The measurement and analysis of road surface roughness". MIRA Report No. 1970/5.
- LIZELL, M [1988]** "Semi-active damping". Proc. I.Mech.E, International Conference on Advanced Suspensions, pp.83-92.

- LOUAM, N; WILSON, D.A; SHARP, R.S [1988]** "Optimal control of a vehicle suspension incorporating the time delay between front and rear wheel inputs". *Vehicle System Dynamics*, 17, pp.317-336
- MILLER, L.R [1988]** "The effect of hardware limitations on an on/off semi-active suspension". *Proc. I.Mech.E, International Conference on Advanced Suspensions*, pp.199-206.
- MIZUGUCHI,M; SUDA, T; CHIKAMORI, S; KOBOYASHI, K [1984]** "Chassis electronic control systems for the Mitsubishi 1984 Galant". SAE paper 840258.
- NAG [1987]** "The Numerical Algorithms Group Fortran library - mark 13". NAG Ltd, Wilkinson House, Jordan Hill Road, Oxford, UK, OX2 8DR.
- PARKER, G.A; LAU, K.S [1988]** "A novel valve for semi-active vehicle suspension systems". *Proc. I.Mech.E, International Conference on Advanced Suspensions*, pp.69-74.
- POYSER, J [1987]** "Development of a computer controlled suspension system". *Int. J. of Vehicle Design*, Vol.8, No.1, pp.74-86.
- REUTER, R.J [1989]** "Speed dependent damping for the 1989 Cadillac Allante". SAE paper 890178.
- ROBSON, J.D [1979]** "Road surface description and vehicle response". *Int. J. of Vehicle Design*, Vol.1, No.1.
- RYBA, D [1973]** "Possible improvements in ride comfort". *Vehicle System Dynamics*, 2, pp.1-32.
- RYBA, D [1974 a]** "Improvements in dynamic characteristics of automobile suspensions, (Part 1, Two mass systems)". *Vehicle System Dynamics*, 3, pp.17-46.

- RYBA, D [1974 b]** "Improvements in dynamic characteristics of automobile suspensions, (Part 2, Three mass systems)". *Vehicle System Dynamics*, 3, pp.55-98.
- SCHWARZENBACH, J; GILL, K.F [1984]** "System Modelling and Control". Edward Arnold, 2nd. Ed. ISBN 0 7131 3518 2.
- SHARP, R.S; HASSAN, S.A [1984]** "The fundamentals of passive automotive suspension systems". Soc. of Environmental Engineers, Conference on Dynamics in Automotive Engineering, Cranfield Inst. Tech., pp.104-115.
- SHARP, R.S; HASSAN, S.A [1986 a]** "An evaluation of passive automotive suspension systems with variable stiffness and damping parameters". *Vehicle System Dynamics*, 15, pp.335-350.
- SHARP, R.S; HASSAN, S.A [1986 b]** "The relative performance capabilities of passive, active and semi-active car suspension systems". *Proc. I.Mech.E*, 200, D3, pp.219-228.
- SHARP, R.S; HASSAN, S.A [1987]** "On the performance capabilities of active automobile suspension systems of limited bandwidth". *Vehicle System Dynamics*, 16, pp.213-225.
- SHARP, R.S; HASSAN, J.H [1988]** "Performance predictions for a pneumatic active car suspension system". *Proc. I.Mech.E*, Vol.202(D4), pp.243-250.
- SHARP, R.S; CROLLA, D.A [1987 a]** "Road vehicle suspension system design - a review". *Vehicle System Dynamics*, 16, pp.167-192.
- SHARP, R.S; CROLLA, D.A [1987 b]** "Intelligent suspension for road vehicles - current and future developments". *Proc. EAEC Conference, Strasbourg*, 2, pp.579-601.

- SHARP, R.S [1989]** "On the accurate representation of tyre shear forces by a multi-radial spoke model". Proc. 11th IAVSD Symposium (Ed. R. Anderson), Kingston, Ont, pp.528-541.
- THOMPSON, A.G [1976]** "An active suspension with optimal linear state feedback". Vehicle System Dynamics, 5, pp.187-203.
- THOMPSON, A.G; PEARCE, C.E.M [1979]** "An optimal suspension for an automobile on a random road". SAE paper 790478.
- THOMPSON, A.G [1984]** "Optimal and sub-optimal linear active suspensions for road vehicles". Vehicle System Dynamics, 13, pp.61-72.
- TSUTSUMI, Y; SATO, H; KAWAGUCHI, H; HIROSE, M [1990]** "Development of piezo TEMS (Toyota electronic modulated suspension)". SAE paper 901745.
- VAN DE VEGTE, J [1990]** "Feedback Control Systems". Prentice Hall, 2nd. Ed. ISBN 0 13 313651 5.
- WILSON, D.A; SHARP, R.S; HASSAN, S.A [1986]** "Application of linear optimal control theory to the design of automobile suspensions". Vehicle System Dynamics, 15, pp.105-118.
- WRIGHT, P.G; WILLIAMS, D.A [1984]** "The application of active suspension to high performance road vehicles". Proc. I.Mech.E, C239/84.
- YOKOYA, Y; ASAMI, K; HAMAJIMA, T; NAKASHIMA, N [1984]** "Toyota electronic modulated suspension (TEMS) system for the 1983 Soarer". SAE paper 840341.
- YOKOYA, Y; KIZU, R; KAWAGUCHI, H; OHASHI, K [1990]** "Integrated control system between active control suspension and four wheel steering for the 1989 Celica". SAE paper 901748.